ELECTROKINETIC-ASSISTED MEMBRANE PHOTOBIOREACTOR (EK-MPBR)

FOR MUNICIPAL WASTEWATER TREATMENT

A Thesis

Presented to

The Faculty of Graduate Studies
of
Lakehead University

by
Maryam Amini

In partial fulfilment of requirements

for the degree of

Doctor of Philosophy

Abstract

Membrane technology and phycoremediation, which utilizes algae for nutrient removal, are two major emerging technologies for wastewater treatment. Membrane photobioreactors (MPBRs) integrate these technologies and provide promising technology to render wastewater for reuse in the industrial or agricultural domains. One of the main current limitations of this technology is membrane fouling, and developing a proper technique to address this issue in MPBRs has remained a gap in this sector.

With the major aim of alleviating membrane fouling in MPBRs, this study modified the design of the current MPBRs to utilize an electric field. Using graphite sheet as anode and stainless steel mesh as simultaneous membrane support and a cathode on each side of the membrane module was developed to ameliorate membrane performance. This novel design helps to repel biomass from the membrane surface with the charge introduced by a low voltage direct current (DC) electric field. The membrane performance of the electrokinetic-assisted MPBR (EK-MPBR) as well as the biological performance of this recently developed technology, have been investigated. Synthetic municipal wastewater was treated by an EK-MPBR and ran in parallel with a control MPBR for 49 days, where EK-MPBR demonstrated significant improvement in terms of membrane fouling inhibition with 50% less fouling frequency. Considerable enhancement in phosphorus (P) removal was another advantage of the EK-MPBR compared to the control MPBR with the EK-MPBR having 56% better P removal. Involved electrokinetic phenomena such as electrophoresis, electroosmosis, and electrochemical reactions contributed to the performance of EK-MPBRs in terms of cell size reduction, dewaterability, and bacterial growth and agglomeration inhibition, respectively, leading to change in algal morphology.

Furthermore, the effect of solid retention time (SRT) on the biological and membrane performances of the EK-MPBRs was studied. SRT of 40, 20, and 10 days were investigated in treating municipal wastewater for 80, 80, and 45 days, respectively. The results suggested that while the SRTs of 20 and 10 days showed similar TMP increases and fouling behaviour over 45 days of operation, the prolonged SRT of 40 days exhibited 75% more fouling. The SRT of 10 days outperformed the 20 and 40 day SRTs in terms of nutrient removal (N and P) efficiency and biomass productivity due to the changes in the biological properties of the algal biomass caused

by the combination of factors, including electrokinetic and SRT. All three SRTs showed superior phosphorus removal efficiency compared to the conventional MPBRs (>96.7 % compared to <50 % for the conventional MPBR) and met the discharge standard for chemical oxygen demand (COD).

The results of this study suggest that the EK-MPBRs are a promising technology for simultaneous biomass production and wastewater treatment. The optimization of the operating condition and the design to improve nitrogen removal efficiency and biomass production will augment the application of electrified MPBRs.

Keywords: Phycoremediation, Wastewater treatment, Algae, Membrane photobioreactor, Nutrients removal, Electrokinetic, Solid retention time

Acknowledgements

First, I would like to express my gratitude to my doctoral advisors Professor Eltayeb Mohamedelhassan and Professor Baoqiang Liao for offering me the opportunity to conduct this research, for guiding me on general research directions, and for their knowledge and academic thoughts. The research presented here would not have been explored without their scientific insights.

I am deeply grateful to my entire committee for their time and insightful comments and guidance. I am aware that the final stages of this project were demanding their time and attention and I am so appreciative of the time they gave me. Dr. Ebrahim Rezaei and Dr. Liang Cui, I am honoured to have you on my committee. I am also thankful to Dr. Wa Gao who served as an external examiner for my comprehensive exam and Dr. Aicheng Chen who served as an external committee member to my defence

I also owe my sincere gratitude to Lakehead University for offering the opportunity to study, and for supporting me throughout the program, and for providing funding for this research. I would like to thank the Dean of Science and Environmental Study, Dr. Todd Randall, and the Faculty of Graduate Studies and International Student Centre, especially Ms. Laura Pudas, for their exceptional support and commitment. I would also like to single out Dr. Brenda Magajna for special thanks. Her tremendous support, incisive feedback, patience, humour, and honesty will be cherished forever.

Great thanks go to Dr. Pedram Fatehi, Mr. Greg Krepka, Ms. Johane Joncas and Dr. Weijue Gao for the training and testing services provide for the research. Special thanks is due to Mr. Glenn Clausen for great insights and for setting up the experimental apparatus. Deep gratitude also goes to my cohort: Dr. Meijia Zhang, Dr. Alnour Bokhary, and Yichen Liao, for much help and kindness. Special appreciation is for Dr. Azadeh Bahrami for her continuous support. I would also like to thank all my friends who have helped me to make it to this stage in the process.

Most importantly, I am incredibly thankful to my family: my late mother, my father, my aunts, my brothers and all of my family members who provided the foundation for a broader life. I am grateful for all their love as well as their support. My life has also become especially enriched in many ways by Sheila and John Noyes who have become my Canadian family. They have

illuminated my life with hope, encouragement, and love. My deepest appreciation is to them, and it will continue unabated. I cannot imagine having accomplished this goal without their support and love.

Table of contents

List of tables

LIST OF FIGURES

List of Nomenclature and Abbreviations

Nomenclature

r_x	productivity of the biomass (mg/L.d)
X	average biomass concentration (g/L)
Q_{waste}	biomass wasting rate (L/d)
V_{MPBR}	working volume of the membrane photobioreactor (L)
ΔP	transmembrane pressure difference (kPa)
J	permeate flux (L/m^2.h)
R_p	pore-clogging filtration resistance (m^{-1})
R_c	cake layer filtration resistance (m^{-1})
R_m	virgin membrane filtration resistance (m^{-1})
R_t	total filtration resistance (m^{-1})
μ	permeate dynamic viscosity (Pa.s)
$J_{backwash}$	backwash flux (L/m^2.h)
Q_p	flow rate of permeate water ($^{m^3}/_{s}$)
A	effective surface area of the membrane (m^2)
v_p	electrophoretic velocity of charged particles (m/s)
ε	permittivity of the electrolyte ($^{F}/_{m}$)
ζ	zeta potential of the particles (v)
E	electric field strength ($^{V}/_{m}$)
ΔU	applied voltage (V)
d	distance between the electrodes (m)
I	applied current (A)
σ	conductivity of the bulk solution ($^{S}/_{m}$)

Abbreviations

AC	Alternative current
ANOVA	Analysis of variance
BES	Bio-electrochemical system
BOD	Biological oxygen demand
BSA	Bovine serum albumin
CA	Cellulose acetate
CCP	Carbon cloth phenolic
CFD	Computational fluid dynamics
CFV	Cross-flow velocity
CO_2	Carbon dioxide
COD	Chemical oxygen demand
CR	Congo red
CNT	Carbon nanotube
DBS	Sodium dodecyl benzene-sulfonate
DC	Direct current
DEP	Dielectrophoresis
E	Electric field gradient
EIS	Electrical impedance spectroscopy
EK-MPBR	Elctrokinetic-assistedmembrane photobioreactor
EMBR	Electrically-assisted membrane bioreactor
EMPBR	Electrokinetic membrane photobioreactor
EO	Electroosmosis
EP	Electrophoresis
EPS	Extracellular polymeric substances (mg/g MLSS)
EWOD	Electrowetting-on-dielectric
F/M	Food-microorganism
FO	Forward osmosis
HEMBR	Hybrid electro membrane bioreactor
HRT	Hydraulic retenton time (d)

iDEP	Insulator-based DEP
MBR	Membrane bioreactor
MF	Microfiltration
MLSS	Mixed liquor suspended solids (g/L)
MWCNT	Multi-walled carbon nanotube
N/P	Nitrogen/Phosphorus
PBR	Photobioreactor
PN/PS	Protein to polysaccharide
PSD	Particle size distribution
PVDF	Polyvinylidene difluoride
QS	Quorum sensing
RO	Reverse osmosis
SAnMBR	Submerged anaerobic membrane bioreactor
SMP	Soluble organic matter (mg/L)
SRT	Solid retention time (d)
SWCNT	Single-walled carbon nanotube
TFC	Thin-film composite
TFN	Thin-film nanocomposite
TMP	Transmembrane pressure (kPa)
TN	Total nitrogen
TP	Total phosphorus

Chapter 1 Introduction

1.1 Overview

Algal-related technologies have received a lot of attention in recent years due to the versatile application of biomass [1]. As a product of these technologies, biomass can be used in industries such as pigment [2], biofuel [3], fish food [4], and phycoremediation, which is defined as the elimination of toxic and non-toxic elements in water and wastewater using algae [5]. However, the demand for the algae in the large-scale applications is much greater than the natural reproducing rate of this microorganism. Hence, cultivation systems have to be developed to satisfy the fast-growing algae demands.

The two common cultivation methods are open ponds and photobioreactors (PBRs). PBRs are considered as having improved photosynthesis and reduced footprints. In open ponds, contamination of algal cultures and lack of control over operational parameters are some of the bottlenecks that occur [6]. With these open ponds' challenges, PBRs have been developed to overcome the culturing issues. It should be noted that improvements to PBR technology have been made to eliminate some of the disadvantages such as biomass washout, poor stability, and harvesting limitations [7]. The combination of membrane technology with PBR has successfully resulted in improved cultivation and PBR performance.

Membrane photobioreactors (MPBR) incorporate simultaneous algal cultivation and wastewater treatment technology. The membrane in MPBRs can be located either at a side-stream tank or as a submerged membrane in PBRs. Membranes help the PBR to prevent biomass washout and enable better control of operational parameters such as hydraulic retention time (HRT) and solids retention time (SRT) [8]. However, similar to other separation technologies, membrane separation has its own drawbacks. One of the major challenges that impede wide applications of membranes and increases the operating and capital costs of this technology is membrane fouling. Membrane fouling is the accumulation of foulants, including biological, organic, and inorganic foulants, on membrane surfaces or inside pores that block the pores for fluid flow. Fouling eventually leads to a decrease in membrane flux and an increase in transmembrane pressure (TMP). This increases

the energy consumption and cost and ultimately chemical cleaning is required in order to reinstate membrane permeability which also results in a decrease in membrane lifespan [9].

Due to the significance of membrane fouling phenomena in membrane separations, considerable efforts and progress have been made to understand the mechanisms of membrane fouling and to develop strategies for membrane fouling control [10]. Physical, chemical, and biological methods have been widely applied for membrane fouling control in water and wastewater treatment [11]. Physical methods include the use of aeration, sparging, and cross-flow velocity (CFV) to create shear forces on membrane surfaces to reduce membrane fouling [12]. Furthermore, back pulse washing has also been widely used for fouling control in hollow fibre membranes [13]. Chemical methods involve the use of chemical cleaning agents to remove foulants from membrane surfaces and inside pores. Typical chemical cleaning agents include oxidants (e.g. sodium hypochlorite), bases (e.g. NaOH), inorganic and organic acids, and chelating agents (citric acid and EDTA) [14]. Biological methods use an enzyme to remove organic foulants [15]. Although these methods are effective in membrane fouling control, they either have a high energy consumption (physical methods) or use chemicals (chemical methods) or expensive enzymes, thus, continuous efforts have been made in searching for new and more efficient methods for membrane fouling control [14].

One of the new approaches for fouling mitigation uses the interaction between charged particles and the membrane which is defined as electrokinetic phenomenon [13]. This technique uses an external electric field to control the foulants' movement and attachment to the surface of the membrane. The electrokinetic approach is potentially an environmentally friendly and cost-effective technique for membrane fouling control and process intensification [16]. Integration of electrokinetic fouling mitigation with membrane bioreactors (MBRs) has promisingly contributed to the biological wastewater treatment techniques [17]. Electrified membrane bioreactors have been developed and studied in recent years [18-20]. Membrane fouling has been reported to be decreased by the electrokinetic presence in the MBRs [21-24]. The improvement in biological performance and removal efficiency of MBRs under the effect of electric field have also been reported [22,25,26]. Although electrically-assisted MBRs has improved the membrane performance by reducing the fouling and increasing nutrient removal, there is an increasing need for further development regarding reducing energy cost and membrane cleaning cycle [14].

Therefore, incorporating electric fields in biological wastewater treatment has been studied and found effective in fouling control and biological performance [22]. However, its application for simultaneous microalgae production and wastewater treatment, which MPBRs can offer, has remained a gap. Furthermore, the implication of electrified phycoremediation in MPBRs and its membrane fouling has not been examined yet. In addition, membrane fouling behaviour under different SRTs in MPBRs has remained a gap in this novel research area and more studies are required to promote electrified MPBRs.

1.2 Objectives

The overall objective of this study is to develop novel electro-phycoremediation techniques in wastewater treatments using microalgae with high efficiency which is not achievable with current technologies. As such, this study aims to determine the feasibility of EK-MPBRs, to identify the critical factors influencing fouling and biological performance in an electrified MPBR, and to investigate the development of membrane fouling. The specific research objectives were as follows:

(1) develop an EK-MPBR process with a novel modified design of membrane module configuration for the treatment of synthetic municipal wastewater and investigate the effects of electric field on the biological performance of the MPBR and compare it with a control MPBR;

(2) investigate the effect of electric field on membrane fouling for the EK-MPBR system;

(3) identify the effects of SRT on the biological performance of an EK-MPBR for the treatment of synthetic municipal wastewater; and

(4) investigate the effects of SRT variations on the membrane performance of the EK-MPBR.

1.3 Scope of this thesis

The present research developed a novel electrokinetic-assisted MPBR (EK-MPBR) with a modified novel design of membrane module configuration to control membrane fouling for treating synthetic municipal wastewater. The effect of applied low voltage electric field on the

biological performance and membrane fouling were studied. Furthermore, the effect of SRT variation on biological and membrane performance of EK-MPBRs was also investigated for the first time. Based on the experimental results, the feasibility and potential of EK-MPBRs for electro-phycoremediation were briefly evaluated. The thesis is organized in the following order:

Chapter 1 briefly describes the research background, objectives, and thesis organization.

Chapter 2 focuses on a literature review about electrochemical approaches for fouling mitigation. The literature introduces membrane separation technology and its fouling mechanism followed by electrokinetic phenomena and its contribution for fouling inhibition. Membrane photobioreactor and its application in wastewater treatment is also discussed.

In **Chapter 3**, a laboratory-scale electrokinetic-assisted membrane photobioreactor (EK-MPBR) was developed and operated in parallel to a control MPBR without an electric field over 60 days for synthetic municipal wastewater treatment. The parameters, including biomass production, biomass productivity, COD removal, and nutrient (N and P) removal were evaluated.

Chapter 4 investigates the physico-chemical properties of microalgae and its membrane fouling propensity under the effect of the electric field. Various characterizations, including transmembrane pressure (TMP), filtration resistance composition, soluble microbial products (SMP), extracellular polymeric substances (EPS), particle size distribution (PSD), and microscopic observation, were evaluated and compared with the control MPBR.

Chapter 5 covers the application of an EK-MPBR treating synthetic municipal wastewater effluent at three SRTs of 10, 20, and 40 d. Influences of SRT on the EK-MPBR biological performance and biomass properties were investigated.

Chapter 6 studies the effects of SRT on membrane fouling based on a series of characterizations, such as TMP, filtration resistance composition, PSD, micromorphology, SMP, and EPS.

Chapter 7 contains the conclusions from this study and recommendations for further studies in this area.

1.4 References

1. Antar, M.; Lyu, D.; Nazari, M.; Shah, A.; Zhou, X.; Smith, D.L. Biomass for a sustainable bioeconomy: An overview of world biomass production and utilization. *Renewable and Sustainable Energy Reviews* **2021**, *139*, 110691.
2. Cai, Y.; Liu, Y.; Liu, T.; Gao, K.; Zhang, Q.; Cao, L.; Wang, Y.; Wu, X.; Zheng, H.; Peng, H. Heterotrophic cultivation of Chlorella vulgaris using broken rice hydrolysate as carbon source for biomass and pigment production. *Bioresource Technology* **2021**, *323*, 124607.
3. Saravanan, A.; Kumar, P.S.; Jeevanantham, S.; Karishma, S.; Vo, D.-V.N. Recent advances and sustainable development of biofuels production from lignocellulosic biomass. *Bioresource Technology* **2022**, *344*, 126203.
4. Ansari, F.A.; Guldhe, A.; Gupta, S.K.; Rawat, I.; Bux, F. Improving the feasibility of aquaculture feed by using microalgae. *Environmental Science and Pollution Research* **2021**, *28*, 43234-43257.
5. Hu, R.; Cao, Y.; Chen, X.; Zhan, J.; Luo, G.; Ngo, H.H.; Zhang, S. Progress on microalgae biomass production from wastewater phycoremediation: metabolic mechanism, response behavior, improvement strategy and principle. *Chemical Engineering Journal* **2022**, 137187.
6. Luo, Y.; Le-Clech, P.; Henderson, R.K. Simultaneous microalgae cultivation and wastewater treatment in submerged membrane photobioreactors: a review. *Algal Research* **2017**, *24*, 425-437.
7. Bilad, M.; Discart, V.; Vandamme, D.; Foubert, I.; Muylaert, K.; Vankelecom, I.F. Coupled cultivation and pre-harvesting of microalgae in a membrane photobioreactor (MPBR). *Bioresource technology* **2014**, *155*, 410-417.
8. Honda, R.; Boonnorat, J.; Chiemchaisri, C.; Chiemchaisri, W.; Yamamoto, K. Carbon dioxide capture and nutrients removal utilizing treated sewage by concentrated microalgae cultivation in a membrane photobioreactor. *Bioresource technology* **2012**, *125*, 59-64.
9. Akther, N.; Sodiq, A.; Giwa, A.; Daer, S.; Arafat, H.; Hasan, S. Recent advancements in forward osmosis desalination: A review. *Chemical Engineering Journal* **2015**, *281*, 502-522.

10. Xie, M.; Shon, H.K.; Gray, S.R.; Elimelech, M. Membrane-based processes for wastewater nutrient recovery: technology, challenges, and future direction. *Water research* **2016**, *89*, 210-221.
11. Liao, Y.; Bokhary, A.; Maleki, E.; Liao, B. A review of membrane fouling and its control in algal-related membrane processes. *Bioresource technology* **2018**, *264*, 343-358.
12. Hilal, N.; Ogunbiyi, O.O.; Miles, N.J.; Nigmatullin, R. Methods employed for control of fouling in MF and UF membranes: a comprehensive review. *Separation Science and Technology* **2005**, *40*, 1957-2005.
13. Bagheri, M.; Mirbagheri, S.A. Critical review of fouling mitigation strategies in membrane bioreactors treating water and wastewater. *Bioresource technology* **2018**, *258*, 318-334.
14. Fan, H.; Xiao, K.; Mu, S.; Zhou, Y.; Ma, J.; Wang, X.; Huang, X. Impact of membrane pore morphology on multi-cycle fouling and cleaning of hydrophobic and hydrophilic membranes during MBR operation. *Journal of Membrane Science* **2018**, *556*, 312-320.
15. Zitomer, D.H.; Bachman, T.; Vogel, D. Thermophilic anaerobic digester with ultrafilter for solids stabilization. *Water Science and Technology* **2005**, *52*, 525-530.
16. Wei, C. Nutrient removal and fouling reduction in electrokinetic membrane bioreactor at various temperatures. **2009**.
17. Meng, F.; Zhang, S.; Oh, Y.; Zhou, Z.; Shin, H.-S.; Chae, S.-R. Fouling in membrane bioreactors: An updated review. *Water research* **2017**, *114*, 151-180.
18. Asif, M.B.; Maqbool, T.; Zhang, Z. Electrochemical membrane bioreactors: State-of-the-art and future prospects. *Science of the total environment* **2020**, *741*, 140233.
19. Zhang, L.; Wang, L.; Zhang, Y.; Wang, D.; Guo, J.; Zhang, M.; Li, Y. The performance of electrode ultrafiltration membrane bioreactor in treating cosmetics wastewater and its anti-fouling properties. *Environmental research* **2022**, *206*, 112629.
20. Ostermeyer, P.; Bonin, L.; Leon-Fernandez, L.F.; Dominguez-Benetton, X.; Hennebel, T.; Rabaey, K. Electrified bioreactors: the next power-up for biometallurgical wastewater treatment. *Microbial Biotechnology* **2022**, *15*, 755-772.
21. Predolin, L.M.; Moya-Llamas, M.-J.; Vasquez-Rodriguez, E.D.; Jaume, A.T.; Rico, D.P. Effect of current density on the efficiency of a membrane electro-bioreactor for removal of

micropollutants and phosphorus, and reduction of fouling: a pilot plant case study. *Journal of Environmental Chemical Engineering* **2021**, *9*, 104874.

22. Corpuz, M.V.A.; Borea, L.; Senatore, V.; Castrogiovanni, F.; Buonerba, A.; Oliva, G.; Ballesteros Jr, F.; Zarra, T.; Belgiorno, V.; Choo, K.-H. Wastewater treatment and fouling control in an electro algae-activated sludge membrane bioreactor. *Science of the Total Environment* **2021**, *786*, 147475.
23. Wang, L.; Wu, Y.; Fu, Y.; Deng, L.; Wang, Y.; Ren, Y.; Zhang, H. Low electric field assisted surface conductive membrane in AnMBR: Strengthening effect and fouling behavior. *Chemical engineering journal* **2022**, *431*, 133185.
24. Karimi, L.; Hazrati, H.; Gharibian, S.; Shokrkar, H. Investigation of various anode and cathode materials in electrochemical membrane bioreactors for mitigation of membrane fouling. *Journal of Environmental Chemical Engineering* **2021**, *9*, 104857.
25. Belli, T.; Battistelli, A.; Costa, R.; Vidal, C.; Schlegel, A.; Lapolli, F. Evaluating the performance and membrane fouling of an electro-membrane bioreactor treating textile industrial wastewater. *International Journal of Environmental Science and Technology* **2019**, *16*, 6817-6826.
26. Su, F.; Liang, Y.; Liu, G.; Mota Filho, C.R.; Hu, C.; Qu, J. Enhancement of anti-fouling and contaminant removal in an electro-membrane bioreactor: significance of electrocoagulation and electric field. *Separation and Purification Technology* **2020**, *248*, 117077.

Chapter 2 Literature review

A membrane photobioreactor (MPBR) is a system that integrates a membrane module into a photobioreactor (PBR). Depending on the function of the membrane in the PBR, membrane photobioreactors can be divided into carbonation MPBRs and biomass retention MPBRs. The latter is mainly used for wastewater treatment and is the focus of this study. Like other membrane technologies, MPBRs also suffer from membrane fouling which affects performance and its application to a large extent. There are some methods to mitigate membrane fouling in MPBRs [1]. To better gain an understanding of the fouling in MPBRs, a background in membrane technology, the classification of the mechanisms of membrane fouling, and membrane fouling mitigation techniques are described below.

A recently developed technique, Electro-Membrane photobioreactor appeared to improve the performance of MPBRs with the major aim of improving biological performance and membrane filtration. However, there are few studies that applied a low-voltage electric field to enhance biological and membrane performance using microalgae to treat synthetic municipal wastewater has remained a gap in this field. Furthermore, the effect of solid retention time variation on electrified MPBRs has not been studied yet. The underlying mechanisms of electrokinetics and their application in membrane technology and MPBRs, including industrial application, are subsequently defined in this chapter. However, limited studies in this novel research area resulted in a knowledge gap. Therefore, further studies could promote this technology by better understanding its advantages/disadvantages of this technology.

2.1 Membrane Technology and MPBR background

Membrane technology is a mature separation technique and has been widely used in numerous industries, including water and wastewater purification, biotechnology, food processing, pulp and paper manufacturing, mining and mineral processing, and petroleum and chemical industries [2]. As compared to other separation techniques, membrane technology has many advantages, such as simplicity of operation, ease of scale-up, low energy consumption, no chemical usage, and high efficiency and productivity [3]. Membrane fouling is a major challenge in membrane separation technology, and there are numerous studies focusing on membrane fouling mitigation techniques [4]. The fouling rate of membranes determines the cost of the operation and its efficiency, as the

flux will decrease as the membrane is fouled. Consequently, the pressure across the membrane, which is called transmembrane pressure (TMP), increases and chemical or physical cleaning would be required that will, eventually, decrease the membrane's lifetime [5].

In biological wastewater treatment using membrane technology, the challenge of membrane fouling is a dominant issue due to debris of the cells and their attachment to the membrane. Membrane bioreactors (MBRs) and membrane photobioreactors (MPBRs) are the most common membrane-assisted biological treatment. MBR integrates phycoremediation with solid/liquid separation by membrane filtration by utilizing bacteria or a combination of bacteria and algae as biomass. MPBR, however, uses microalgae as biomass for water treatment and simultaneously benefits from the nutrients in wastewater to grow and cultivate microalgae. MPBR is the focus of the current study, and the factors affecting its performance are discussed accordingly.

2.2 Factors affecting MPBR performance

2.2.1 Wastewater type

Nutrients in wastewater, especially nitrogen and phosphorus, are of great importance in microalgae growth in MPBRs since they are considered as a feed of the microalgae [6]. Fe, Mg, B, Mo, K, Co, Zn, and Mb are also required as trace metals and are consumed by microalgae from wastewater. Therefore, the quantity of these elements in wastewater can determine the efficiency of MPBR in terms of both treatment and biomass production. It is possible for microalgae to experience both morphological and physical changes due to excess or deficiency of the above-mentioned nutrients [7]. Recent studies regarding MPBRs for the purpose of microalgae cultivation have mainly focused on secondary effluent (either synthetic or real)[8,9]. In secondary effluent, the level of organic carbon is lower as opposed to primary effluent, which benefits MPBRs in terms of biomass production and removal efficiency of N and P. The low organic carbon level inhibits the excessive growth of bacteria and, therefore, enhances the algal concentration and accumulation[8]. Many studies have examined the feasibility of MPBRs for the treatment of real municipal wastewater [10-12] and other wastewater (e.g., commercial laundry wastewater [13], pulp and paper wastewater [14], and textile wastewater[15,16]). It should be noted that raw or real wastewater contains high concentrations of pollutants, like suspended solids, ammonia nitrogen and heavy colour, which can inhibit the growth or cause the death of microalgae through

photoinhibition and toxicity [17,18]. Therefore, there should be an appropriate pretreatment or a specific system design for the treatment of the above-mentioned wastewater with microalgae.

2.2.2 Microalgae species

In traditional microalgae cultivation, high biomass productivity is the main goal. However, when selecting microalgae species for nutrient recovery from wastewater, the composition of wastewater is generally very complex and variable, so their adaptability must also be considered. Of the many microalgae, *Chlorella vulgaris* (*C. vulgaris*) is the most commonly used microalgae for biomass production and wastewater treatment due to its high productivity and strong adaptability [19]. Znad et al. studied the removal of nutrients in various wastewaters, such as primary wastewater (PWW), secondary wastewater (SWW) and petroleum effluent (PE) in different volume ratios using *C. vulgaris.* It has been reported that even in oily wastewater, the nutrient in wastewater provided nutrients for the microalgae growth, reaching a concentration of 1.6 g / L of biomass in 13 days, which shows the adaptability of C. vulgaris in different media [20]. Besides *Chlorella vulgaris*, *Chlorella sp.*, *Chlorella emersonii*, *Chlorella sorokiniana*, *Scenedesmus quadricauda* and some other species have also been adopted for wastewater treatment due to some strength. For example, *Chlorella Species* have shown higher adaptability and survival than *Chlorella vulgaris* in the treatment of low-nutrient secondary wastewater [9].

2.2.3 Lighting

Microalgae use light as an energy source for photosynthesis. The sources of light can be artificial sources (e.g., LED and fluorescence) or natural sources, e.g., sunlight, which latter becomes less common because of its instability [21]. However, artificial lights are mostly used for lab-scale, indoor cultivations and MPBR systems. The factors associated with light in MPBRs are light intensity and wavelength and light-dark cycle that can affect microalgae growth.

Light intensity has a direct impact on biomass production and, subsequently, nutrient removal [22]. In general, the optimized light intensity can enhance the efficiency of nutrient and CO_2 uptake [23] and is microalgae species dependent [6]. Additionally, the light wavelength is another factor contributing to the performance of MPBRs. It directly affects the light utilization of microalgae and, henceforth, its growth and nutrient removal [24]. In the case of *C. vulgaris,* the studies have

indicated that red light (620–630 nm) leads to more productive cultivation [25] whereas blue light (475 nm) is more suitable in terms of nutrient uptake [24]. Overall, the agreed wavelength beneficial for microalgae growth is in the region of the red and the blue light [26]. In terms of the light-dark cycle, two parameters can be determined, which are optimizing energy cost and biomass production. A previous study examined the effectiveness of continuous light for microalgae growth where it was found applying a suitable light-dark cycle is more beneficial for biomass production than continuous light, and it also benefits MPBR in terms of energy saving [27].

2.2.4 CO_2

CO_2 is typically the carbon source for microalgae growth and is provided by aeration in MPBRs. This source is preferred by microalgae over other common sources of carbon, such as pure CO_2, flue gas and soluble carbonate [28-30]. The other important role of aeration in MPBRs is membrane fouling mitigation. However, there are studies that show a correlation between excessive aeration and compromised biomass growth and increased fouling [31,32]. The intense shear force induced by excessive aeration can damage the cells and cause cell lysis and, therefore, negatively impact membrane fouling. As such, proper aeration should be provided in MPBRs and is generally in the range of 0.15-8.0 L/min [6].

2.2.5 Hydraulic retention time (HRT) and Solid retention time (SRT)

Hydraulic retention time (HRT) and solid retention time (SRT) are the two main operational parameters that control MPBR performance. These parameters depend on factors such as wastewater characteristics, treatment targets, type of biological treatment and climatic conditions, and selecting a proper HRT and SRT correlate with the microalgae production and nutrient removal from wastewater [33]. The typical HRTs for MPBRs vary between 6 h to 5 d and are higher than open ponds or PBRs [34]. The longer HRT leads to higher nutrient removal from the wastewater [8]. On the other hand, the shorter HRT shortens the retention time during which the microalgae assimilate the nutrients from the reactor. To date, there are many studies that investigate the proper HRT in MPBRs for optimized microalgae growth and nutrient removal [35-37]. A recent study by Vu et al. (2022) using *C. vulgaris* and activated sludge showed that 5 days of HRT resulted in 30% higher nutrient removal compared to that of 3 days [38]. Another study

showed that while a shorter HRT did not affect the total nitrogen removal, the proper phosphorus removal was only achieved at a longer HRT (7 days) in a microalgal-based membrane bioreactor in treating synthetic wastewater(TN and TP of 1012 and 318 mg/L, respectively) [39]. However, it is well-accepted that the impact of HRT on biomass production should be considered along with other conditions, such as SRT[6].

Another operational parameter that significantly contributes to MPBR performance is solid retention time (SRT) which determines the ratio of food to the microorganism in the system. Previous studies have reported that the longer the SRT is, the more concentration of microalgae will be achieved[40,41]. Furthermore, there is research indicating that the lower SRT of 5 days has led to the highest biomass productivity (132 g m^{-3} d^{-1}) [8]. A recent study has shown that there was not a linear relationship between SRT and membrane fouling performance, and different SRT of 10, 20, and 30 days behaved differently [42]. This is because there are some interrelated factors to the membrane fouling, such as particle size, microalgae concentration and extracellular substances that are also affected by SRT[42]. Nutrient removal is another parameter of MPBR performance and is influenced by this operational parameter. Generally, the longer SRT results in more microalgae uptake of the nutrient. However, it is reported by some researchers that SRT can affect differently on phosphorus and nitrogen removal [43,44]. For example, prolonged SRT led to better phosphorus removal (28.38 ± 7.16%, 48.36 ± 5.91%, and 54.95 ± 4.36% for SRTs of 10, 20, and 30, respectively), while the nitrogen removal was reported lower at longer SRT(18.05 ± 9.96, 19.26 ± 4.58, and 14.60 ± 1.78 mg/L for SRTs of 10, 20 and 30 days, respectively)[44]. In summary, it is generally recommended that MPBRs operate at SRTs between 15 and 25 days [6].

2.3 Membrane fouling

2.3.1 Mechanisms of membrane fouling

The two main drawbacks that significantly hinder the membrane's performance are membrane fouling and concentration polarization [45]. The latter is considered to be the solute accumulation around the membrane surfaces, creating a boundary layer that decreases the effective driving force across the membrane surfaces [46]. However, membrane fouling is defined as the adsorption or chemical reaction of foulants with the membrane that causes agglomeration of flocs on the

membrane surface and even membrane pore blocking [45] followed by precipitation and cake formation [47]. During the last decades, considerable efforts and progress have been made to understand the mechanisms of membrane fouling and the effects of membrane materials, feed-biomass characteristics, hydrodynamic conditions, and operating conditions on membrane fouling [48]. It is well accepted that the mechanism of membrane fouling is a complicated matter. However, it has been considered to be a dependent parameter to the hydrodynamic conditions of the membrane systems and properties of the particles, as well as the membrane. In order to better understand membrane fouling, fouling has been categorized into different classifications based on the foulants' type or the attachment strength of the fouling materials to the membrane [48,49]. Although each categorization has its benefits, this study focuses on the foulants' type and further review and discuss the suitable electrokinetic process for studying the fouling of the membrane.

Membrane fouling can be classified into general groups of biofouling, organic fouling, and inorganic fouling based on the biological and chemical characteristics of membrane foulants [50]. The following sections are brief descriptions of the fouling types.

2.3.1.1 Biofouling (Biosolids)

Biofouling is considered as the deposition, growth, and, finally, accumulation of the sludge or microbial flocs, which further creates the biocake (gel) layer on the membrane's surface. The fact that microorganisms can grow, reproduce, and move across surfaces is a detrimental characteristic of biofouling [51]. Besides, organic matter, as the by-product of microorganisms, also causes fouling. Organic matter, which is soluble organic matter (SMP) and extracellular polymeric substances (EPS) are considered organic foulants in this paper because of their chemical properties. For this reason, it is out of the scope of this section.

In assessing biofouling, like any other phenomenon, studying the parameters affecting biofouling is of concern which will be mentioned in Table 2.1. There are a lot of studies conducted to evaluate the factors affecting biofouling, and significant ones are characterized below in terms of the membrane, solution, and microorganism characteristics [52].

Table 2-1 Factors affecting biofouling

Membrane characteristics	Solution characteristics	Microorganism characteristics
hydrophilic-hydrophobic properties of the membrane surface	suspended matter	charge
membrane surface charge	dissolved organic matter	nutrition status
membrane surface roughness	viscosity	hydrophobicity
chemical composition	pH	growth phase
surface tension	temperature	density
porosity	shear forces	the composition of the mixed population

Biofouling is widely accepted as fouling that is hard to be cleaned [53], and most biofouling preventions are done as a pretreatment. While the elimination of biofouling is mostly done by biocides (anti-microorganisms), one cannot guarantee the removal of microorganisms on the surface of the membrane. During the filtration process, these microorganisms can cause pore blocking and decrease the effective driving force across the membrane. Besides the declination of the flux, biofouling can also cause the membrane (especially cellulose acetate membranes) biodegradation [51]. Acidic by-products of the organisms can be gathered on the surface of the membrane, which can finally damage the surface. Although biodegradation is not fouling, it can cause a significant problem for the membrane that cannot be neglected.

Table 2.2 shows a summary of biofouling hindering methods. These methods include the use of electrokinetic phenomena, modification of process conditions, biological control, modification of membrane surface properties, the use of chemicals and oxidants, etc.

2.3.1.2 Organic fouling

Natural organic matter, algal, polysaccharides, proteins, and humic substances are all considered organic foulants. These foulants can be adsorbed and decomposed. Organic foulants are in the range of 0.001 to 0.1 μm and are smaller than microbial flocs and larger than biopolymers which can quickly deposit on the membrane's surfaces. Hence, colloidal fouling is considered a subgroup of organic fouling [54]. In light of this fact, nanofiltration, ultrafiltration, and microfiltration membranes are the common membranes studied for organic fouling.

Organic fouling depends on hydrophobicity, charge, and membrane materials. If both membrane and organic compounds are hydrophobic, the organics will be repulsed by the membrane [55]. From the charge characteristic, if both membrane and the organics have the same charge because of the electrostatic forces, the foulant will be repelled by the surface of the membrane [56]. However, the fouling happens when the hydrodynamic forces on the particles, namely permeation drag force caused by flow current through the membrane pore, exceeds the electrostatic force both between the colloids (organic foulant) and between colloids and the membrane surface [57]. As a result, particles are accumulated inside the pores or on the top of the membrane.

In terms of the material, most organic membranes (e.g., polymers) and inorganic membranes (e.g., ceramic) are amorphoteric, and both membrane types can show positive or negative surface charge [58]. As both pH and surface charge affect the fouling mechanisms, the consideration of the membrane type is essential in the scope of organic fouling. For further investigation of the factor involved in the organic foulant, Figure 2.1 summarizes the major parameters that have been considered for studying organic fouling.

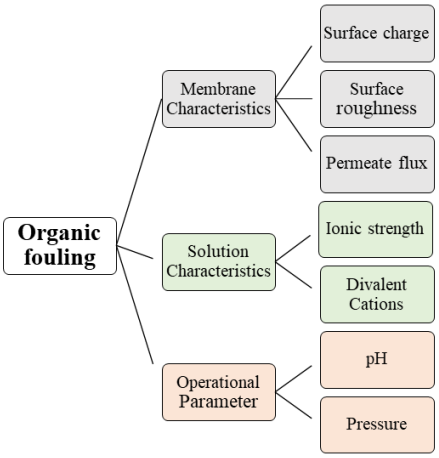

Figure 2-1 Factors affecting organic fouling

2.3.1.3 Inorganic fouling

Metals ions including Ca^{2+}, Mg^{2+}, Al^{3+}, $Fe^{2+/3+}$, heavy metals (i.e., lead, cadmium, nickel, arsenic, etc.), radionuclides (i.e., strontium and uranium), and anions (i.e., CO_3^{2-}, SO_4^{2-}, PO_4^{3-}, and OH^-) are some of the main inorganic foulants [58]. These ions, which exist in the influent, can cause chemical reactions and precipitate and foul the membrane pores. Most of the inorganic fouling, which is named mineral scale deposits [59], is treated before membrane filtration. Some of the inhibition techniques utilize chemical additives (antiscalants, acids, and nanofiltration). Green additives, such as polyaminoamide dendrimer (PAMAMs), are investigated for membrane inorganic fouling control [59]. The combination of inorganic and organic matter, which results in enhanced fouling effects, became an important area for fouling studies [60]. It is acknowledged that inorganic colloids can adsorb organic foulants, which are likely to have an impact on the fouling of the membrane [61]. Various factors have been criticized for inorganic fouling, including flow velocity, pressure, divalent cations concentrations, temperature, pH, ionic strength, and surface charge [62]. Since these factors have been studied before, this paper continues to focus on the role of the electrokinetic in membrane technology.

2.3.2 Methods to control membrane fouling

Due to the significance of membrane fouling phenomena in membrane separations, considerable efforts and progress have been made to understand the mechanisms of membrane fouling and to develop strategies for membrane fouling control [63]. Physical, chemical, and biological methods have been widely applied for membrane fouling control in water and wastewater treatment [64]. Although these methods are effective in membrane fouling control, they either have a high energy consumption (physical methods) or use chemicals (chemical methods) or expensive enzymes; thus, continuous efforts have been made in searching for new and more efficient methods for membrane fouling control [65]. The above-mentioned methods are briefly discussed below.

2.3.2.1 Physical methods

Physical methods include the use of aeration, sparging, and cross-flow velocity (CFV) to create shear forces on membrane surfaces to reduce membrane fouling [66]. Furthermore, back pulse washing has also been widely used for fouling control in hollow fibre membranes [67].

2.3.2.2 Chemical methods

Chemical methods involve the use of chemical cleaning agents to remove foulants from membrane surfaces and inside pores. Typical chemical cleaning agents include oxidants (e.g. sodium hypochlorite), bases (e.g. NaOH), inorganic and organic acids, and chelating agents (citric acid and EDTA) [65].

2.3.2.3 Biological Methods

In-situ fouling control might be preferred to ex-situ fouling mitigation techniques [68]. Biological method is the currently most-used in-situ method to control fouling. One of the biological methods method uses an enzyme to remove organic foulants which is called quorum quenching(QQ) [69]. Enzymatic disruption (ED) and energy uncoupling (EU) are the other two main biological approach that has shown great potential for effective biofouling control [70].

2.3.2.4 Electrokinetics in fouling mitigation

Recent studies have demonstrated the application of electric field to control membrane fouling [71,72]. This method employs electrochemical mechanisms such as electrocoagulation, electroosmosis, and electrophoresis which control fouling by degradation of pollutants and, at the same time, controlling the mobility, and deposition of particles onto the membrane surface [71,73].

2.4 Fundamentals of electrokinetic phenomena

To properly address the use of electrokinetics for membrane fouling control and performance enhancement, the fundamentals of electrokinetic phenomena will be outlined and briefly discussed with an emphasis on its applications in membrane technology.

Electrokinetics is the application of an electric field to a porous medium-water-electrolyte system. The phenomenon was first established by Reuss in 1809 [74]. The transport processes relevant to control fouling in membranes include electrophoresis (EP), dielectrophoresis (DEP), and electroosmosis (EO) (Figure 2.2).

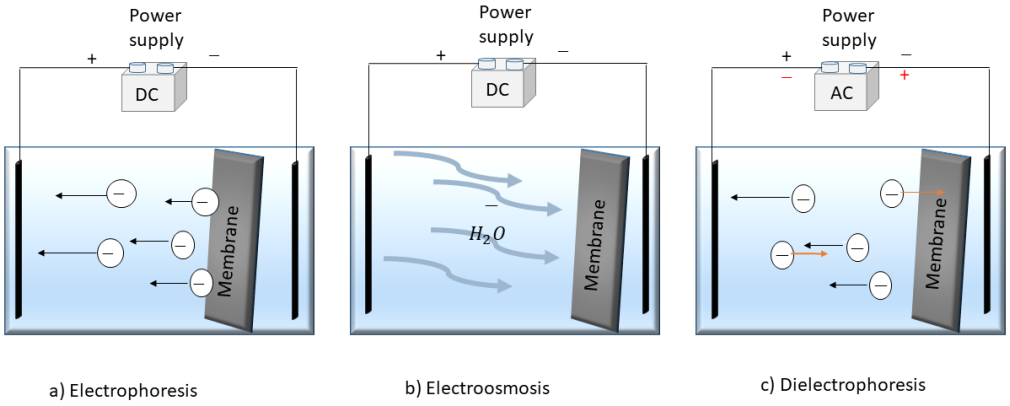

Figure 2-2 Electrokinetic movements, a) Electrophoresis (EP), b) Electroosmosis (EO), c) Dielectrophoresis (DEP) (modified from Ensano et al. 2016 [71])

Exerted by an electric field, charged particles and foulants can be repelled from the surface of the membrane. The use of an electric field instead of chemically assisted fouling control and cleaning processes makes the electrokinetic approach appealing because of environmental issues that can be associated with the use of chemicals. Additionally, applying an electric field is easy to operate and control [75,76]. With such benefits, electrokinetics has gained more interest as a fouling mitigation technique. To gain insight into this technique, electrokinetic phenomena related to the membrane processes are discussed in the following sections.

2.4.1 Electrokinetic Processes

Foulants have different charges and electrostatic characteristics [77]. Thus, foulants can be repelled or attracted to the surfaces of the membranes and the electrodes. The phenomena affiliated with electrokinetics from membrane separation perspectives (electrophoresis, dielectrophoresis, and electroosmosis) are discussed in the following sections, along with electrolysis reactions of water.

2.4.2 Electrophoresis (EP)

EP is the movement of charged particles or dispersed solids of colloidal size in solutions under the influence of a direct current (DC) electric field towards the electrode with the opposite charge.

2.4.3 Dielectrophoresis (DEP)

DEP is the movement of polarizable particles, with dimensions between 1 and 100 μm, in a non-uniform electric field towards the electrode [78]. DEP is independent of the direction of the electric field and, therefore, can be effective at both DC and AC (alternating current) potentials. When particles move due to the positive electric field gradient, it is considered a positive DEP, whereas a negative electric gradient creates a negative DEP [79]. It is worthwhile to note that this stimulus happens just when a spatial of the electric field intensity exists [80]. Furthermore, it only occurs when the electric field is more or about 10^6 Vm^{-1} which is very large but can be reached by micrometre electrode dimensions and spacing and applied potential of 1 to 10 V [80].

2.4.3 Electroosmosis (EO)

Apart from EP and DEP, EO is another electrokinetic effect that helps reduce membrane fouling as well. In contrast to EP, where charged particles move in the solution, EO is the movement of water through a solid porous media such as a membrane due to an applied DC electric field. In this process, water is moved from the anode (positively charged electrode) to the cathode (i.e. negatively charged electrode) if the membrane is negatively charged. EO has frequently been demonstrated as a possible mechanism for electric-enhanced filtration and can be used for the removal of both organic and inorganic contaminants [58]. For instance, EO flow was suggested to

occur on inorganic membrane surfaces using a 500 to 4500 V/m electric field gradient to intensify the microfiltration of synthetic activated sludge effluent [81]. Due to the forced movement of liquid through the membrane, EO can increase the permeation flux and can be used for fouling mitigation on membrane surfaces [81]. Table 2-2 shows a comparative summary of the electrokinetic phenomena mentioned above.

Table 2-2 Summary of the features and applications of the EO, EP, and DEP (modified from Amini et al. 2019 [82])

Processes	**EP**	**DEP**	**EO**
Major mechanism	Movement of the charged particles/ions	Movement of the charged particles/ions	Movement of the fluid
Stationary phase	Liquid	Liquid	Capillary
Disadvantages/ Advantages	-Needs to use corrosion resistance electrodes -Needs pH modification -The risk of short circuit -Possibility of production of toxic by product	- Joule heating generated by electric field effect particles movement and properties of the feed - Higher particle speed compared to EP	- Joule heating generated by electric field effect particles movement and properties of the feed
Applications	-Surface potential and streaming potential -Protein separation	-Gas Sensors and detection instruments -Separation of the minerals	-Drain porous media -Measuring surface charge of the porous media -Sludge dewatering
Power source	DC	AC	DC
Symbols	$v_{ep} = \frac{\varepsilon_m \xi}{\mu}(E)$	$F = 2\pi r^3 \varepsilon_o Re(K) \nabla E^2$	$q_{eo} = k_e E$
SI-units	$m\ s^{-1}$	N	$m\ s^{-1}$

v_{ep} electrophoresis induced velocity, ε_m permittivity of the medium solution, ξ zeta potential, μ dynamic viscosity of the solution, E electric field gradient, r radius of the sphere, ε_o permittivity of free space, $Re(K)$ Clasius Mossotti function, ∇ del operator, q_{eo} electroosmosis flow velocity, k_e coefficient of electroosmosis permeability.

2.4.5 Electrochemical reactions at the electrodes

It is often important to consider the electrochemical reactions caused by the electric field around the electrodes. Electrolysis reactions of water occur at the electrodes in an electrokinetic process. The reactions result in oxidation at the anode generating an acid front, and reduction at the cathode producing a base front as [83]:

The oxidation reaction at the anode:

$$2\,H_2O_{(l)} \rightarrow\ O_{2\,(g)} + 4\,H^+_{(aq)} +\ 4\,e^- \qquad E_0 = -1.229\ \text{V} \qquad (2.1)$$

and the reduction reaction at the cathode:

$$4\,H_2O_{(l)} +\ 4\,e^- \rightarrow\ 2\,H_{2\,(g)} + 4\,OH^-_{(aq)} \qquad E_0 = -0.828\ \text{V} \qquad (2.2)$$

Where, $O_{2(g)}$ is oxygen in the gaseous phase, $H^+_{(aq)}$is hydrogen in the aqueous phase, $H_{2\,(g)}$ is hydrogen in the gaseous phase, and $OH^-_{(aq)}$ is hydroxyl ion in the aqueous phase.

The metal terminals produce ions which react or combine with the ions in the solution. The mechanisms of the reactions of metals at the anode and in the solution are:

Anode:

$$M \rightarrow M^{m+} + m\,e^- \qquad (2.3)$$

In the solution:

$$M^{m+} + m\,H_2O \rightarrow M(OH)_m + m\,H^+ \qquad (2.4)$$

Where, M is metal, M^{m+} is a metal ion, and $M(OH)_m$ is metal hydroxides that react as coagulants. The $M(OH)_m$ have been investigated as a neutralizer of the electrostatic charge of the foulants.

2.5 Application of electrokinetics in membrane technology

Among the versatile applications of the electrokinetic transport phenomena, from the fossil-fired power plant to biomaterials, membrane fouling control piques a lot of interest [58]. Under the influence of an electric field, the charged particles, liquid or both of them, can be subjected to movement. The schematic diagram of the movement of the charged particles in the presence of an electric field is shown in Figure 2.3. Examples of the selected applications will be presented as the fouling monitoring, fouling measuring, and fouling mitigation techniques that are reviewed in this paper.

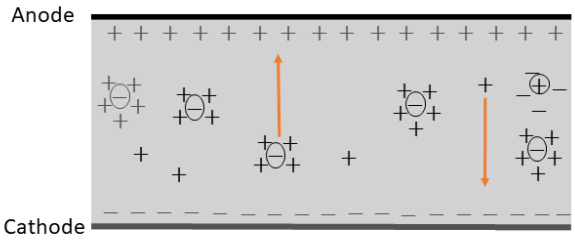

Figure 2-3 The schematic of charged particles' movement in the presence of an electric field

2.5.1 Electrokinetic application in membrane fouling mitigation

This section discusses how electrokinetic properties and phenomena help fouling mitigation and control. The study of electrokinetics can be further subdivided into the parameters affecting different fouling types.

2.5.1.1 Electrokinetic approach for organic fouling control

One of the electrokinetic phenomena which have been employed for fouling abatement of the colloidal size particles is DEP [84]. In most ultrafiltration and microfiltration processes, the colloidal particles in the solute will deposit on the membrane surface. By using an alternating electric field, the colloidal particles can have positive or negative dipole differences relative to the dielectric of the solution. This diversity of the dielectric constant is referred to as positive and negative DEP (attractive and repulsive DEP, respectively) [80]. Among positive and negative DEP, negative DEP is more desirable because it repels colloids from the membrane surface. The effect and the range of the dielectrophoretic forces are more than that of the electric double layer, and its magnitude can be felt by the particles from micrometres distance from the electrode surface [80]. The schematic diagram of colloid particles in different DEP configurations is shown in Figure 2-4.

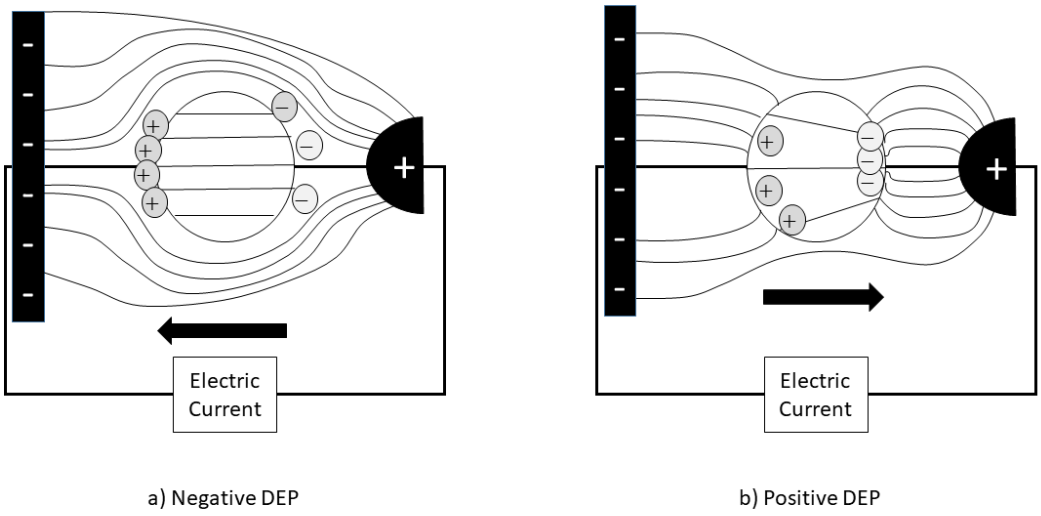

Figure 2-4 Two different dielectrophoretic movements a) negative DEP b) positive DEP modified from [85]

Molla and Bhattacharjee [84] investigated DEP created by parallel electrode array and its role on the colloidal fouling of the membrane, followed by modelling the colloidal fouling behaviour. A further study was conducted to examine the effect of the electrode configuration and the voltage on the influence of the DEP on the fouling mitigation of the microfiltration membrane [86]. Hawari et al. (2017) evaluated the space between electrodes and the voltage input on the anti-fouling behaviour on a submerged membrane bioreactor (SMBR). They observed that using DEP doubled the permeate flux and hindered fouling [87]. It should be noted that increasing the electric field will cause greater DEP, and the fouling will be minimized more.

The use of the direct electric field in minimizing membrane fouling is intensified during the last decade [88,89]. The main electrokinetic processes triggered with DC electric field are EO and EP. The applications of EP in minimizing organic fouling largely appear in the conductive membrane era (See Table 2.4). Before the presence of conductive membranes, the membrane should be put between the electrodes that hindered the effective electric field caused by electrodes [90]. In order to overcome this drawback, researchers used a high voltage, which increased the operating cost

[88]. A further way to tackle this issue is using a conductive membrane within which the membrane usually acts as a cathode. The schematic diagram of this process is shown in Figure 2.5.

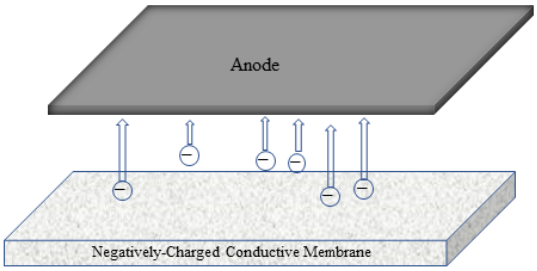

Figure 2.5 The particle movement at the presence of the conductive membrane

The conductive membrane can repel organic compounds by an electrophoretic movement that needs low energy and a conductive surface. Furthermore, the membrane can be easily cleaned and decreased fouling [91]. Tailoring conductive membranes has mainly three different approaches; using conductive polymers [92] and coating or adding conductive materials on the membrane's surface [93]. Table 2-3 summarizes relevant studies of conductive membranes for fouling control.

Table 2-3 Conductive membrane for fouling mitigation

Material	**Type of the membrane**	**Type of fouling**	**Year of the study**	**Ref.**
CNT-PVDF	UF	Organic fouling	2014	[94]
Composite of stainless steel with PVDF membrane	MF in MBR	Organic fouling, inorganic fouling and biofouling	2015	[95]
Conductive membrane modified with PPy	-	Organic fouling, inorganic fouling and biofouling	2013	[96]
Conductive membrane (GO/MWCNTs)	NF	palm oil mill effluent (POME)	2018	[97]
RGO/PVDF coated carbon cloth	-	oil field waste water	2016	[98]
The carbon paper-based FO TFC	FO	Bio and organic fouling	2016	[99]

Studying fouling reduction using a conductive membrane was investigated by Salehi and Madaeni [100]. The results showed that higher protein adsorption was achieved with a nonconductive membrane in comparison to a conductive membrane. It is suggested that the electrostatic field on the surface of the conductive membrane acts as a barrier against the negatively charged BSA, which is attributed to the lower membrane fouling.

The use of CNT for conducting membranes and its role in organic fouling mitigation have been studied by various researchers [3,90]. They concluded that organic fouling was successfully decreased by the electrostatic force and electrophoresis movement of organic matter. Another study contributed by Zhang and Vecitis [94] examined a different configuration and electrode type for electrophoresis movement. They used a cathode made by a conducting CNT-polyvinylidene fluoride (PVDF) mesh over the Polyethersulphone membrane. The carbon cloth phenolic (CCP) was chosen as an anode. They observed that the best order for organic fouling reduction is that the solution first moves through the porous anode, then through the conductive cathode, followed by the UF membrane.

Modification of the membrane surface for enhancing commercial UF membrane surface charge and wettability has been studied [101]. Among the existing techniques, electrophoresis-UV grafting is of great interest due to its simplicity, low cost, and versatile application [102]. Wei et al. [102] reported that electrophoresis-UV grafting exhibited fewer NOM fouling due to better surface charge compared with the unmodified membrane.

The combination of the electrokinetic with the submerged anaerobic membrane bioreactor (SAnMBR) has shown a lot of interest in fouling reduction research. Using an active anode (i.e., Al) and DC electric field exhibited remarkable fouling reduction caused by EPS (Extracellular Polymeric Substances) [103]. Since the EPS is a negatively charged particle, it can be destabilized by the anodes cations released by the oxidation of anode (Al^{3+}) [104]. These particles can be moved by electrophoretic motion toward the anode and thus neutralize the negative charge, which can further result in lower organic fouling [105].

2.5.1.2 Factor affecting electrokinetic approach for organic fouling control

pH: pH value is important for organic materials as their properties are often dependent on the pH. Some organic matter, such as BSA, exhibits different surface charges based on their amorphic structures. They can be positively or negatively charged in acidic media (at pH < 4.4, BSA is positively charged while it is negatively charged at pH > 4.4) [106]. Because of the correlation of pH with the surface charge, determining this parameter is worthy of consideration. Furthermore, pH has a dominant effect on the behaviours of organic foulants such as humic acids. The humic acids show different configurations based on the pH due to inter-chain electrostatic repulsion [62]. At some range of pH, the smaller macromolecule configuration of humic acids has been reported [107].

Electrode surface area and charge: As the surface charge of the organic matter and the electrodes influence the created electrostatic force, adhesion, and fouling, careful attention must be exerted on this parameter. The study for BSA adsorption on the gold electrode (positive charge) showed that the rate and the amount of protein adsorption are generally depending on the polarity and magnitude of the applied potential of the electrode. The more adhesion occurs, the more surface area of the electrode that will be occupied by foulants and therefore, the efficiency of the electrodes and applied electric field will be decreased.

Foulant chemical structure: The foulant chemical structure can show different adhesion parameters on the surface of the electrodes. Electrochemical reactions around the electrode will produce radiant. The radiance with the functional group in d-orbitals is strongly adsorptive [108]. The study of the chemical properties of the colloidal particles will help understand the fouling behaviour and needs to be further investigated.

Current density: The increment in current density causes an increase in the driving force of the filtration process, as reported by Lindstrand et al. [109]. Since the flux has been increased due to a higher driving force, the fouling rate for organic fouling was faster when the applied current was higher. The other study also reported that the organic fouling of the anion exchange membrane is directly affected by the current density. The increase in the current density showed more fouling

compared to the lower current due to higher transportation of the sodium dodecylbenzene-sulphonate (DBS) through the membrane [109].

2.5.1.3 Electrokinetic approach for inorganic fouling control

Dissolved heavy metals in the fluid can be removed from the membrane surface by applying an electric field. A study on the hardness removal of the seawater (Ca^{2+}, Mg^{2+}, So_4^{2-}) by electrokinetic pretreatment showed that electrocoagulation, EP along with EO could remove 13% to 91% of inorganic ions from seawater using different electrode configurations and electric current [75], although the foulant distribution mechanisms were not studied. Other studies revealed that the EP force and the use of stainless steel cathode in SMBR could successfully abate the inorganic fouling on the surface of the membrane and electrodes [110].

2.5.1.4 Factor affecting electrokinetic approach for inorganic fouling

pH: The investigation of pH on the inorganic fouling has been considered as a parameter that is one of the main characteristics of the solution. Sulphate is an inorganic foulant that is in wastewater effluent and is the factor that is considered for the quality of the filtered solution. The study conducted to evaluate the relationship between pH and sulphate removal revealed that the best sulphate removal in the bioelectrochemical system (BES) can be achieved at the pH range between 4.5 to 8.5 [111]. Nevertheless, most of the sulphate pollutants exist in acidic wastewater with a pH of around 3-4. In order to adjust the pH level, basic additives such as sodium hydroxide are added to the solution. Furthermore, the total hardness removal efficiency by different pH levels has been studied by Malakootian and Yousefi [112]. They found that within the pH range of 5.3 to 10.1, the total hardness removal increased with the pH. Nevertheless, the evaluation of the pH in the presence of the membrane is not studied.

Current density: One more factor that has a profound impact on inorganic fouling is the current density. Murugananthan et al. [113] found the removal of the sulphur ion (S^{2-}) directly depended on the current density. Even though the sulphite (SO_3^{2-}) and sulphate (SO_4^{2-}) ion removal was low, another study by Saiba et al. [114] indicates that the removal of the inorganic foulants increases with the current density. Moreover, Abdulkarem et al. [75] investigated the effect of the current

density on the removal of the foulant, such as SO_4^{2-}, Mg^{2+}, and Ca^{2+} using the electrodes made of aluminum and stainless steel as the anode and cathode, respectively. Three different configurations of electrodes with different current densities have been studied. They found that the current density increased the formation of the $Ca(OH)_2$, $CaCO_3$, $Mg(OH)_2$, and $MgCO_3$ concentrations. Yet, the relationship between the current density and the membrane fouling was not examined.

Electrode materials: Considerable studies have been conducted to investigate the inorganic removal efficiency associated with the electrode materials. Three titanium, iron, and aluminum metals were studied to evaluate the effect of the anode materials on S^{2-} removal efficiency [113]. According to the study, unlike stable electrodes such as titanium, soluble anodes such as Al and Fe showed a decent potential for the removal of sulphur species, although more studies are needed in this area.

2.5.1.5 Electrokinetic approach for biofouling control

Within the scope of biofouling, studies are mainly in two parts that are the inactivation of biomaterial (bio-inactivity) and anti-adhesive surfaces for bio-fouling approaches. As many bacteria have a negative charge, it is widely accepted that negatively charged membranes have fewer bio-adhesion properties. The electrostatic force will repel negatively charged biomaterials from the membrane surface, although this force should be strong enough to be able to move them far from the surface. Otherwise, they will stick on the surface, and biofouling will start. In doing so, the electric current will strengthen the electrostatic force. This movement of the charged particles in the relatively stationary fluid, called EP, as previously discussed, can enhance the anti-adhesive characteristic of the membrane. On the other hand, the biofoulants attached to the positively charged surface could not grow very well [115]. The strong electrostatic force between the positively charged surface and negatively charged bacteria impedes the division and reproduction of the bacteria [116]. Hence, the effect of the electrokinetic stimuli on the biofouling control, which can either reduce adsorption or inhibit microbial metabolisms, is established [117]. The electrokinetic-assisted antibacterial processes have been studied from different perspectives, including damaging cell membranes, biocides and antibacterial agents introduced by an electric

field (such as hydrogen peroxide), and interference of metal ions with the physiology of microbes[118,119]. In this study, we will discuss it as an electro-assisted antibacterial. There are many other studies that revealed that in the Membrane bioreactors (MBRs), the high DC (more than 1.4 Vcm^{-1}) would affect the microorganisms (which includes bacteria). It is well accepted that the desired DC voltage potential range for aerobic microorganisms is between 0.28 and 1.14 Vcm^{-1} [120]. Because of that, many electrokinetic MBRs operate at this range. One can look at this issue from a different view. In other words, outside the scope of MBRs, an electric field can be applied as an antibacterial agent. So, it can help the inactivation of the biomaterials followed by less biofouling. The electric current will usually be applied by electrodes in the membrane filtration. The mechanisms that cause the antibacterial property of the electro-assisted membrane filtration are mainly due to chemical reactions that happen around and on the surface of the electrodes. These chemical reactions and inactivation phenomena have been categorized into two main possible explanations; direct inactivation by the electrodes surfaces and indirect inactivation by electrochemical production of active chemicals ($Cl^{\cdot}$ or $HO^{\cdot}$) [121]. In a cathodic current, the production of $HO^{\cdot}$ and $HO_2^{\cdot}$ can cause bacterial inactivation. While in anodic current, there are two main processes that can happen; 1- Direct inactivation by electrode surface, 2- indirect inactivation by electrochemical production of $Cl^{\cdot}$ and $HO^{\cdot}$. Between those two ways, anodic oxidation has been investigated more. Cathode surface has a negative charge and can reduce organic and bacterial adhesion followed by reducing fouling which has been studied less than anodic inactivation. The influence of the anodic and cathodic current on bacterial adhesion without any applied membrane is studied [122]. It is observed that bacterial inactivation in the anodic current was much more than that of the cathodic current. However, the other study done by Kim et al. [123] showed that in the case of membrane existence, the electrophoretic movement caused by conductive membranes could reduce the biofouling on the surface of the membrane. Perez-Roa et al. [124] applied small electric pulses (0.5-5 V) to prevent biofilm formation. They found that the biofouling was reduced by 50% at the applied 5 V at 200Hz. It should be noted that the role of more bacterial activity on the membrane surface should be further investigated. CNT-based membranes are other types of conductive membranes that have been studied in recent years[90]**.**

Anti-organic fouling properties of CNT-based conductive membranes are discussed in previous sections. Here, we will focus on their biofouling mitigation abilities which mainly rely on their

antimicrobial properties [125]. Some studies investigated the antimicrobial property of both single-walled and multi-walled CNTs (SWCNTs and MWCNTs, respectively). The studies identified that the size of the CNTs is a key parameter which mostly affects the antibacterial property of the CNT. Based on their study, SWCNTs cause less bacterial activity [126]. Fan et al. [127] addressed the effect of electromigration on the biofouling of the electropolarized CNTs/ceramic membrane. They found that the adhesion between the bacteria and the membrane surface was weakened by the movement of bacteria driven from electrophoretic and electroosmotic mobility under both cathodic and anodic polarization. Besides, the permeate flux obtained by electropolarization was 8.1 times larger than that without electropolarization for biofoulant-containing feed water. Also, microbubbles which may be created on the electrode surface can physically reduce fouling on the electrode surface [128]. These microbubbles are produced by the electrochemical reactions around the electrodes. Water will be split into hydrogen and oxygen gasses around the electrodes (O_2 gas at the anode and H_2 gas at the cathode) as a result of electric current and hydrolysis. These gasses in the form of bubbles not only decrease the surface area where foulants can settle but also can sweep them away from the membrane surface.

As the initial stage of biofouling is the adsorption of biofoulants on the membrane surface, the electrostatic force caused by a surface charge of the membrane is one of the crucial parameters related to the biofouling [53], although further investigation and monitoring of the average surface charge are suggested.

Another method that exploits electrokinetic forces for biofouling mitigation was investigated by Huang et al. [129]. They used a combination of DEP and electrowetting-on-dielectric (EWOD) techniques to abate biofoulants sedimentation. Manipulation bio-fluid (or bioparticles) by wrapping them with other substances (such as silicone oil), which is EWOD, simultaneously using dielectric coated electrodes showed fewer BSA adsorbed on the surface. As electrowetting has attracted more interest in recent years, more research has been done on its application in fouling control [130]. Geng and Cho [131] examined a slippery liquid infused porous surface integrated with EWOD and DEP without a membrane, leading to moved bio-fouled protein from the membrane surface.

2.5.1.6 Factor affecting electrokinetic approach for biofouling control

Electrode surface area and charge: The attachment of biofoulants on the surface of the electrode is of main concern to scientists researching electrokinetic-assisted biofouling inhibitions. Bacterial adhesion on the electrodes' surfaces causes a reduction of the performance of the electrode due to both decreasing the surface of the electrode and increasing the required electric cost [132]. Hence, the mechanisms of biofilm creation and development on the surface of the electrode should be well addressed and investigated.

The surface charge of the foulant: The surface charge which is related to surface energy must be investigated in the fouling behaviour studies. Many studies have shown the significant influence of the surface charge and energy on the adsorption and adhesion of biofouling organisms. Gatley-Montross et al. [133] addressed the surface charge effect on the attachment pattern of five biofouling organisms. They observed that adhesion is a multivariate parameter that depends on the types of microorganisms, the chemistry of the surface, a dispersive component of surface energy, etc. They found that the diversity that existed between the studies for biofouling behaviour of the same foulant reveals the importance of the chemical property of the surface, which should be further studied.

Table 2-4 shows a summary of the factors affecting the electrokinetic approach for each type of fouling. The table suggests that factors studied for each type of fouling are limited, and this gap can be covered by further studies on the role of electrokinetics in fouling mitigation and membrane performance.

Table 2-4 Factors affecting electrokinetic approach

Organic fouling	Inorganic fouling	Biofouling
pH	pH	Electrode surface area and charge
Electrode surface area and charge	Current density	The surface charge of the foulant
Foulant chemical structure	Electrode materials	-
Current density	-	-

2.5.2 The application of electrokinetic technology for performance enhancement in membrane processes

In addition to membrane fouling mitigation and control, electrokinetic technology has also been used for process efficiency enhancements in various membrane processes. The enhanced membrane technology helped attain a higher microalgae production, dewatering potential, rejection, better nutrient and chemical oxygen demand (COD) removal, and improved flux and coagulation continuously.

2.5.2.1 Enhanced microalgae growth and harvesting

Electro technologies have been effective in microalgae production enhancement as well as downstream processing of microalgae, such as the dewatering of microalgae. It has been reported that a high voltage gradient (2. 7 kV/cm) could improve *C. vulgaris* by 51 % in 50 min of treatment [134]. Another study has shown the effectiveness of an applied electric field of (voltage: 25 V) in increasing the biomass yield of Haematococcus pluvialis [135]. The improvement of the harvesting potential of microalgae using an electric field has also been investigated and reported in the literature [136,137]. Electrochemical harvesting is an approach based on the movement of charged particles [138]. By applying an electric field, the charged microalgae will flocculate and float in the suspension by the produced electrochemical gas and move toward the electrode with the opposite charge [137]. This technique can be a substitute for chemical flocculants in the harvesting stage of microalgae production [139].

2.5.2.2 Enhanced chemical oxygen demand (COD) and nutrients removal in MBRs

Alshawabkeh et al. [140] studied the effect of a DC electric field on the COD removal of the aerobic-activated sludge. Based on the investigations, the COD removal by the applied field depends on the field level and the exposure time. They found that the DC fields of 0.28 to 1.14 V/cm enhanced COD removal, while lower and higher exposure had a negative impact on COD removal efficiency. Bani-Melhem and Elektorowicz [73] reported that the COD removal rate increased from 75-90% to 85-95% by applying the intermittent DC field of 1 to 6 V/cm (15 min ON/45 min OFF) using iron electrodes. Tafti et al. [141] suggested that at a low current density,

the biomass could highly oxidize the organic materials resulting in a high COD removal efficiency. This oxidation of the organic contaminants is on account of the electrokinetic phenomena due to electric current. However, higher current densities, which can ultimately cause either a strong electrical pulse or a high concentration of ions, may be attributed to the adverse COD removal efficiency [119]. Hosseinzadeh et al. [142] conducted research by designing a hybrid electro membrane bioreactor (HEMBR). They argued that compared to the conventional MBR, the COD removal of HEMBR was increased from 80 % to 85 %.

Nitrogen and phosphorous are usually considered nutrients in the bioreactors. Nutrients in the forms of $N-NH_4^+$, $N-NO_3$, $N-NH_3$, and PO_4-P can be found in the wastewater. These compounds are assessed in the processes to evaluate treatment performance. The applied electric field from the electrochemical processes results in better nutrient removal [143]. The reduction and oxidation around the electrodes result in denitrification and electrocoagulation, which are the determining reasons for improved removal. To put more detail on it, the reduction of the $N-NO_3$ to nitrogen gas is a favourable phenomenon in the presence of electrodes. Incorporating the hydrogen gas generated around the cathode motivates the denitrification process according to the following reactions [144]:

At the cathode: $$3\,H_2O\ + 3\,e^- \rightarrow \frac{3}{2}\,H_{2(g)} + 3\,OH^-_{(aq)} \qquad (2.5)$$

Reduction of NO_3-N: $$NO_3{}^- + 2.5\,H_2 \rightarrow 0.5N_2 + 2H_2O + OH^- \qquad (2.6)$$

The phosphorous removal contributed by the electric field is explained by the oxidation and reduction reactions around the electrodes [145]. The proposed reaction for electrocoagulation, with the aluminum anode as an example, is explained by the following reaction [73]:

In the solution:

$$Al^{3+}{}_{(aq)} + PO_{4\,(aq)}^{3-} \rightarrow AlPO_{4(s)} \qquad (2.7)$$

Thus, with applying an electric field, the phosphorous compound will precipitate as a solid form, that is a leading cause for enhanced P removal of EMBRs compared to MBRs.

Borea et al. [143] reported that higher removal efficiency of 96.06 % and 69.34 %, respectively, for orthophosphate (PO_4-P) and ammonia nitrogen (NH_4-N) was achieved with an applied field

of 1 and 3 V/cm, as compared to the conventional MBR. As reported by Khalid Bani-Melhem and Maria Elektorowicz, the intermittent DC electric field resulted in 98% $PO_4 - P$ removal, which is higher than conventional MBRs [73]. Zhang et al. [146] conducted a study of a controlled MBR via EMBR with the titanium anode (Ti-MBR) and stainless steel anode (Fe-MBR). Based on their report, the $NH_4 - N$ removal of the conventional MBR(88.9%) was higher than that of the EMBRs (81.9% for Fe-MBR and 52.4% for Ti-MBR). It should be noted that this reduction in nutrient removal is attributed to the effect of the direct current on the nitrifying bacteria or process [147].

2.5.2.3 Enhanced coagulation and sedimentation

Despite the chemical method and microorganisms for coagulation of the pollutant, electrical-assisted sedimentation and coagulation arise as a favourable substitute for the conventional method. According to Mollah et al. [148], electrocoagulation is favourable for controlled and rapid reactions and small systems due to the economic and environmental benefits. It is often argued that chemical additives have some consequences, such as the production of undesirable by-products or an increase in the sludge amount in the reactor [142], while, as mentioned earlier, the ions released around the electrodes can combine with the ions in the solution and produce coagulant. This process, electrocoagulation, along with the other advantages of using an electric field, brought about further studies on the electrocoagulation process to be applied either in situ or ex-situ as a pretreatment of feed for membrane processes. Electrocoagulation as a pretreatment was introduced as a fouling prevention technique. The high concentration of some solutes causes scaling and fouling that can gradually inhibit the performance of the membrane. In doing so, electrocoagulation has been proposed prior to the filtration process in some research. Den et al. [149] conducted a study of an electrocoagulation unit for silica removal as a pretreatment. They argued that with an initially high concentration of silica, the electrocoagulation enhanced the silica removal by 80%. A study conducted by Vasudevan et al. [150] showed that electrocoagulation could remove phosphate from drinking water by 98%.

In-situ electrocoagulation, a combination of membrane process with electrocoagulation, admittedly holds certain advantages. Prevention of the movement of the ions toward the membrane, which can gradually cause membrane fouling, is one of the main advantages. Mavrov

et al. [151] added an electrode to a flat sheet membrane for selenium removal. They could reach up to 98% of removal in the first 20 min of the operation. The application of electrocoagulation in MBR can also be cited. Designing electro bioreactors that could successfully combine electrocoagulation with MBR was first conducted by [152]. Having identified the undesirable fouling issues of MBRs, electrically-assisted membrane bioreactors (EMBRs) gain significant development. It is noteworthy to mention that the applications of the EMBRs include organic compound removal [153], oily wastewater treatment [154] and the removal of heavy metals [155]. This process showed enhanced membrane flux and removal efficiency, which will be discussed in the following sections.

2.5.2.4 Improved membrane flux

Besides enhancing fouling mitigation by electrokinetics, the permeation through the membrane can be improved by the aeration caused by the electric field and electroosmosis (EO) [156]. The backwashing caused by the hydrogen evolution reaction provides the mechanical force for moving particles from the surface of the membrane and is considered self-cleaning in some papers [157]. Lalia et al. [158] examined the role of conductive carbon nanostructures in PVDF membranes. Based on their report, the flux recovery caused by the formation of micro-bubbles on the surface of the conductive membrane provides a fast and consequent cycle of cleaning followed by inhibition of flux decline during the filtration period.

The permeate enhancement by electroosmosis has been investigated for many years. Electroosmosis helps the permeation by enhancing the boundary layer and mass transfer, although a comprehensive understanding of this mechanism is not reported yet. Despite this fact, the computational fluid dynamics (CFD) modelling of electroosmosis flux enhancement showed that the split velocity (caused by osmotic flow) has a major effect on the friction factor of the membrane, concentration polarization, and mass transfer [159].

Bayar et al. [160] found that the use of EO and EP technology significantly increased membrane flux in an SMBR. In their study, they used continuous DC with a voltage range of 30-50 V for 140 min. Two to four-fold increases in the membrane were achieved in the presence of an electric field, as compared to MBR without an electric field. This could attribute to the role of EO and EP.

Although EO showed a lower impact on the flux enhancement compared to EP, the magnitude of EO changed during the filtration. At a higher voltage (i.e. 50 V), the dominant phenomenon for improved flux was determined as an electrophoresis movement, while at a lower voltage, the electroosmosis had a greater impact on flux enhancement. They also observed that, in the presence of the cake layer and TMP, the electroosmosis flow increased due to the accumulation of negatively charged foulant (such as SMP and colloids) in the pore and on the surface of the membrane. The summary of the electrically assisted flux enhancement is shown in Table 2-5.

Table 2-5 Electrically assisted flux enhancement

Methods	Mechanism of flux enhancement	Ref.
Aeration	Turbulence caused by hydrogen microbubble produced within conductive membranes	[161]
Backwashing	Extrusion of the gases from the pores of the conductive membranes	[157]
Boundary layer and mass transfer	Reducing the friction factor and boundary layer thickness caused by electroosmosis movement	[159,162]

2.5.2.5 Enhanced rejections in membrane separations

The selectivity of the membrane for the solutes and the rejection ability is undoubtedly one of the main factors determining membranes' performance. Among all types of membranes, UF and MF membranes have received much more attention since they are less expensive and energy-intensive [163,164]. Yet, the trade-off between permeability and selectivity of both UF and MF membranes has yet to be developed. The application of conductive membranes, which utilize electrostatic repulsion, is one of the most recent advances in this research field. Zhang et al. [165] studied the dye rejection ability of the conductive polyvinylidene fluoride (PVDF) using an electric field voltage of 20 V. Increasing voltage from 0 to 20 V enhanced Congo red (CR) rejection (97.93%) ability which is attributed to the enhanced electrostatic repel force. As reported by Yu et al. [161], CR rejection (100%) of conductive polyvinylidene fluoride (PVDF)-Ni membrane was obtained by the electric field of 10 mA. Such rejection is attributed to the positive effects of the electrostatic forces and aeration extrusion. Maintaining a high water flux and high rejection value of conductive membranes showed great potential for overcoming the inhibitory trade-off that exists in membrane technology.

Liu et al. [166] argued that hydrophilic poly (1,5-diaminoanthraquinone) /reduced graphene oxide (PDAAQ/rGO) nanohybrid blended polyvinylidene fluoride (PVDF) membrane with an external electric field of 1.0 V cm^{-1} exhibited increased BSA rejection.

2.6 Industrial applications

2.6.1 Lab-scale industrial effluents and solutions treatment

As membrane technology has been regularly used in waste treatment operations, developing the existing techniques in order to increase the efficiency and efficacy of the membrane process has a major environmental and economic impact. This large impact is caused by the high volume and investment cost of industrial membrane separation facilities [89]. Many industries are looking for means to decrease the footprints of conventional treatment processes. To overcome fouling issues accompanied by membranes, especially when treating large amounts of charged particles that exist in industrial wastes and solutions, the use of electric fields and repulsions have been considered as possible ways of fouling control. This Ek-assisted method has been summarized in Table 2-6.

Table 2-6 Lab-scale separation processes for industrial effluent applications

The Feed	Type of the membrane	Electrical field strength	Research highlights	Additional operating cost due to electricity/energy demand	Ref.
Real Wastewater Sample from an Electronics/ Optoelectronics Fabrication Plant Wastewater	Ceramic microfiltration membrane	DC, 58 V/cm	Increased Perfluorinated compounds and DOC removal	0.171-1.54/m3 USD	[167]
Chemical Industrial Tailwater	Microfiltration membrane	DC, 25 V, 50 V,75 V and 100 V	Increased rejection of humic substances and decreased fouling	-	[168]
Industrial Enzyme Solutions	Ultrafiltration membrane	DC, 0-70 V	3-7 times flux increase by increasing the applied voltage	-	[88]
Textile Wastewater	Membrane bioreactor	DC, 0-12 V	Lower fouling, Better mixed liquor filterability	-	[169]

Coal Chemical Industry	Membrane bioreactor	DC, 1.33 mA/cm^2	Reduction of SMP and SRF, Increased floc size	0.036 kWh/m^3	[170]
Domestic Wastewater	Membrane bioreactor	DC, 12 V	13% reduction of membrane fouling and improved COD removal	-	[171]

Beside the lab-scale experiments listed in Table 2.7, a pilot plant with electrokinetic integration with the existing plant has been reported by Hosseinzadeh et al. [142]. Reportedly, they were pioneers in applying the electric field in the continuous treatment of municipal wastewater. The integrated electrocoagulation with flat sheet membrane bioreactor improved biomass characteristics and decreased membrane fouling. Although the cost associated with applied power was not evaluated, further investigation on cost analyses has been proposed.

Some studies used electrocoagulation as a pretreatment for the membrane bioreactor process on a large scale. Kim et al. [172] reported a pilot-scale MBR integrated with electrocoagulation for phosphorous removal. This pilot plant treats municipal wastewater with a capacity of 50 m^3/day located in Guri, South Korea. With the applied voltage of 1.38-1.99 V, the total phosphorous removal improved by 100% (two-times) compared to the MBR. Another pilot-scale study reported that applied voltage gradient to the existing municipal wastewater treatment plant in the City of l'Assomption, Quebec showed reduced membrane fouling and stable TMP [110].

2.6.2 Industrial scale

Based on the available literature, there is no study that reported the industrial-scale application of EK-assisted membrane technologies. A close and large perspective for the scalability of these technologies depends on their cost and energy demand evaluations that are not reported in the literature. The cost correlated with the electrode materials, energy cost, and probable design adjustment costs are those that should be considered in the scale-up of EK-assisted technologies. The feasibility of the industrial application of electrokinetic phenomena in an industrial-scale application is the gap that is highlighted for further research.

2.7 References

1. Liao, Y.; Bokhary, A.; Maleki, E.; Liao, B. A review of membrane fouling and its control in algal-related membrane processes. *Bioresource technology* **2018**, *264*, 343-358.
2. Tijing, L.D.; Woo, Y.C.; Choi, J.-S.; Lee, S.; Kim, S.-H.; Shon, H.K. Fouling and its control in membrane distillation—A review. *Journal of membrane science* **2015**, *475*, 215-244.
3. Ahmed, F.; Lalia, B.S.; Kochkodan, V.; Hilal, N.; Hashaikeh, R. Electrically conductive polymeric membranes for fouling prevention and detection: A review. *Desalination* **2016**, *391*, 1-15.
4. Sohn, W.; Guo, W.; Ngo, H.H.; Deng, L.; Cheng, D.; Zhang, X. A review on membrane fouling control in anaerobic membrane bioreactors by adding performance enhancers. *Journal of water process engineering* **2021**, *40*, 101867.
5. Antony, A.; Low, J.H.; Gray, S.; Childress, A.E.; Le-Clech, P.; Leslie, G. Scale formation and control in high pressure membrane water treatment systems: A review. *Journal of membrane science* **2011**, *383*, 1-16.
6. Luo, Y.; Le-Clech, P.; Henderson, R.K. Simultaneous microalgae cultivation and wastewater treatment in submerged membrane photobioreactors: a review. *Algal research* **2017**, *24*, 425-437.
7. Mercer, P.; Armenta, R.E. Developments in oil extraction from microalgae. *European journal of lipid science and technology* **2011**, *113*, 539-547.
8. Xu, M.; Li, P.; Tang, T.; Hu, Z. Roles of SRT and HRT of an algal membrane bioreactor system with a tanks-in-series configuration for secondary wastewater effluent polishing. *Ecological engineering* **2015**, *85*, 257-264.
9. Boonchai, R.; Seo, G. Microalgae membrane photobioreactor for further removal of nitrogen and phosphorus from secondary sewage effluent. *Korean journal of chemical engineering* **2015**, *32*, 2047-2052.
10. Dargahi, A.; Shokoohi, R.; Asgari, G.; Ansari, A.; Nematollahi, D.; Samarghandi, M.R. Moving-bed biofilm reactor combined with three-dimensional electrochemical

pretreatment (MBBR–3DE) for 2, 4-D herbicide treatment: application for real wastewater, improvement of biodegradability. *RSC advances* **2021**, *11*, 9608-9620.

11. Biswas, K.; Taylor, M.W.; Turner, S.J. dsrAB-based analysis of sulphate-reducing bacteria in moving bed biofilm reactor (MBBR) wastewater treatment plants. *Applied microbiology and biotechnology* **2014**, *98*, 7211-7222.
12. Kowalski, M.S.; Devlin, T.R.; di Biase, A.; Oleszkiewicz, J.A. Effective nitrogen removal in a two-stage partial nitritation-anammox reactor treating municipal wastewater–Piloting PN-MBBR/AMX-IFAS configuration. *Bioresource technology* **2019**, *289*, 121742.
13. Bering, S.; Mazur, J.; Tarnowski, K.; Janus, M.; Mozia, S.; Morawski, A.W. The application of moving bed bio-reactor (MBBR) in commercial laundry wastewater treatment. *Science of the total environment* **2018**, *627*, 1638-1643.
14. Chen, F.; Zeng, S.; Luo, Z.; Ma, J.; Zhu, Q.; Zhang, S. A novel MBBR–MFC integrated system for high-strength pulp/paper wastewater treatment and bioelectricity generation. *Separation science and technology* **2020**, *55*, 2490-2499.
15. Liu, Y.; Wang, N.; Wei, Y.; Dang, K.; Li, M.; Li, Y.; Li, Q.; Mu, R. Pilot study on the upgrading configuration of UASB-MBBR with two carriers: Treatment effect, sludge reduction and functional microbial identification. *Process biochemistry* **2020**, *99*, 211-221.
16. Yang, X.; Crespi Rosell, M.; López Grimau, V. A review on the present situation of wastewater treatment in textile industry with membrane bioreactor and moving bed biofilm reactor. *Desalination and water treatment* **2018**, *103*, 315-322.
17. Chen, X.; Li, Z.; He, N.; Zheng, Y.; Li, H.; Wang, H.; Wang, Y.; Lu, Y.; Li, Q.; Peng, Y. Nitrogen and phosphorus removal from anaerobically digested wastewater by microalgae cultured in a novel membrane photobioreactor. *Biotechnology for biofuels* **2018**, *11*, 1-11.
18. Chang, H.; Quan, X.; Zhong, N.; Zhang, Z.; Lu, C.; Li, G.; Cheng, Z.; Yang, L. High-efficiency nutrients reclamation from landfill leachate by microalgae Chlorella vulgaris in membrane photobioreactor for bio-lipid production. *Bioresource technology* **2018**, *266*, 374-381.
19. Coronado-Reyes, J.A.; Salazar-Torres, J.A.; Juarez-Campos, B.; Gonzalez-Hernandez, J.C. Chlorella vulgaris, a microalgae important to be used in Biotechnology: a review. *Food science and technology* **2020**.

20. Znad, H.; Al Ketife, A.M.; Judd, S.; AlMomani, F.; Vuthaluru, H.B. Bioremediation and nutrient removal from wastewater by Chlorella vulgaris. *Ecological engineering* **2018**, *110*, 1-7.
21. Chen, C.-Y.; Yeh, K.-L.; Aisyah, R.; Lee, D.-J.; Chang, J.-S. Cultivation, photobioreactor design and harvesting of microalgae for biodiesel production: a critical review. *Bioresource technology* **2011**, *102*, 71-81.
22. Zhen-Feng, S.; Xin, L.; Hong-Ying, H.; Yin-Hu, W.; Tsutomu, N. Culture of Scenedesmus sp. LX1 in the modified effluent of a wastewater treatment plant of an electric factory by photo-membrane bioreactor. *Bioresource technology* **2011**, *102*, 7627-7632.
23. Simionato, D.; Basso, S.; Giacometti, G.M.; Morosinotto, T. Optimization of light use efficiency for biofuel production in algae. *Biophysical chemistry* **2013**, *182*, 71-78.
24. Blair, M.F.; Kokabian, B.; Gude, V.G. Light and growth medium effect on Chlorella vulgaris biomass production. *Journal of environmental chemical engineering* **2014**, *2*, 665-674.
25. Zhao, Y.; Wang, J.; Zhang, H.; Yan, C.; Zhang, Y. Effects of various LED light wavelengths and intensities on microalgae-based simultaneous biogas upgrading and digestate nutrient reduction process. *Bioresource technology* **2013**, *136*, 461-468.
26. Das, P.; Lei, W.; Aziz, S.S.; Obbard, J.P. Enhanced algae growth in both phototrophic and mixotrophic culture under blue light. *Bioresource technology* **2011**, *102*, 3883-3887.
27. Sforza, E.; Simionato, D.; Giacometti, G.M.; Bertucco, A.; Morosinotto, T. Adjusted light and dark cycles can optimize photosynthetic efficiency in algae growing in photobioreactors. *PloS one* **2012**, *7*, e38975.
28. Woertz, I.; Feffer, A.; Lundquist, T.; Nelson, Y. Algae grown on dairy and municipal wastewater for simultaneous nutrient removal and lipid production for biofuel feedstock. *Journal of environmental engineering* **2009**, *135*, 1115.
29. Lam, M.K.; Lee, K.T.; Mohamed, A.R. Current status and challenges on microalgae-based carbon capture. *International journal of greenhouse gas control* **2012**, *10*, 456-469.
30. Sutherland, D.L.; Howard-Williams, C.; Turnbull, M.H.; Broady, P.A.; Craggs, R.J. The effects of CO2 addition along a pH gradient on wastewater microalgal photo-physiology, biomass production and nutrient removal. *Water research* **2015**, *70*, 9-26.

31. Meng, F.; Yang, F.; Shi, B.; Zhang, H. A comprehensive study on membrane fouling in submerged membrane bioreactors operated under different aeration intensities. *Separation and purification technology* **2008**, *59*, 91-100.
32. Joshi, J.; Elias, C.; Patole, M. Role of hydrodynamic shear in the cultivation of animal, plant and microbial cells. *The Chemical Engineering journal and the biochemical engineering journal* **1996**, *62*, 121-141.
33. Judd, S.; van den Broeke, L.J.; Shurair, M.; Kuti, Y.; Znad, H. Algal remediation of CO2 and nutrient discharges: a review. *Water research* **2015**, *87*, 356-366.
34. Yoon, S.-H.; Kim, H.-S.; Yeom, I.-T. The optimum operational condition of membrane bioreactor (MBR): cost estimation of aeration and sludge treatment. *Water research* **2004**, *38*, 37-46.
35. Gao, F.; Peng, Y.-Y.; Li, C.; Cui, W.; Yang, Z.-H.; Zeng, G.-M. Coupled nutrient removal from secondary effluent and algal biomass production in membrane photobioreactor (MPBR): effect of HRT and long-term operation. *Chemical engineering journal* **2018**, *335*, 169-175.
36. Zhang, M.; Leung, K.-T.; Lin, H.; Liao, B. The biological performance of a novel microalgal-bacterial membrane photobioreactor: Effects of HRT and N/P ratio. *Chemosphere* **2020**, *261*, 128199.
37. Solmaz, A.; Işık, M. Optimization of membrane photobioreactor; the effect of hydraulic retention time on biomass production and nutrient removal by mixed microalgae culture. *Biomass and bioenergy* **2020**, *142*, 105809.
38. Vu, M.T.; Nguyen, L.N.; Mofijur, M.; Johir, M.A.H.; Ngo, H.H.; Mahlia, T.; Nghiem, L.D. Simultaneous nutrient recovery and algal biomass production from anaerobically digested sludge centrate using a membrane photobioreactor. *Bioresource technology* **2022**, *343*, 126069.
39. Ashadullah, A.; Shafiquzzaman, M.; Haider, H.; Alresheedi, M.; Azam, M.S.; Ghumman, A.R. Wastewater treatment by microalgal membrane bioreactor: evaluating the effect of organic loading rate and hydraulic residence time. *Journal of environmental management* **2021**, *278*, 111548.

40. Honda, R.; Boonnorat, J.; Chiemchaisri, C.; Chiemchaisri, W.; Yamamoto, K. Carbon dioxide capture and nutrients removal utilizing treated sewage by concentrated microalgae cultivation in a membrane photobioreactor. *Bioresource technology* **2012**, *125*, 59-64.
41. Ahmed, Z.; Cho, J.; Lim, B.-R.; Song, K.-G.; Ahn, K.-H. Effects of sludge retention time on membrane fouling and microbial community structure in a membrane bioreactor. *Journal of membrane science* **2007**, *287*, 211-218.
42. Zhang, M.; Leung, K.-T.; Lin, H.; Liao, B. Evaluation of membrane fouling in a microalgal-bacterial membrane photobioreactor: Effects of SRT. *Science of the total environment* **2022**, 156414.
43. Hu, W.; Yin, J.; Deng, B.; Hu, Z. Application of nano TiO2 modified hollow fiber membranes in algal membrane bioreactors for high-density algae cultivation and wastewater polishing. *Bioresource technology* **2015**, *193*, 135-141.
44. Zhang, M.; Leung, K.-T.; Lin, H.; Liao, B. Effects of solids retention time on the biological performance of a novel microalgal-bacterial membrane photobioreactor for industrial wastewater treatment. *Journal of environmental chemical engineering* **2021**, *9*, 105500.
45. Jagannadh, S.N.; Muralidhara, H. Electrokinetics methods to control membrane fouling. *Industrial & engineering chemistry research* **1996**, *35*, 1133-1140.
46. Al Mamun, M.; Bhattacharjee, S.; Pernitsky, D.; Sadrzadeh, M. Colloidal fouling of nanofiltration membranes: Development of a standard operating procedure. *Membranes* **2017**, *7*, 4.
47. Hoek, E.M.; Elimelech, M. Cake-enhanced concentration polarization: a new fouling mechanism for salt-rejecting membranes. *Environmental science & technology* **2003**, *37*, 5581-5588.
48. Wang, Z.; Mei, X.; Ma, J.; Grasmick, A.; Wu, Z. Potential foulants and fouling indicators in MBRs: a critical review. *Separation science and technology* **2013**, *48*, 22-50.
49. Al Mamun, M.A.; Sadrzadeh, M.; Chatterjee, R.; Bhattacharjee, S.; De, S. Colloidal fouling of nanofiltration membranes: A novel transient electrokinetic model and experimental study. *Chemical engineering science* **2015**, *138*, 153-163.

50. Meng, F.; Chae, S.-R.; Drews, A.; Kraume, M.; Shin, H.-S.; Yang, F. Recent advances in membrane bioreactors (MBRs): membrane fouling and membrane material. *Water research* **2009**, *43*, 1489-1512.
51. Nguyen, T.; Roddick, F.A.; Fan, L. Biofouling of water treatment membranes: a review of the underlying causes, monitoring techniques and control measures. *Membranes* **2012**, *2*, 804-840.
52. Milović, N.M.; Wang, J.; Lewis, K.; Klibanov, A.M. Immobilized N-alkylated polyethylenimine avidly kills bacteria by rupturing cell membranes with no resistance developed. *Biotechnology and bioengineering* **2005**, *90*, 715-722.
53. Liu, C.; Zhang, D.; He, Y.; Zhao, X.; Bai, R. Modification of membrane surface for anti-biofouling performance: Effect of anti-adhesion and anti-bacteria approaches. *Journal of membrane science* **2010**, *346*, 121-130.
54. Amy, G. Fundamental understanding of organic matter fouling of membranes. *Desalination* **2008**, *231*, 44-51.
55. Hong, S.; Elimelech, M. Chemical and physical aspects of natural organic matter (NOM) fouling of nanofiltration membranes. *Journal of membrane science* **1997**, *132*, 159-181.
56. Nghiem, L.D.; Schäfer, A.I.; Elimelech, M. Removal of natural hormones by nanofiltration membranes: measurement, modeling, and mechanisms. *Environmental science & technology* **2004**, *38*, 1888-1896.
57. Teychene, B.; Loulergue, P.; Guigui, C.; Cabassud, C. Development and use of a novel method for in line characterisation of fouling layers electrokinetic properties and for fouling monitoring. *Journal of membrane science* **2011**, *370*, 45-57.
58. Llorente, I.; Fajardo, S.; Bastidas, J. Applications of electrokinetic phenomena in materials science. *Journal of solid state electrochemistry* **2014**, *18*, 293-307.
59. Demadis, K.D.; Neofotistou, E.; Mavredaki, E.; Tsiknakis, M.; Sarigiannidou, E.-M.; Katarachia, S.D. Inorganic foulants in membrane systems: chemical control strategies and the contribution of "green chemistry". *Desalination* **2005**, *179*, 281-295.
60. Arkhangelsky, E.; Wicaksana, F.; Tang, C.; Al-Rabiah, A.A.; Al-Zahrani, S.M.; Wang, R. Combined organic–inorganic fouling of forward osmosis hollow fiber membranes. *Water research* **2012**, *46*, 6329-6338.

61. Schulz, M.; Soltani, A.; Zheng, X.; Ernst, M. Effect of inorganic colloidal water constituents on combined low-pressure membrane fouling with natural organic matter (NOM). *Journal of membrane science* **2016**, *507*, 154-164.
62. Al-Amoudi, A.S. Factors affecting natural organic matter (NOM) and scaling fouling in NF membranes: a review. *Desalination* **2010**, *259*, 1-10.
63. Xie, M.; Shon, H.K.; Gray, S.R.; Elimelech, M. Membrane-based processes for wastewater nutrient recovery: technology, challenges, and future direction. *Water research* **2016**, *89*, 210-221.
64. Alkhatib, A.; Ayari, M.A.; Hawari, A.H. Fouling mitigation strategies for different foulants in membrane distillation. *Chemical engineering and processing-Process intensification* **2021**, *167*, 108517.
65. Fan, H.; Xiao, K.; Mu, S.; Zhou, Y.; Ma, J.; Wang, X.; Huang, X. Impact of membrane pore morphology on multi-cycle fouling and cleaning of hydrophobic and hydrophilic membranes during MBR operation. *Journal of membrane science* **2018**, *556*, 312-320.
66. Hilal, N.; Ogunbiyi, O.O.; Miles, N.J.; Nigmatullin, R. Methods employed for control of fouling in MF and UF membranes: a comprehensive review. *Separation science and technology* **2005**, *40*, 1957-2005.
67. Bagheri, M.; Mirbagheri, S.A. Critical review of fouling mitigation strategies in membrane bioreactors treating water and wastewater. *Bioresource technology* **2018**, *258*, 318-334.
68. Brepols, C.; Drensla, K.; Janot, A.; Trimborn, M.; Engelhardt, N. Strategies for chemical cleaning in large scale membrane bioreactors. *Water science and technology* **2008**, *57*, 457-463.
69. Zitomer, D.H.; Bachman, T.; Vogel, D. Thermophilic anaerobic digester with ultrafilter for solids stabilization. *Water science and technology* **2005**, *52*, 525-530.
70. Liu, Q.; Ren, J.; Lu, Y.; Zhang, X.; Roddick, F.A.; Fan, L.; Wang, Y.; Yu, H.; Yao, P. A review of the current in-situ fouling control strategies in MBR: Biological versus physicochemical. *Journal of industrial and engineering chemistry* **2021**, *98*, 42-59.
71. Ensano, B.; Borea, L.; Naddeo, V.; Belgiorno, V.; De Luna, M.D.; Ballesteros Jr, F.C. Combination of electrochemical processes with membrane bioreactors for wastewater treatment and fouling control: a review. *Frontiers in environmental science* **2016**, 57.

72. El Kateb, M.; Trellu, C.; Darwich, A.; Rivallin, M.; Bechelany, M.; Nagarajan, S.; Lacour, S.; Bellakhal, N.; Lesage, G.; Heran, M. Electrochemical advanced oxidation processes using novel electrode materials for mineralization and biodegradability enhancement of nanofiltration concentrate of landfill leachates. *Water research* **2019**, *162*, 446-455.
73. Bani-Melhem, K.; Elektorowicz, M. Performance of the submerged membrane electro-bioreactor (SMEBR) with iron electrodes for wastewater treatment and fouling reduction. *Journal of membrane science* **2011**, *379*, 434-439.
74. Reuss, F.F. Sur un nouvel effet de l'électricité galvanique. *Mem. Soc. Imp. Natur. Moscou* **1809**, *2*, 327-337.
75. Abdulkarem, E.; Ahmed, I.; Abu-Zahra, M.; Hasan, S. Electrokinetic pretreatment of seawater to decrease the Ca2+, Mg2+, SO42− and bacteria contents in membrane desalination applications. *Desalination* **2017**, *403*, 107-116.
76. Corbatón-Báguena, M.-J.; Álvarez-Blanco, S.; Vincent-Vela, M.-C.; Ortega-Navarro, E.; Pérez-Herranz, V. Application of electric fields to clean ultrafiltration membranes fouled with whey model solutions. *Separation and purification technology* **2016**, *159*, 92-99.
77. Kochkodan, V.; Hilal, N. A comprehensive review on surface modified polymer membranes for biofouling mitigation. *Desalination* **2015**, *356*, 187-207.
78. Pethig, R. Dielectrophoresis: Status of the theory, technology, and applications. *Biomicrofluidics* **2010**, *4*, 022811.
79. Labeed, F.H.; Coley, H.M.; Thomas, H.; Hughes, M.P. Assessment of multidrug resistance reversal using dielectrophoresis and flow cytometry. *Biophysical journal* **2003**, *85*, 2028-2034.
80. Masliyah, J.H.; Bhattacharjee, S. *Electrokinetic and colloid transport phenomena*; John Wiley & Sons: 2006.
81. Chiu, T.; Garcia, F.G. Critical flux enhancement in electrically assisted microfiltration. *Separation and purification technology* **2011**, *78*, 62-68.
82. Amini, M.; Mohamedelhassan, E.; Liao, B. Electrokinetic membrane bioreactors. *Advances in membrane technologies* **2020**, 195.
83. Acar, Y.B.; Alshawabkeh, A.N. Principles of electrokinetic remediation. *Environmental science & technology* **1993**, *27*, 2638-2647.

84. Molla, S.H.; Bhattacharjee, S. Prevention of colloidal membrane fouling employing dielectrophoretic forces on a parallel electrode array. *Journal of membrane science* **2005**, *255*, 187-199.
85. Hawari, A.H.; Du, F.; Baune, M.; Thöming, J. A fouling suppression system in submerged membrane bioreactors using dielectrophoretic forces. *Journal of environmental sciences* **2015**, *29*, 139-145.
86. Du, F.; Ciaciuch, P.; Bohlen, S.; Wang, Y.; Baune, M.; Thöming, J. Intensification of cross-flow membrane filtration using dielectrophoresis with a novel electrode configuration. *Journal of membrane science* **2013**, *448*, 256-261.
87. Larbi, B.; Hawari, A.; Du, F.; Baune, M.; Thöming, J. Impact of the pulsed voltage input and the electrode spacing on the enhancement of the permeate flux in a dielectrophoresis based anti-fouling system for a submerged membrane bioreactor. *Separation and purification technology* **2017**, *187*, 102-109.
88. Enevoldsen, A.D.; Hansen, E.B.; Jonsson, G. Electro-ultrafiltration of industrial enzyme solutions. *Journal of membrane science* **2007**, *299*, 28-37.
89. Krzeminski, P.; Leverette, L.; Malamis, S.; Katsou, E. Membrane bioreactors–a review on recent developments in energy reduction, fouling control, novel configurations, LCA and market prospects. *Journal of membrane science* **2017**, *527*, 207-227.
90. Dudchenko, A.V.; Rolf, J.; Russell, K.; Duan, W.; Jassby, D. Organic fouling inhibition on electrically conducting carbon nanotube–polyvinyl alcohol composite ultrafiltration membranes. *Journal of membrane science* **2014**, *468*, 1-10.
91. Van Der Borden, A.J.; Van Der Werf, H.; Van Der Mei, H.C.; Busscher, H.J. Electric current-induced detachment of Staphylococcus epidermidis biofilms from surgical stainless steel. *Applied and environmental microbiology* **2004**, *70*, 6871-6874.
92. Price, W.; Too, C.; Wallace, G.G.; Zhou, D. Development of membrane systems based on conducting polymers. *Synthetic metals* **1999**, *102*, 1338-1341.
93. Liu, J.; Liu, L.; Gao, B.; Yang, F. Cathode membrane fouling reduction and sludge property in membrane bioreactor integrating electrocoagulation and electrostatic repulsion. *Separation and purification technology* **2012**, *100*, 44-50.

94. Zhang, Q.; Vecitis, C.D. Conductive CNT-PVDF membrane for capacitive organic fouling reduction. *Journal of membrane science* **2014**, *459*, 143-156.
95. Huang, J.; Wang, Z.; Zhang, J.; Zhang, X.; Ma, J.; Wu, Z. A novel composite conductive microfiltration membrane and its anti-fouling performance with an external electric field in membrane bioreactors. *Scientific reports* **2015**, *5*, 9268.
96. Liu, L.; Liu, J.; Bo, G.; Yang, F.; Crittenden, J.; Chen, Y. Conductive and hydrophilic polypyrrole modified membrane cathodes and fouling reduction in MBR. *Journal of membrane science* **2013**, *429*, 252-258.
97. Ho, K.; Teow, Y.; Mohammad, A.; Ang, W.; Lee, P. Development of graphene oxide (GO)/multi-walled carbon nanotubes (MWCNTs) nanocomposite conductive membranes for electrically enhanced fouling mitigation. *Journal of membrane science* **2018**, *552*, 189-201.
98. Zhang, Y.; Liu, L.; Yang, F. A novel conductive membrane with RGO/PVDF coated on carbon fiber cloth for fouling reduction with electric field in separating polyacrylamide. *Journal of applied polymer science* **2016**, *133*.
99. Liu, Q.; Qiu, G.; Zhou, Z.; Li, J.; Amy, G.L.; Xie, J.; Lee, J.Y. An effective design of electrically conducting thin-film composite (TFC) membranes for bio and organic fouling control in forward osmosis (FO). *Environmental science & technology* **2016**, *50*, 10596-10605.
100. Salehi, E.; Madaeni, S. Influence of conductive surface on adsorption behavior of ultrafiltration membrane. *Applied surface science* **2010**, *256*, 3010-3017.
101. Kull, K.R.; Steen, M.L.; Fisher, E.R. Surface modification with nitrogen-containing plasmas to produce hydrophilic, low-fouling membranes. *Journal of membrane science* **2005**, *246*, 203-215.
102. Wei, X.; Wang, R.; Li, Z.; Fane, A.G. Development of a novel electrophoresis-UV grafting technique to modify PES UF membranes used for NOM removal. *Journal of membrane science* **2006**, *273*, 47-57.
103. Hasan, B.O.; Nathan, G.J.; Ashman, P.J.; Craig, R.A.; Kelso, R.M. The use of turbulence generators to mitigate crystallization fouling under cross flow conditions. *Desalination* **2012**, *288*, 108-117.

104. Wilen, B.-M.; Jin, B.; Lant, P. The influence of key chemical constituents in activated sludge on surface and flocculating properties. *Water research* **2003**, *37*, 2127-2139.
105. Elektorowicz, M.; Hasan, S.; Oleszkiewicz, J. A novel submerged membrane electrobioreactor achieves high removal efficiencies. *Journal of water environmental technololgy* **2011**, *23*, 60-62.
106. Beykal, B.; Herzberg, M.; Oren, Y.; Mauter, M.S. Influence of surface charge on the rate, extent, and structure of adsorbed Bovine Serum Albumin to gold electrodes. *Journal of colloid and interface science* **2015**, *460*, 321-328.
107. Ghosh, K.; Schnitzer, M. Macromolecular structures of humic substances. *Soil science* **1980**, *129*, 266-276.
108. Manica, D.P.; Mitsumori, Y.; Ewing, A.G. Characterization of electrode fouling and surface regeneration for a platinum electrode on an electrophoresis microchip. *Analytical chemistry* **2003**, *75*, 4572-4577.
109. Lindstrand, V.; Jönsson, A.-S.; Sundström, G. Organic fouling of electrodialysis membranes with and without applied voltage. *Desalination* **2000**, *130*, 73-84.
110. Hasan, S.W.; Elektorowicz, M.; Oleszkiewicz, J.A. Start-up period investigation of pilot-scale submerged membrane electro-bioreactor (SMEBR) treating raw municipal wastewater. *Chemosphere* **2014**, *97*, 71-77.
111. Liang, F.; Xiao, Y.; Zhao, F. Effect of pH on sulfate removal from wastewater using a bioelectrochemical system. *Chemical engineering journal* **2013**, *218*, 147-153.
112. Malakootian, M.; Yousefi, N. The efficiency of electrocoagulation process using aluminum electrodes in removal of hardness from water. *Journal of environmental health science & engineering* **2009**, *6*, 131-136.
113. Murugananthan, M.; Raju, G.B.; Prabhakar, S. Removal of sulfide, sulfate and sulfite ions by electro coagulation. *Journal of hazardous materials* **2004**, *109*, 37-44.
114. Saiba, A.; Kourdali, S.; Ghernaout, B.; Ghernaout, D. In Desalination, from 1987 to 2009, the birth of a new seawater pretreatment process: Electrocoagulation-an overview. *Desalination and water treatment* **2010**, *16*, 201-217.

115. Gottenbos, B.; Grijpma, D.W.; van der Mei, H.C.; Feijen, J.; Busscher, H.J. Antimicrobial effects of positively charged surfaces on adhering Gram-positive and Gram-negative bacteria. *Journal of antimicrobial chemotherapy* **2001**, *48*, 7-13.
116. Jucker, B.A.; Harms, H.; Zehnder, A. Adhesion of the positively charged bacterium Stenotrophomonas (Xanthomonas) maltophilia 70401 to glass and Teflon. *Journal of bacteriology* **1996**, *178*, 5472-5479.
117. Li, C.; Guo, X.; Wang, X.; Fan, S.; Zhou, Q.; Shao, H.; Hu, W.; Li, C.; Tong, L.; Kumar, R.R. Membrane fouling mitigation by coupling applied electric field in membrane system: Configuration, mechanism and performance. *Electrochimica Acta* **2018**.
118. Dong, Y.-H.; Wang, L.-H.; Zhang, L.-H. Quorum-quenching microbial infections: mechanisms and implications. *Philosophical transactions of the Royal Society B: biological Sciences* **2007**, *362*, 1201-1211.
119. Wei, V.; Elektorowicz, M.; Oleszkiewicz, J. Influence of electric current on bacterial viability in wastewater treatment. *Water research* **2011**, *45*, 5058-5062.
120. Ho, K.; Teow, Y.; Ang, W.; Mohammad, A. An Overview of Electrically-enhanced Membrane Bioreactor (EMBR) for Fouling Suppression. *Journal of engineering science & technology review* **2017**, *10*.
121. Vecitis, C.D.; Schnoor, M.H.; Rahaman, M.S.; Schiffman, J.D.; Elimelech, M. Electrochemical multiwalled carbon nanotube filter for viral and bacterial removal and inactivation. *Environmental science & technology* **2011**, *45*, 3672-3679.
122. Hong, S.H.; Jeong, J.; Shim, S.; Kang, H.; Kwon, S.; Ahn, K.H.; Yoon, J. Effect of electric currents on bacterial detachment and inactivation. *Biotechnology and bioengineering* **2008**, *100*, 379-386.
123. Kim, J.-O.; Jung, J.-T.; Yeom, I.-T.; Aoh, G.-H. Electric fields treatment for the reduction of membrane fouling, the inactivation of bacteria and the enhancement of particle coagulation. *Desalination* **2007**, *202*, 31-37.
124. Perez-Roa, R.E.; Tompkins, D.T.; Paulose, M.; Grimes, C.A.; Anderson, M.A.; Noguera, D.R. Effects of localised, low-voltage pulsed electric fields on the development and inhibition of Pseudomonas aeruginosa biofilms. *Biofouling* **2006**, *22*, 383-390.

125. Sivaraj, D.; Vijayalakshmi, K. Substantial effect of magnesium incorporation on hydroxyapatite/carbon nanotubes coatings on metallic implant surfaces for better anticorrosive protection and antibacterial ability. *Journal of analytical and applied pyrolysis* **2018**, *135*, 15-21.
126. Kang, S.; Herzberg, M.; Rodrigues, D.F.; Elimelech, M. Antibacterial effects of carbon nanotubes: size does matter! *Langmuir* **2008**, *24*, 6409-6413.
127. Fan, X.; Zhao, H.; Quan, X.; Liu, Y.; Chen, S. Nanocarbon-based membrane filtration integrated with electric field driving for effective membrane fouling mitigation. *Water research* **2016**, *88*, 285-292.
128. Hashaikeh, R.; Lalia, B.S.; Kochkodan, V.; Hilal, N. A novel in situ membrane cleaning method using periodic electrolysis. *Journal of membrane science* **2014**, *471*, 149-154.
129. Huang, P.-W.; Wang, T.-T.; Lin, S.-W.; Chang, Y.-C.; Fan, S.-K. Dielectrophoretic cell concentrator on EWOD-based chips. In Proceedings of the 2006 1st IEEE International Conference on Nano/Micro Engineered and Molecular Systems, 2006; pp. 1418-1421.
130. Zhang, P.; Lin, L.; Zang, D.; Guo, X.; Liu, M. Designing Bioinspired Anti-Biofouling Surfaces based on a Superwettability Strategy. *Small* **2017**, *13*, 1503334.
131. Geng, H.; Cho, S.K. Anti-biofouling droplet manipulation by slippery liquid infused porous surface (SLIPS) integrated with electrowetting and liquid-dielectrophoresis. In Proceedings of the 2018 IEEE Micro Electro Mechanical Systems (MEMS), 2018; 261-264.
132. Wang, C.; Song, H.; Zhang, Q.; Wang, B.; Li, A. Parameter optimization based on capacitive deionization for highly efficient desalination of domestic wastewater biotreated effluent and the fouled electrode regeneration. *Desalination* **2015**, *365*, 407-415.
133. Gatley-Montross, C.M.; Finlay, J.A.; Aldred, N.; Cassady, H.; Destino, J.F.; Orihuela, B.; Hickner, M.A.; Clare, A.S.; Rittschof, D.; Holm, E.R. Multivariate analysis of attachment of biofouling organisms in response to material surface characteristics. *Biointerphases* **2017**, *12*, 051003.
134. Nezammahalleh, H.; Ghanati, F.; Adams II, T.A.; Nosrati, M.; Shojaosadati, S.A. Effect of moderate static electric field on the growth and metabolism of Chlorella vulgaris. *Bioresource technology* **2016**, *218*, 700-711.

135. Kim, J.Y.; Lee, C.; Jeon, M.S.; Park, J.; Choi, Y.-E. Enhancement of microalga Haematococcus pluvialis growth and astaxanthin production by electrical treatment. *Bioresource technology* **2018**, *268*, 815-819.
136. Fayad, N.; Yehya, T.; Audonnet, F.; Vial, C. Harvesting of microalgae Chlorella vulgaris using electro-coagulation-flocculation in the batch mode. *Algal research* **2017**, *25*, 1-11.
137. Misra, R.; Guldhe, A.; Singh, P.; Rawat, I.; Stenström, T.A.; Bux, F. Evaluation of operating conditions for sustainable harvesting of microalgal biomass applying electrochemical method using non sacrificial electrodes. *Bioresource technology* **2015**, *176*, 1-7.
138. Amaro, H.M.; Guedes, A.C.; Malcata, F.X. Advances and perspectives in using microalgae to produce biodiesel. *Applied energy* **2011**, *88*, 3402-3410.
139. Uduman, N.; Bourniquel, V.; Danquah, M.K.; Hoadley, A.F. A parametric study of electrocoagulation as a recovery process of marine microalgae for biodiesel production. *Chemical engineering journal* **2011**, *174*, 249-257.
140. Alshawabkeh, A.N.; Shen, Y.; Maillacheruvu, K.Y. Effect of DC electric fields on COD in aerobic mixed sludge processes. *Environmental engineering science* **2004**, *21*, 321-329.
141. Tafti, A.D.; Mirzaii, S.M.S.; Andalibi, M.R.; Vossoughi, M. Optimized coupling of an intermittent DC electric field with a membrane bioreactor for enhanced effluent quality and hindered membrane fouling. *Separation and purification technology* **2015**, *152*, 7-13.
142. Hosseinzadeh, M.; Bidhendi, G.N.; Torabian, A.; Mehrdadi, N.; Pourabdullah, M. A new flat sheet membrane bioreactor hybrid system for advanced treatment of effluent, reverse osmosis pretreatment and fouling mitigation. *Bioresource technology* **2015**, *192*, 177-184.
143. Borea, L.; Naddeo, V.; Belgiorno, V. Application of electrochemical processes to membrane bioreactors for improving nutrient removal and fouling control. *Environmental Science and pollution research* **2017**, *24*, 321-333.
144. Lee, J.; Lee, K.; Park, K.; Maeng, S. Hydrogenotrophic denitrification in a packed bed reactor: effects of hydrogen-to-water flow rate ratio. *Bioresource technology* **2010**, *101*, 3940-3946.

145. Aouni, A.; Fersi, C.; Ali, M.B.S.; Dhahbi, M. Treatment of textile wastewater by a hybrid electrocoagulation/nanofiltration process. *Journal of hazardous materials* **2009**, *168*, 868-874.
146. Zhang, J.; Satti, A.; Chen, X.; Xiao, K.; Sun, J.; Yan, X.; Liang, P.; Zhang, X.; Huang, X. Low-voltage electric field applied into MBR for fouling suppression: Performance and mechanisms. *Chemical engineering journal* **2015**, *273*, 223-230.
147. Liu, L.; Liu, J.; Gao, B.; Yang, F.; Chellam, S. Fouling reductions in a membrane bioreactor using an intermittent electric field and cathodic membrane modified by vapor phase polymerized pyrrole. *Journal of membrane science* **2012**, *394*, 202-208.
148. Mollah, M.Y.; Morkovsky, P.; Gomes, J.A.; Kesmez, M.; Parga, J.; Cocke, D.L. Fundamentals, present and future perspectives of electrocoagulation. *Journal of hazardous materials* **2004**, *114*, 199-210.
149. Den, W.; Wang, C.-J. Removal of silica from brackish water by electrocoagulation pretreatment to prevent fouling of reverse osmosis membranes. *Separation and purification technology* **2008**, *59*, 318-325.
150. Vasudevan, S.; Sozhan, G.; Ravichandran, S.; Jayaraj, J.; Lakshmi, J.; Sheela, M. Studies on the removal of phosphate from drinking water by electrocoagulation process. *Industrial & engineering chemistry research* **2008**, *47*, 2018-2023.
151. Mavrov, V.; Stamenov, S.; Todorova, E.; Chmiel, H.; Erwe, T. New hybrid electrocoagulation membrane process for removing selenium from industrial wastewater. *Desalination* **2006**, *201*, 290-296.
152. Bani-Melhem, K.; Elektorowicz, M. Development of a novel submerged membrane electro-bioreactor (SMEBR): performance for fouling reduction. *Environmental science & technology* **2010**, *44*, 3298-3304.
153. Nguyen, L.N.; Hai, F.I.; Kang, J.; Price, W.E.; Nghiem, L.D. Removal of trace organic contaminants by a membrane bioreactor–granular activated carbon (MBR–GAC) system. *Bioresource technology* **2012**, *113*, 169-173.
154. Ibanez, J.G.; Takimoto, M.M.; Vasquez, R.C.; Basak, S.; Myung, N.; Rajeshwar, K. Laboratory experiments on electrochemical remediation of the environment: electrocoagulation of oily wastewater. *Journal of chemical education* **1995**, *72*, 1050.

155. Abdel-Ghani, N.; Hefny, M.; El-Chaghaby, G.A. Removal of lead from aqueous solution using low cost abundantly available adsorbents. *International journal of environmental science & technology* **2007**, *4*, 67-73.
156. Yu, W.; Liu, Y.; Xu, Y.; Li, R.; Chen, J.; Liao, B.-Q.; Shen, L.; Lin, H. A conductive PVDF-Ni membrane with superior rejection, permeance and antifouling ability via electric assisted in-situ aeration for dye separation. *Journal of membrane science* **2019**.
157. Ahmed, F.E.; Hilal, N.; Hashaikeh, R. Electrically conductive membranes for in situ fouling detection in membrane distillation using impedance spectroscopy. *Journal of membrane science* **2018**, *556*, 66-72.
158. Lalia, B.S.; Ahmed, F.E.; Shah, T.; Hilal, N.; Hashaikeh, R. Electrically conductive membranes based on carbon nanostructures for self-cleaning of biofouling. *Desalination* **2015**, *360*, 8-12.
159. Liang, Y.; Chapman, M.; Weihs, G.F.; Wiley, D. CFD modelling of electro-osmotic permeate flux enhancement on the feed side of a membrane module. *Journal of membrane science* **2014**, *470*, 378-388.
160. Bayar, S.; Karagunduz, A.; Keskinler, B. Influences of electroosmosis and electrophoresis on permeate flux and membrane fouling in submerged membrane bioreactors (SMBRs). *Water science and technology* **2016**, *74*, 766-776.
161. Yu, W.; Liu, Y.; Xu, Y.; Li, R.; Chen, J.; Liao, B.-Q.; Shen, L.; Lin, H. A conductive PVDF-Ni membrane with superior rejection, permeance and antifouling ability via electric assisted in-situ aeration for dye separation. *Journal of membrane science* **2019**, *581*, 401-412.
162. Liang, Y.; Weihs, G.F.; Wiley, D. CFD modelling of electro-osmotic permeate flux enhancement in spacer-filled membrane channels. *Journal of membrane science* **2016**, *507*, 107-118.
163. Jiang, M.; Ye, K.; Deng, J.; Lin, J.; Ye, W.; Zhao, S.; Van der Bruggen, B. Conventional ultrafiltration as effective strategy for dye/salt fractionation in textile wastewater treatment. *Environmental science & technology* **2018**, *52*, 10698-10708.
164. Lin, J.; Ye, W.; Baltaru, M.-C.; Tang, Y.P.; Bernstein, N.J.; Gao, P.; Balta, S.; Vlad, M.; Volodin, A.; Sotto, A. Tight ultrafiltration membranes for enhanced separation of dyes and

Na2SO4 during textile wastewater treatment. *Journal of membrane science* **2016**, *514*, 217-228.

165. Zhang, Y.; Yu, W.; Li, R.; Xu, Y.; Shen, L.; Lin, H.; Liao, B.-Q.; Wu, G. Novel conductive membranes breaking through the selectivity-permeability trade-off for Congo red removal. *Separation and purification technology* **2019**, *211*, 368-376.
166. Liu, H.; Zhang, G.; Zhao, C.; Liu, J.; Yang, F. Hydraulic power and electric field combined antifouling effect of a novel conductive poly (aminoanthraquinone)/reduced graphene oxide nanohybrid blended PVDF ultrafiltration membrane. *Journal of materials chemistry A* **2015**, *3*, 20277-20287.
167. Tsai, Y.-T.; Yu-Chen Lin, A.; Weng, Y.-H.; Li, K.-C. Treatment of perfluorinated chemicals by electro-microfiltration. *Environmental science & technology* **2010**, *44*, 7914-7920.
168. Wei, K.; Shen, C.; Han, W.; Li, J.; Sun, X.; Shen, J.; Wang, L. Advance treatment of chemical industrial tailwater by integrated electrochemical technologies: electrocatalysis, electrodialysis and electro-microfiltration. *Chemical engineering journal* **2017**, *310*, 13-21.
169. Belli, T.; Battistelli, A.; Costa, R.; Vidal, C.; Schlegel, A.; Lapolli, F. Evaluating the performance and membrane fouling of an electro-membrane bioreactor treating textile industrial wastewater. *International journal of environmental science and technology* **2019**, 1-10.
170. Hou, B.; Kuang, Y.; Han, H.; Liu, Y.; Ren, B.; Deng, R.; Hursthouse, A.S. Enhanced performance and hindered membrane fouling for the treatment of coal chemical industry wastewater using a novel membrane electro-bioreactor with intermittent direct current. *Bioresource technology* **2019**, *271*, 332-339.
171. Bani-Melhem, K.; Smith, E. Grey water treatment by a continuous process of an electrocoagulation unit and a submerged membrane bioreactor system. *Chemical engineering journal* **2012**, *198*, 201-210.
172. Kim, H.-G.; Jang, H.-N.; Kim, H.-M.; Lee, D.-S.; Chung, T.-H. Effect of an electro phosphorous removal process on phosphorous removal and membrane permeability in a pilot-scale MBR. *Desalination* **2010**, *250*, 629-633.

Chapter 3 The biological performance of a novel electrokinetic-assisted membrane photobioreactor (EK-MPBR) for wastewater treatment

Adapted from: Maryam Amini*, Eltayeb Mohamedelhassan, Baoqiang Liao
Membranes 2022, 12(6), 587

*Department of Biotechnology, Lakehead University,
955 Oliver Road, Thunder Bay, ON P7B 5E1, Canada

Abstract

Developing an effective phycoremediation system, especially by utilizing microalgae, could provide a valuable approach in wastewater treatment for simultaneous nutrient removal and biomass generation, which would help control environmental pollution. This research aims to study the impact of low-voltage direct current (DC) application on *Chlorella vulgaris* properties and the removal efficiency of nutrients (N and P) in a novel electrokinetic-assisted membrane photobioreactor (EK-MPBR) in treating synthetic municipal wastewater. Two membrane photobioreactors ran in parallel for 49 days with and without an applied electric field (current density: 0.261 A/m^2). Mixed liquid suspended soils (MLSS) concentration, chemical oxygen demand (COD), floc morphology, total phosphorus (TP), and total nitrogen (TN) removals were measured during the experiments. The results showed that EK-MPBR achieved biomass production comparable to the control MPBR. In EK-MPBR, an over 97% reduction in phosphate concentration was achieved compared to 41% removal in the control MPBR. The control MPBR outperformed the nitrogen removal of EK-MPBR (68% compared to 43% removal). Induced DC electric field led to lower pH, lower zeta potential, and smaller particle sizes in the EK-MPBR as compared with MPBR. The results of this novel study investigating the incorporation of *Chlorella vulgar*is in an electrokinetic-assisted membrane photobioreactor indicate that this is a promising technology for wastewater treatment.

3.1 Introduction

Wastewater treatment is a growing concern because wastewater contains pollutants such as nitrogen and phosphorus, which in excess can threaten wildlife and marine life [1,2]. Algae can assimilate these nutrients from wastewater and prevent eutrophication [3–6]. Phycoremediation, or biological treatment that utilizes algae for nutrient removal from wastewater, is one of the recent technologies gaining attention due to its low cost and environmental footprint [5,7,8]. Membrane photobioreactor technology (MPBR), as one of the biological wastewater treatment systems, is widely used for simultaneous wastewater treatment and microalgae production [9]. This technology has gained momentum due to promising nutrient removal and the high quality of effluent, together with the production of concentrated microalgae [10,11]. The biomass production of MPBRs has industrial applications, including biofuel, foods, and feeds [12–14].

Several studies on MPBR have been conducted by various research groups with different microalgae species and MPBR configurations [15–18]. These studies have demonstrated the advantages of MPBR systems for nutrient removal and microalgae biomass production compared to the conventional microalgae system [19].

Chlorella vulgaris (C. vulgaris) is an extensively used microalgae in MPBRs for wastewater treatment [8,20,21]. It is also produced for human nutrition and biodiesel feedstock applications [12,14,22]. *C. vulgaris* can grow in diverse environments [23–25] such as high temperatures, e.g., up to 40 °C [14], acidic and alkaline (pH from 3 to 11.5) [20–22], light intensity [22], and high salinity. The most studied condition affecting their growth is light, but few studies focus on the effect of a low-voltage continuous electric field on photosynthesis and growth efficiency [14].

There are several parameters that affect the phycoremediation process [8]. Wastewater characteristics are one of the factors that have been studied. One recent study investigated the implications of urban wastewater concentration and induced stress on the growth of *Chlorella fusca* [26]. Using real wastewater instead of synthetic wastewater is another recent research focus on the growth study of *C. vulgaris* and its bioremediation of primary (PE) and secondary (SE) urban effluents [27]. Some report-ed researchers have focused on operating conditions such as hydraulic retention time (HRT), solid retention time (SRT), and turbulent pulsation [28–30].

Some studies investigated the effect of a low-voltage electric field on the growth and nitrogen and phosphorus removal efficiency of C. vulgaris [31,32]. Other research groups have studied the

application of moderate and short-term electric fields in stimulating the growth and metabolism of C. vulgaris [13,33]. They found that in batch culture, a short-term applied electric field could improve the biomass growth of microalgae [13,33]. A study using an applied pulse electric field recently revealed the potential for increased lipid content from *C. vulgaris* [34].

Studies that incorporate electric fields in membrane bioreactors (MBR) have found improved chemical oxygen demand removal (COD) as well as nitrogen and phosphorus removal were observed by applying a short-term electric field in membrane bioreactors (MBR), where activated sludge was used [35–38]. To date, only one study has integrated an electric field into an MBR with algae and activated sludge [2]. However, the combination of an electric field with a membrane photobioreactor utilizing algae as biomass has not yet been investigated.

The current study examines the effect of a low-voltage continuous electric field on the microalgae growth rate, biomass quality, and overall nutrient removal (N and P) of an MPBR with *C. vulgaris* in treating synthetic municipal wastewater. An MPBR and an electrokinetic-assisted MPBR (EK-MPBR) with *C. vulgaris* were operated in parallel for 49 days to investigate the electric field effects on biomass production, biomass productivity, COD removal, and nutrient (N and P) removals. This is the first study on EK-MPBR, and the results demonstrate that it is a promising technology that simultaneously removes nutrients and reproduces microalgae.

3.2 Materials and Methods

3.2.1 Chemicals

All chemicals mentioned in the following sections that were used for microalgae cultivation, wastewater preparation and measurements were purchased from Sigma-Aldrich (Merck, Darmstadt, Germany). Deionized water was prepared in the laboratory.

3.2.2 Microalgae and Culture Conditions

The microalgae *C. vulgaris* was purchased from the Canadian Phycological Culture Centre of the University of Waterloo, ON, Canada. The medium solution was prepared with the following composition and amounts in 1 L of solution [39,40]:

0.66 g NH_4Cl (≥99.5%), 0.625 g $MgSO_4$ (≥ 99.8 %), 0.1105 g $CaCl_2.2H_2O$ (≥99.0%), 0.1142 g H_3BO_3 (≥99.5%), 0.0498 g $FeSO_4.7H_2O$ (≥99.0%), 0.0882 $ZnSO_4.7H_2O$ (≥99.0%), 0.0144 g $MnCl_2.4H_2O$ (≥99.0%), 0.0118 g $Na_2MoO_4.2H_2O$ (≥99.5%), 0.0157 g $CuSO_4.5H_2O$ (≥98%),

0.004 g $CoCl_2.6H_2O$ (≥97%), 0.64 g ethylenediamine tetraacetic acid (EDTA)-2 $Na.2H_2O$ (≥98%), 0.6247 g KH_2PO_4 (≥99.0%), 1.3251 g K_2HPO_4 (≥98%). All components were added to deionized (DI) water and insulated to avoid contamination. The cultivation continued for 25 days to reach the desired concentration of 1.2 g/L of dried biomass under continuous aeration and light illumination at room temperature.

3.2.3 Operating Conditions

The feed of the reactors was a synthetic municipal wastewater effluent (after bio-logical chemical oxygen demand (COD) removal). The amount of the trace element in one litre feed summarized in Table 3.1 included 0.0025 g NaCl (≥99.0%), 0.082 g $MgSO_4.7H_2O$ (≥ 99.8 %), 0.005 g $CaCl_2.2H_2O$ (≥99.0%), 0.02490 g $FeSO_4.7H_2O$ (≥99.0%), 0.00044 $ZnSO_4.7H_2O$ (≥99.0%), 0.00022 g $MnCl_2.4H_2O$ (≥99.0%), 0.00126 g $Na_2MoO_4.2H_2O$ (≥99.5%), 0.00039 g $CuSO_4.5H_2O$ (≥98%), 0.00041 g $CoCl_2.6H_2O$ (≥97%) , 0.09553 NH_4Cl (≥99.5%), 0.01537 g KH_2PO_4 (≥99.0%), 0.3 g NaHCO3 (≥95%) and 0.01874 g Glucose (≥99.5%). All the components were added to distilled water. The reactors were fed semi-continuously with a liquid level controller sensor and a peristaltic pump, and the feed was kept in a refrigerator at 4–5 °C. The level of the suspensions in the reactors was kept constant by a level sensor (LC40, Flowline Inc., Los Alamitos, CA, USA), and feed was pumped by a peristaltic pump (Model 77122-12, Masterflex®C/L®PWR, Cole-Parmer, USA). The permeation pumps were programmed to operate in 3-min-on and 2-min-off modes for permeation and relaxation to control membrane fouling. The reactors were operated for 49 days, and hydraulic retention time (HRT) and solid retention time (SRT) were maintained at 2.5 days and 30 days, respectively. During the operation, HRT was controlled by applied membrane flux. Once the transmembrane pressure (TMP) of the MPBRs reached about 30 kPa, physical cleaning was used to remove the foulant layer of the membrane module. The pH of the feed for the MPBR was adjusted using NaOH (≥97%) and HCl (≥37%) solutions.

Table 3-1 Characteristics of synthetic wastewater.

Water Quality Index	Average Value (mg/L)
Nitrogen	25 ± 2
Phosphorus ($PO_4 - P$)	3.5 ± 0.3
Chemical Oxygen Demand	20 ± 2.5

3.2.4 Experimental Set-Up

The experiments were conducted using two lab-scale submerged MPBRs. The reactors were filled with 10 L of culture medium. White LED lamps were used to provide illumination. The reactors were put in a magnet stir to mix the algal solution slightly. The schematic diagram of the experimental set-up is shown in Figure 3.1. Table 3.2 summarizes the basic parameters of the membrane module and the operating conditions. Polyvinylidene fluoride (PVDF) flat sheet membranes with the pore size of 0.4 µm was used. The surface area of the membrane on each side of the module was 0.03 m^2. The membrane module was immersed in 10 L of the suspension. Two flat sheet rectangular graphite electrodes (surface area of 0.015 ± 0.008 m^2) and two stainless steel meshes were placed in the reactors (with the distance of 0.03 m). The EK-MPBR is connected to a DC power supply system, and the MPBR has the same configuration but without DC power supply. The graphite and stainless steel sheets were connected to the positive and the negative poles of a DC power supply (B & K precision's, Taiwan), respectively. A constant DC electric field (0.261 A/m^2) was applied to the microalgae for the entire operation of the EK-MPBR.

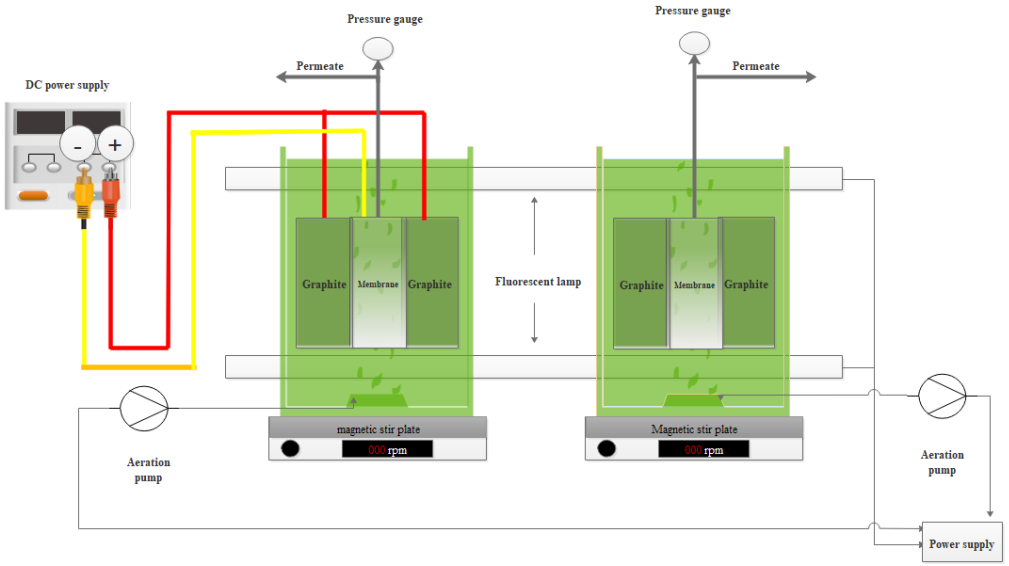

Figure 3-1 Schematic of lab-scale MPBR and EK-MPBR set-up.

Table 3-2 Specification of the membrane module and operating condition

Membrane Module	**MPBR**	**EK-MPBR**
Total membrane surface area	0.03 m^2	0.03 m^2
Membrane materials	Polyvinylidene fluoride (PVDF)	Polyvinylidene fluoride (PVDF)
Membrane type	Flat sheet	Flat sheet
Mean membrane pore size	0.4 µm	0.4 µm
Operational Parameter		
Working volume	10 L	10 L
Temperature	25.75 ± 0.7° C	25.9 ± 0.6° C
pH	8.15 ± 0.15	8.46 ± 0.5
Aeration rate	2.16 ± 0.10 L/min	2.16 ± 0.10 L/min
Illumination intensity	8400 lux	8400 lux
Voltage gradient		0.62 ± 0.02 V/cm
Current density		0.261 A/m^2
Electrodes surface area		0.015 ± 0.008 m^2
Electrodes distance		0.03 m

3.2.5 Zeta Potential and Routine Analysis

The zeta potential of the flocs was determined by using a NanoBrook ZetaPlus (Brookhaven, NY, USA). The samples were diluted in 1 mM KCl solution. Each sample was tested at least twice to confirm the zeta potential value. Smoluchowski's equation was used to determine the zeta potential [41]. A dissolved oxygen (DO) meter (Model 407510, Extech, Nashua, NH, USA), a pH meter (pH 700, Oakton, VA, USA), and a thermometer were used to measure the DO, pH, and temperature of the suspension in the reactor.

3.2.6 Determination of Biomass Characteristics

The MLSS and COD were measured using the standard method [42]. Biomass productivity was calculated based on the following equation [43]:

$$r_x = X \times \frac{Q_{waste}}{V_{MPBR}} = \frac{X}{SRT} \qquad (3.1)$$

where, r_x is biomass productivity (mg/L.d); X is the average biomass concentration (g/L), which in this study equals to average MLSS; Q waste is the reactor biomass wasting rate (L/d), and VMPBR is its working volume (L).

Total nitrogen and phosphorus (TN, TP) were monitored on samples taken every other day. Each sample was duplicated, and the values reported are the averages for each sample. Both TN and TP were measured by spectrophotometry using the alkaline potassium persulfate digestion-UV spectroscopy method [39,44] and the ammonium molybdate spectroscopy method, respectively [44].

3.2.7 Particle Size Distribution and Microalgae Structure

The particle size distribution was measured by a Malvern Mastersize 2000 instrument (Worcestershire, UK) with detention of 0.02–2000 μm. Each sample was measured in triplicate. The range of laser obscuration was 0.1–0.4%.

The structure of the algal cell was studied by an inverted microscope (Olympus IX51, Tokyo, Japan). For each picture, the samples were dropped onto a slide, followed by dispersion with a cover slide. To gather images, each sample was randomly photographed with a digital camera connected to a microscope.

3.2.8 Statistical Analysis

The statistical difference of the parameters in MPBR and EK-MPBR was determined by two-sample t-tests, with the alpha significance level at 0.05 ($p = 0.05$). If $P < 0.05$, the null hypothesis, the mean values corresponding to the parameters are not statistically different, is rejected. The results are presented as mean ± standard deviation. Each sample was at least duplicated and the standard deviation for each data point represents an average of at least two data.

3.3 Results and Discussion

In this study, the performance of the electrokinetic-assisted photobioreactor on phycoremediation is investigated and compared with a control photobioreactor. The effect of the electric field is classified in terms of biomass production, nutrient removal, zeta potential, pH, and floc morphology.

3.3.1 Effect of EF treatment on biomass production

We investigated the effect of the applied electric field on algae growth in photobioreactors. The MLSS concentration was measured and used as an indicator of algal growth throughout the study. The time course measuring the MLSS concentration of the reactor is shown in Figure 3.2. Both MPBRs operated in parallel with an initial concentration of 1.16 ± 0.4 g/L of MLSS. The biomass value and productivity of the control reactor (MPBR) varied from 0.97 g/L to 2.12 g/L and 32.33–70.66 g/Ld, respectively. For the EK-MPBR, the corresponding values were lower than the control, with biomass ranging from 0.62 g/L to 1.59 g/L of MLSS and productivity ranging from 18–53 mg/Ld. However, these values were not significantly different ($p > 0.05$).

In the EK-MPBR, MLSS fluctuation over the first 39 days of the experiment was smoother and relatively higher compared to the control MPBR. This improved productivity suggests that the applied electric field stimulated the growth of microalgae. The present study is consistent with the findings of others that the electric field increased the productivity of *Chlorella vulgaris* by enhancing the transport of substances across the algae cell membrane [45,46]. However, the underlying reason for the stimulated cell growth has remained unknown [46]. The hormetic response of low-dose stimulation and high-dose inhibition seen in Figure 3.2 is an adaptive cell response that is stimulatory in the short term and inhibitory in long-term exposure [47] was also observed in the pre-treatment of *Chlorella vulgaris* with the application of a short-term moderate electric field [13].

Corpuz et al. studied the effect of a long-term applied electric field bioreactor, where they observed a similar trend in the algae-activated sludge bioreactor [2]. In the study of Corpuz et al., it was mentioned that more prolonged exposure to the electric field inhibited microalgae growth starting on day 28. This retardation of microalgae, which is caused mainly by electrochemical reactions around the cathode, was delayed in this study until day 39. Indirect oxidation due to the modified design of the cathode in our study could play a role in growth inhibition caused by hydroxyl radicals. By placing the cathode behind the membrane, the released ions in the permeate could be removed by the permeate pump, and therefore, their accumulation over time is controlled. The indirect oxidation effect on the molecular level in MPBRs could be the focus of future studies.

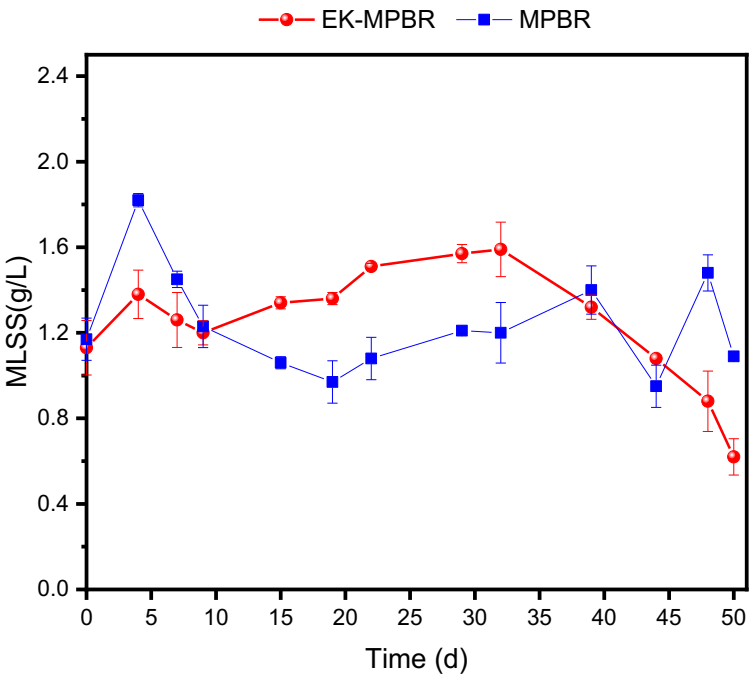

Figure 3-2 Variation of biomass production for MPBRs with and without applied electric field over the experimental period of 49 days. Values and error bars represent average and standard deviation from two technical replicate measurements (n = 2), respectively. Average pH value and temperature for both EK-MPBR and the control MPBR were around 8 and 25 ° c.

3.3.2 Nutrient Removal and Wastewater Treatment Potential

The wastewater treatment performance of EK-MPBR was compared to the control MPBR to determine electric field efficiency in terms of nutrient removal from the wastewater. The efficiency of a phycoremediation system is defined by how well algae can remove nitrogen, phosphorus, and COD from wastewater. Figure 3.3 shows the percentage of nutrient removal of EK-MPBR and MPBR over time. The concentrations of N, P, and COD in the influent were maintained constant at the levels of 25 ± 2 mg/L, 3.5 ± 0.3 mg/L, and 20 ± 2.5 mg/L, respectively. EK-MPBR showed a statistically significant higher phosphorous removal with an overall removal of 97.98 ± 0.02% ($p < 0.05$). This demonstrates the advantage of EK-MPBR for phosphorus removal compared to the overall removal of 41.81 ± 0.05% of the control reactor. The main two phosphorus removal mechanisms in algal systems are biomass adsorption and precipitation of phosphorus [2,25]. In an electric field-assisted system, electrochemical oxidation on the surface of the electrodes and electrochemical reactions in the suspension can also contribute to phosphorus removal. Given a

pH range of 7.5 to 8.5 for EK-MPBR, phosphorus adsorption on the surface of the anode (graphite) is not the dominant mechanism [48]. The improved phosphorus removal in EK-MPBR can be attributed to the occurrence of electrochemical reactions in the suspension and the overall ion strength in the mixed liquor solution [33,49]. A recent study showed that in biomass combined with activated sludge, the applied electric field improved phosphorus removal by 65% compared to its control reactor and was mainly due to electrochemical reactions [2]. The released aluminum ions from the aluminum anode and the generation of phosphate aluminum complex contribute to the removal of phosphorus [50,51]. Although a number of studies have evaluated the effect of electric field on MBRs [2,33,52,53], its effect on molecular adsorption in MPBRs needs to be verified in future studies.

Limited phosphate concentration in the suspension in EK-MPBR can lower the biomass productivity and removal efficiency caused by a low biomass concentration [54]. However, this is in contrast to the MLSS concentration (Figure 3.2). As such, it is likely that the stimulating effect of the electric field outweighed the inhibitory effect of P depletion. Furthermore, the limited phosphate concentration in the suspension in EK-MPBR is beneficial for reducing membrane fouling. The correlation between P depletion and biofilm growth has been reported by other studies [55,56]. The low concentration of P, ranging from 0.05 mg/L to 1.09 mg/L in EK-MPBR, is below the concentration needed for biofilm growth compared to the control MPBR, ranging from 1.79 to 2.39 mg/L [49]. This suggests the existing potential of EK-MPBR for enhanced membrane performance.

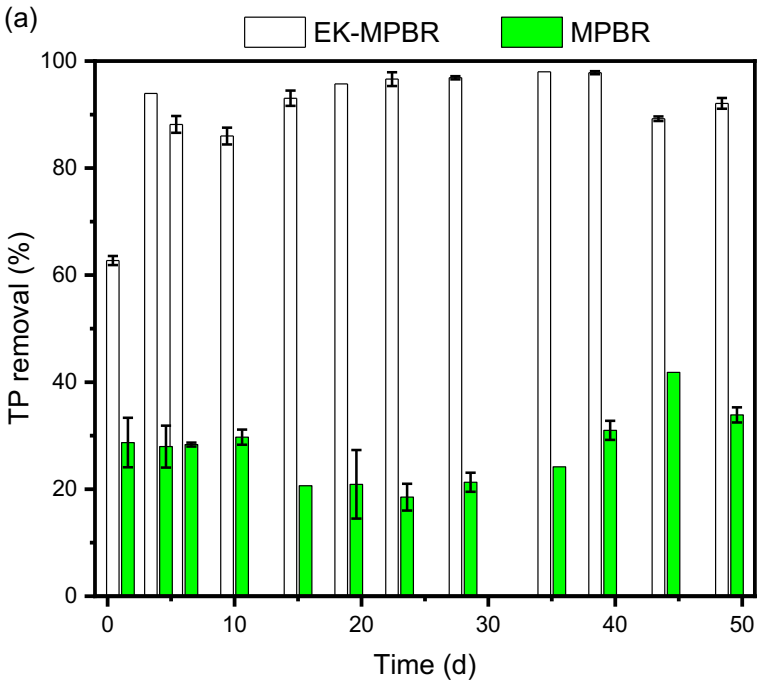
(a)
EK-MPBR
MPBR
TP removal (%)
Time (d)
0
20
40
60
80
100
0
10
20
30
40
50

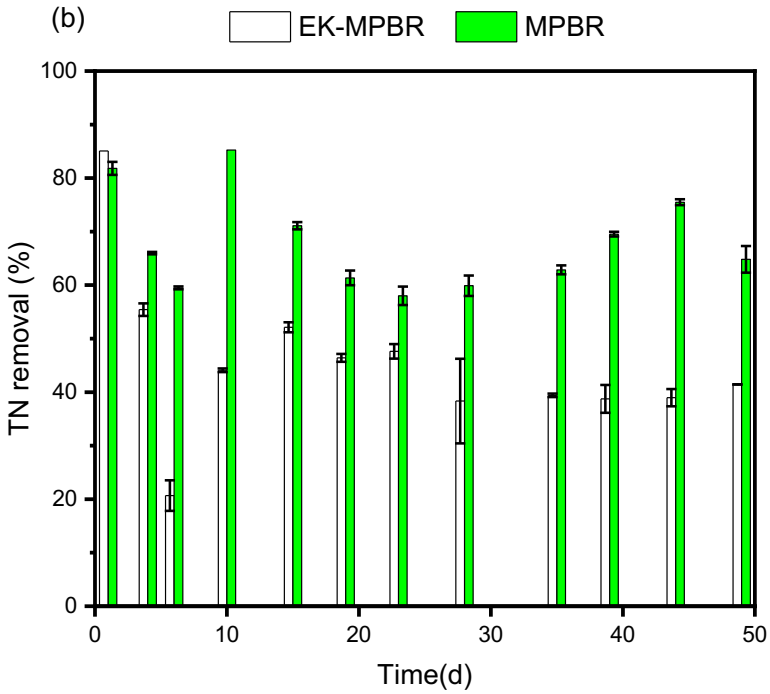
(b)
EK-MPBR
MPBR
TN removal (%)
Time(d)
0
20
40
60
80
100
0
10
20
30
40
50

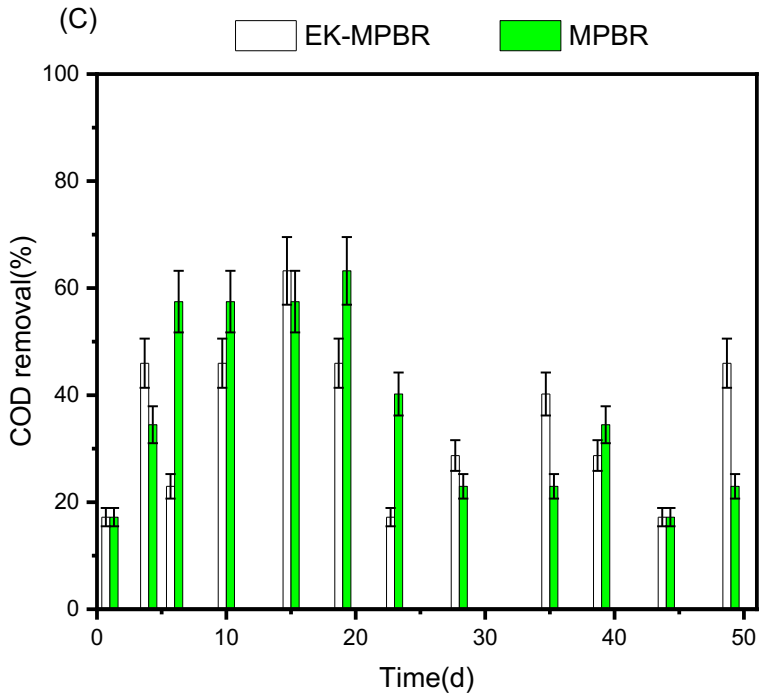

Figure 3-3 Nutrient removal of MPBR and EK-MPBR: (a) comparison of TP removal efficiency, (b) TN removal efficiency, and (c) COD removal efficiency. Values and error bars represent average and standard deviation from two technical replicate measurements (n = 2), respectively.

Despite the significant phosphorus removal of EK-MPBR, the nitrogen removal efficiency of EK-MPBR was depressed to some extent. The better phosphorous removal efficiency compared to the nitrogen removal efficiency in EK-MPBR might be because of their different removal mechanisms. At the water-oxide interface, phosphate removal utilizes an inter-sphere adsorption mechanism that is less affected by ionic strength as compared to nitrogen removal, which has an outer-sphere adsorption mechanism [48]. As shown in Figure 3.3b, EK-MPBR TN removal ranged from 17.82% to 85%, whereas in control MPBR, TN was removed by 58% to 85% ($p < 0.05$). The concentration of TN in the influent was kept at a constant value of 25 ± 2 mg/L for both reactors. The lower nitrogen removal efficiency agrees with other studies that showed that the electric field might interfere with the nitrogen removal process [33,57,58]. The fluctuation over the 49 days in TN removal in EK-MPBR could be attributed to the change in MLSS concentration (Figure 3.2a), zeta potential (Figure 3.4), and ionic strength of the suspension, which may have interfered with nitrification. The lower nitrogen removal in EK-MPBR due to the presence of an

electric field agrees with the study by Zhang et al. [33]. The potential changes in ionic properties of the microalgae could be due to the electrochemical reactions and the incorporation of the electric field, which further have an inhibitory impact on the removal of total nitrogen [33]. However, both EK-MPBR and MPBR showed nitrogen removal comparable to other studies (Table 3.3).

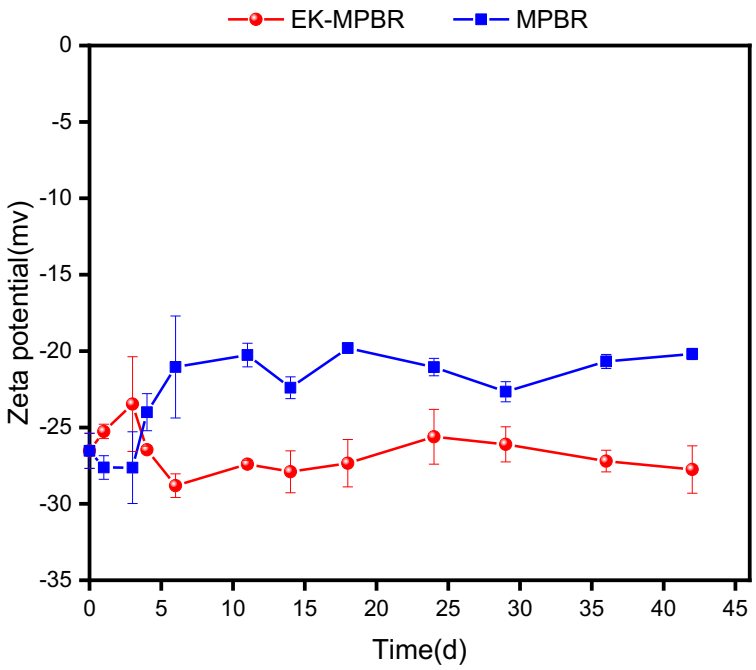

Figure 3-4 Zeta potential variation during EK-MPBR and MPBR operations. Values and error bars represent average and standard deviation from three technical replicate measurements (n = 3), respectively.

Table 3-3 The removal efficiency of MPBRs with *Chlorella vulgaris.*

Source of Water/Wastewater	Type of MPBR	Influent Concentration (mg/L)	Organic Loading Rate (mg/L.d)	HRT and SRT (d)	Membrane Pore Size (μm)	Removal Efficiency%	Ref.
Synthetic municipal wastewater effluent	MPBR	TN: 25 ± 2 TP: 3.5 ± 0.4	TN:10.58 ± 1.02 TP:1.48 ± 0.2	HRT: 2.5 SRT: 30	0.4	68 ± 3 of TN 41.81 ± 0.05 of TP	This Study
Synthetic municipal wastewater effluent	EK-MPBR	TN: 25 ± 2 TP: 3.5 ± 0.4	TN: 10.58 ± 1.02 TP: 1.48 ± 0.2	HRT: 2.5 SRT:30	0.4	43 ± 2 of TN 97.98 ± 0.02 of TP	This Study
Synthetic municipal wastewater	MPBR	N/A		HRT: 2.5 SRT:12.5	N/A	50 of TN 50 of TP	[59]

Synthetic municipal wastewater	MPBR	TN: 14.1 ± 0.5 TP: 2.5 ± 0.2	HRT: 1 SRT: 9	0.04	31 of TN 30 of TP	[43]
Synthetic municipal wastewater	MPBR	TN: 14.1 ± 0.5 TP: 2.5 ± 0.2	HRT: 1 SRT: 30	0.04	32 of TN 25 of TP	[43]

Figure 3.3 c represents the COD concentration over the experimental period. The influent COD concentration for both reactors was kept constant at 20 ± 1.8 mg/L. The COD reduction can be attributed to the thickness of the biofilm, electrochemical oxidation of organic substances, and oxidation of the organic compounds by electrochemically generated oxidants such as hydrogen peroxide [2]. In this study, due to the induced multiple factors, further investigation is needed before highlighting any underlying reasons as the main mechanism of COD removal in EK-MPBR when comparing it with MPBR.

3.3.3 Effect of EF on the Physiology of Microalgae

Zeta potential, pH, and the morphology of biomass are measured as indicators of changes in physiology under the electric field and their effect on the phycoremediation efficiency [60,61]. In both MPBRs, the zeta potential remained negative over the experimental period. Zeta potential is dependent on factors such as pH and ion type and strength [62]. In alkaline conditions, zeta potential increases (i.e., becomes more negative) with pH increase as particles are surrounded by more negative charge in the suspension. The zeta potential values, represented in Figure 3.3, along with the pH data depicted in Figure 3.4, agree with the above statement.

The zeta potential in the control MPBR was higher than that of EK-MPBR. This can be attributed to the higher pH in the reactor compared to EK-MPBR [62]. Furthermore, zeta potential is a function of other factors, such as the composition and concentration of metabolites in the suspension [62]. This could explain the fluctuating behaviour, especially over the first days of the operation, when the microalgae have unstable conditions due to adaptation to the new environment.

Surface charge, as represented by the zeta potential here, can contribute to the nutrient uptake efficiency of the system [63]. In an alkaline solution, the predominant phosphate ions are HPO_4^{2-} and PO_4^{3-} [64]. The higher the surface charge, the stronger the electrostatic repulsion would

interfere with the adsorption of these ions on the algal cell surface [64,65]. Reportedly, the lower surface charge positively affects the adsorption of the orthophosphate by *C. vulgaris* [65].

Sedimentation is another mechanism of phosphorus removal from wastewater that is also affected by surface charge and electrostatic repulsion [66,67]. The phosphate ions form complex salts in wastewater, such as calcium phosphate in the form of sediments [67]. The lower surface charge would enhance sedimentation and phosphorus removal. Therefore, as shown in Figure 3.4, the decreased zeta potential in EK-MPBR (−27 compared to −20 mv in MPBR) can be attributed to the better phosphorus removal efficiency in EK-MPBR (97.98 ± 0.02% in EK-MPBR compared to 41.81 ± 0.05% in MPBR).

The nitrogen removal, however, was affected differently by the surface charge. Due to the increased surface charge, the adsorption of negatively charged hydroxyl ions (OH) that are part of the denitrification process could be decreased [68]. The effect of the electric field on this removal pathway can be further verified through electrochemical analysis of the cells in future studies.

The variation of pH with time is shown in Figure 3.5. While both reactors started with the same pH, the applied electric field lowered pH over time. The electrochemical reaction around the cathode is a determining factor [69]. In alkaline conditions, the following reaction at the cathode can be expected:

$$2H_2O + 2\,e^- \rightarrow H_2(g) + 2\,OH^-(aq) \quad (3.2)$$

As a result of this electrolysis reaction, the pH near the cathode is expected to increase under the applied electric field. However, the results show that other factors may be involved in pH changes. One of the underlying reasons for pH changes could be the materials used and impurities that arise during the strengthening of the carbon in the manufacturing process, which could be released from the electrode to the suspension when placed under the electric field [70].

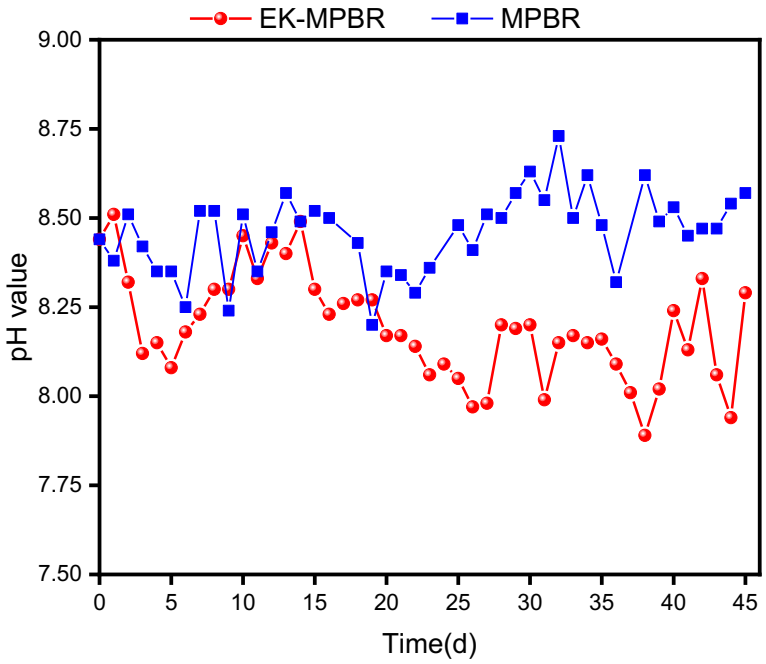

Figure 3-5 pH variation during EK-MPBR and MPBR operations

.

pH is also sensitive to the mechanism of microalgae growth. Considering glucose in the influent, the suspension provides a mixotrophic and/or heterotrophic culture for *C. vulgaris* growth. In both cases, mixotrophic and heterotrophic, pH depends on the microalgae's preferred growth kinetics. While the pH remained unchanged in the mixotrophic condition, heterotrophic culture showed a gradual decrease in the suspension [71]. As shown in Figure 3.6, the lighter suspension over time under the electric field demonstrates heterotrophic dominancy and, therefore, decreased pH.

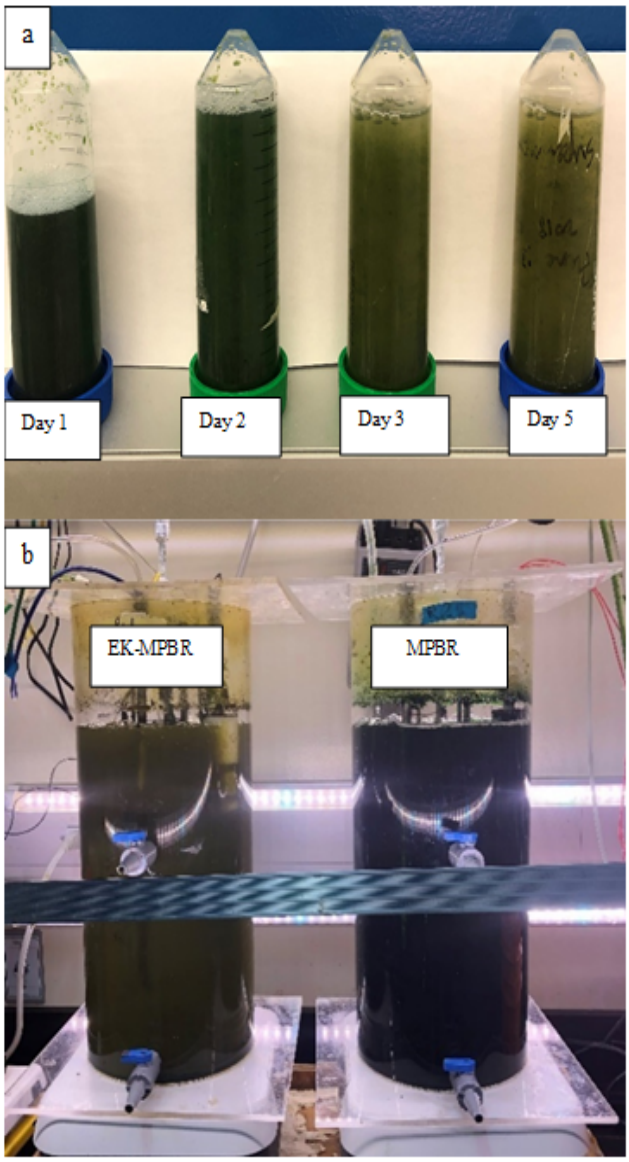

Figure 3-6 The colour of microalgae grown in (a) EK-MPBR from day 1 to day 5 and (b) EK-MPBR and MPBR at day 20.

Figure 3.7 shows the morphology of the suspensions in MPBR and EK-MPBR. One of the main objectives of this investigation is to study possible morphology changes due to the applied electric field. As shown in Figure 3.6, the floc size in the EK-MPBR is smaller than that of the MPBR. This agrees with the higher fraction of smaller particles seen in the particle size distribution (PSD) analysis (Figure 3.8). The fraction of the smaller particles in EK-MPBR (Figure 3.8) can be attributed to floc breakage and disintegration due to the applied electric field and the

electrophoresis phenomenon. Electrophoresis and movement of the charged particles could result in more breakage of the flocs [49]. In electrophoresis, the charged particles tend to move toward the electrode with the opposite charge, which can cause collisions and smaller particle formation. This potentially explains the formation of smaller flocs in EK-MPBR. The conceptual image of the phenomena is presented in Figure 3.9.

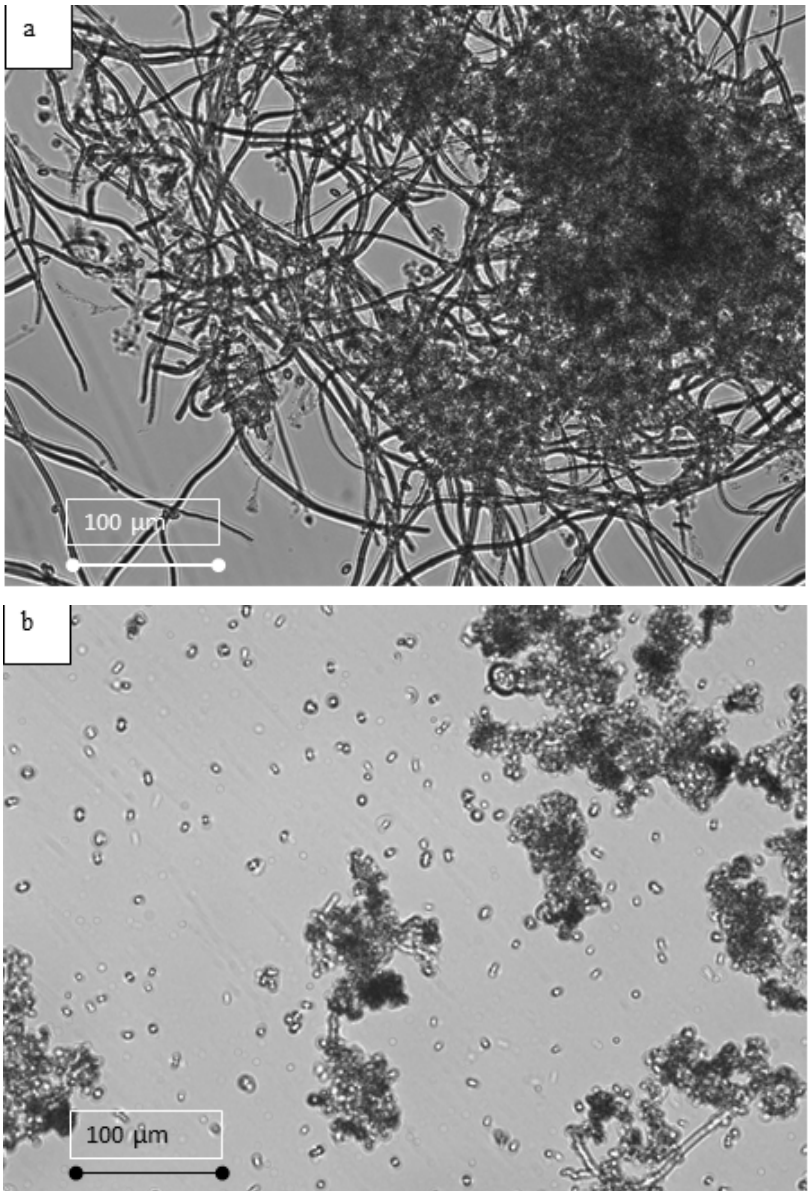

Figure 3-7 Microscopic images representing the morphology of C. vulgaris in (a) MPBR and (b) EK-MPBR.

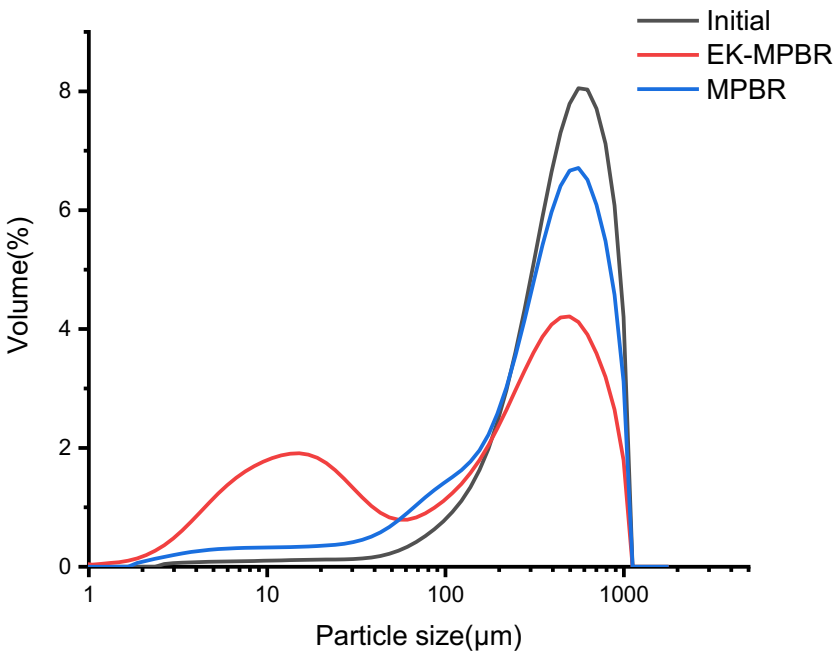

Figure 3-8 Particle size distribution of the floc suspension in the MPBR and EK-MPBR.

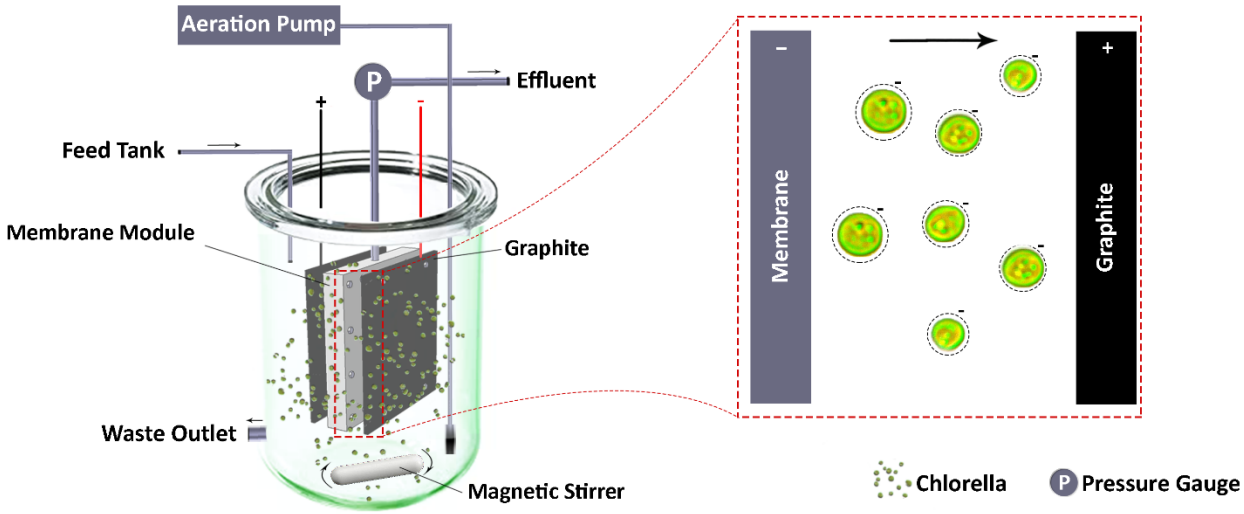

Figure 3-9 Conceptual figure of the electrophoresis movement of charged particles toward the opposite electrode in EK-MPBR.

3.4 Conclusions

A modified membrane photobioreactor that incorporated a low-voltage electric field and the algae *C. vulgaris* was developed. This novel study compared the biomass production and the nitrogen and phosphorus removal efficiency of *C. vulgaris* in the electrokinetic-assisted membrane bioreactor with that of the control.

The biomass production in the EK-MPBR was comparable to that in the MPBR. Nutrient removal was lower and significantly higher in EK-MPBR for total nitrogen and total phosphorus, respectively. This can be explained by electrochemical reactions around the electrodes. The results also showed that increased cell charge and formation of smaller particles under the applied electric field was observed, which may affect biomass production.

The work presented here has implications for future studies of the electric field in MPBRs and may help modify the design of membrane photobioreactors for membrane fouling control. Further research identifying the mortality rate of the algae under different applied currents, molecular changes, and electrokinetically affected assimilation efficiency of the cells will be beneficial for improving electro-phycoremediation techniques in wastewater treatments.

3.5 References

1. Touliabah, H.E.-S.; El-Sheekh, M.M.; Ismail, M.M.; El-Kassas, H. A Review of Microalgae-and Cyanobacteria-Based Biodegradation of Organic Pollutants. *Molecules* **2022**, 27, 1141.
2. Corpuz, M.V.A.; Borea, L.; Senatore, V.; Castrogiovanni, F.; Buonerba, A.; Oliva, G.; Ballesteros Jr, F.; Zarra, T.; Belgiorno, V.; Choo, K.-H. Wastewater treatment and fouling control in an electro algae-activated sludge membrane bioreactor. *Science of the total environment* **2021**, 786, 147475.
3. Lavrinovičs, A.; Murby, F.; Zīverte, E.; Mežule, L.; Juhna, T. Increasing Phosphorus Uptake Efficiency by Phosphorus-Starved Microalgae for Municipal Wastewater Post-Treatment. *Microorganisms* **2021**, 9, 1598.
4. Sousa, C.A.; Sousa, H.; Vale, F.; Simões, M. Microalgae-based bioremediation of wastewaters-Influencing parameters and mathematical growth modelling. *Chemical engineering journal* **2021**, 425, 131412.

5. Priyadharshini, S.D.; Babu, P.S.; Manikandan, S.; Subbaiya, R.; Govarthanan, M.; Karmegam, N. Phycoremediation of wastewater for pollutant removal: A green approach to environmental protection and long-term remediation. *Environmental pollution* **2021**, 290, 117989.
6. Wu, P.; Zhang, X.; Wang, X.; Wang, C.; Faustin, F.; Liu, W. Characterization of the start-up of single and two-stage Anammox processes with real low-strength wastewater treatment. *Chemosphere* **2020**, 245, 125572.
7. Karthik, V.; Saravanan, K.; Bharathi, P.; Dharanya, V.; Meiaraj, C. An overview of treatments for the removal of textile dyes. *Journal of chemical and pharmaceutical sciences* **2014**, 7, 301-307.
8. Verma, R.; Suthar, S.; Chand, N.; Mutiyar, P.K. Phycoremediation of milk processing wastewater and lipid-rich biomass production using Chlorella vulgaris under continuous batch system. *Science of the total environment* **2022**, 833, 155110.
9. Bilad, M.; Azizo, A.; Wirzal, M.; Jia, L.J.; Putra, Z.; Nordin, N.; Mavukkandy, M.; Jasni, M.; Yusoff, A. Tackling membrane fouling in microalgae filtration using nylon 6, 6 nanofiber membrane. *Journal of environmental management* **2018**, 223, 23-28.
10. Gao, F.; Li, C.; Yang, Z.-H.; Zeng, G.-M.; Feng, L.-J.; Liu, J.-z.; Liu, M.; Cai, H.-w. Continuous microalgae cultivation in aquaculture wastewater by a membrane photobioreactor for biomass production and nutrients removal. *Ecological engineering* **2016**, 92, 55-61.
11. Lee, J.-C.; Baek, K.; Kim, H.-W. Semi-continuous operation and fouling characteristics of submerged membrane photobioreactor (SMPBR) for tertiary treatment of livestock wastewater. *Journal of cleaner production* **2018**, 180, 244-251.
12. Walter, U.; Beyer, M.; Klein, J.; Rehm, H.-J. Degradation of pyrene byRhodococcus sp. UW1. *Applied Microbiology and Biotechnology* **1991**, 34, 671-676.
13. Nezammahalleh, H.; Ghanati, F.; Adams II, T.A.; Nosrati, M.; Shojaosadati, S.A. Effect of moderate static electric field on the growth and metabolism of Chlorella vulgaris. *Bioresource technology* **2016**, 218, 700-711.

14. Serra-Maia, R.; Bernard, O.; Gonçalves, A.; Bensalem, S.; Lopes, F. Influence of temperature on Chlorella vulgaris growth and mortality rates in a photobioreactor. *Algal research* **2016**, 18, 352-359.
15. Zhang, M.; Lee, E.; Vonghia, E.; Hong, Y.; Liao, B. Introduction to aerobic membrane bioreactors: Current status and recent developments. *In Current Developments in Biotechnology and Bioengineering*; *Elsevier*: **2020**; pp. 1-23.
16. Bokhary, A.; Maleki, E.; Hong, Y.; Hai, F.I.; Liao, B. Anaerobic membrane bioreactors: Basic process design and operation. *In Current developments in biotechnology and bioengineering; Elsevier:* **2020**; pp. 25-54.
17. Luo, Y.; Le-Clech, P.; Henderson, R.K. Simultaneous microalgae cultivation and wastewater treatment in submerged membrane photobioreactors: a review. *Algal research* **2017**, 24, 425-437.
18. Bilad, M.; Arafat, H.A.; Vankelecom, I.F. Membrane technology in microalgae cultivation and harvesting: a review. *Biotechnology advances* **2014**, 32, 1283-1300.
19. Zhang, M.; Leung, K.-T.; Lin, H.; Liao, B. Membrane fouling in a microalgal-bacterial membrane photobioreactor: Effects of P-availability controlled by N: P ratio. *Chemosphere* **2021**, 282, 131015.
20. Katırcıoğlu Sınmaz, G.; Erden, B.; Şengil, İ. Cultivation of Chlorella vulgaris in alkaline condition for biodiesel feedstock after biological treatment of poultry slaughterhouse wastewater. *International journal of environmental science and technology* **2022**, 1-10.
21. Kothari, R.; Pandey, A.; Ahmad, S.; Singh, H.M.; Pathak, V.V.; Tyagi, V.; Kumar, K.; Sari, A. Utilization of Chlorella pyrenoidosa for Remediation of Common Effluent Treatment Plant Wastewater in Coupling with Co-relational Study: An Experimental Approach. *Bulletin of environmental contamination and toxicology* **2022**, 108, 507-517.
22. Safi, C.; Zebib, B.; Merah, O.; Pontalier, P.-Y.; Vaca-Garcia, C. Morphology, composition, production, processing and applications of Chlorella vulgaris: A review. *Renewable and sustainable energy reviews* **2014**, 35, 265-278.
23. Gao, Y.; Yang, M.; Wang, C. Nutrient deprivation enhances lipid content in marine microalgae. *Bioresource technology* **2013**, 147, 484-491.

24. San Pedro, A.; González-López, C.; Acién, F.; Molina-Grima, E. Marine microalgae selection and culture conditions optimization for biodiesel production. *Bioresource technology* **2013**, 134, 353-361.
25. Schmidt, J.J.; Gagnon, G.A.; Jamieson, R.C. Microalgae growth and phosphorus uptake in wastewater under simulated cold region conditions. *Ecological engineering* **2016**, 95, 588-593.
26. Arrojo, M.Á.; Regaldo, L.; Calvo Orquín, J.; Figueroa, F.L.; Abdala Díaz, R.T. Potential of the microalgae Chlorella fusca (Trebouxiophyceae, Chlorophyta) for biomass production and urban wastewater phycoremediation. *AMB Express* **2022**, 12, 1-14.
27. Salgado, E.M.; Gonçalves, A.L.; Sánchez-Soberón, F.; Ratola, N.; Pires, J.C. Microalgal cultures for the bioremediation of urban wastewaters in the presence of siloxanes. *International journal of environmental research and public health* **2022**, 19, 2634.
28. Huang, H.; Zhong, S.; Wen, S.; Luo, C.; Long, T. Improving the efficiency of wastewater treatment and microalgae production for biofuels. *Resources, conservation and recycling* **2022**, 178, 106094.
29. Novoa, A.F.; Fortunato, L.; Rehman, Z.U.; Leiknes, T. Evaluating the effect of hydraulic retention time on fouling development and biomass characteristics in an algal membrane photobioreactor treating a secondary wastewater effluent. *Bioresource technology* **2020**, 309, 123348.
30. Qiu, S.; Yu, Z.; Hu, Y.; Chen, Z.; Guo, J.; Xia, W.; Ge, S. An evolved native microalgal consortium-snow system for the bioremediation of biogas and centrate wastewater: Start-up, optimization and stabilization. *Water research* **2021**, 196, 117038.
31. Gordalina, M.; Pinheiro, H.M.; Mateus, M.; da Fonseca, M.M.R.; Cesário, M.T. Macroalgae as Protein Sources—A Review on Protein Bioactivity, Extraction, Purification and Characterization. *Applied sciences* **2021**, 11, 7969.
32. Buchmann, L.; Böcker, L.; Frey, W.; Haberkorn, I.; Nyffeler, M.; Mathys, A. Energy input assessment for nanosecond pulsed electric field processing and its application in a case study with Chlorella vulgaris. *Innovative food science and emerging technologies* **2018**, 47, 445-453.

33. Zhang, J.; Satti, A.; Chen, X.; Xiao, K.; Sun, J.; Yan, X.; Liang, P.; Zhang, X.; Huang, X. Low-voltage electric field applied into MBR for fouling suppression: Performance and mechanisms. *Chemical engineering journal* **2015**, 273, 223-230.
34. Canelli, G.; Tevere, S.; Jaquenod, L.; Dionisi, F.; Rohfritsch, Z.; Bolten, C.J.; Neutsch, L.; Mathys, A. A novel strategy to simultaneously enhance bioaccessible lipids and antioxidants in hetero/mixotrophic Chlorella vulgaris as functional ingredient. *Bioresource technology* **2022**, 126744.
35. Salamati Mashhad, N. Investigation of activated sludge properties under different electrical field and in the presence of calcium. *Concordia University*, **2010**.
36. Su, F.; Liang, Y.; Liu, G.; Mota Filho, C.R.; Hu, C.; Qu, J. Enhancement of anti-fouling and contaminant removal in an electro-membrane bioreactor: significance of electrocoagulation and electric field. *Separation and purification technology* **2020**, 248, 117077.
37. Giwa, A.; Dindi, A.; Kujawa, J. Membrane bioreactors and electrochemical processes for treatment of wastewaters containing heavy metal ions, organics, micropollutants and dyes: Recent developments. *Journal of hazardous materials* **2019**, 370, 172-195.
38. Asif, M.B.; Maqbool, T.; Zhang, Z. Electrochemical membrane bioreactors: state-of-the-art and future prospects. *Science of the total environment* **2020**, 741, 140233.
39. Zhang, M.; Leung, K.-T.; Lin, H.; Liao, B. The biological performance of a novel microalgal-bacterial membrane photobioreactor: Effects of HRT and N/P ratio. *Chemosphere* **2020**, 261, 128199.
40. Muñoz, R.; Jacinto, M.; Guieysse, B.; Mattiasson, B. Combined carbon and nitrogen removal from acetonitrile using algal–bacterial bioreactors. *Applied microbiology and biotechnology* **2005**, 67, 699-707.
41. Shaw, D.J. Introduction to colloid and surface chemistry; Butterworths: **1980**.
42. Federation, W.E.; Association, A. Standard methods for the examination of water and wastewater. American Public Health Association (APHA): Washington, DC, USA **2005**, 21.

43. Luo, Y.; Le-Clech, P.; Henderson, R.K. Assessment of membrane photobioreactor (MPBR) performance parameters and operating conditions. *Water research* **2018**, 138, 169-180.
44. China, E. Monitoring and analysis methods for water and wastewater. *China Environmental science press, Beijing* **2002**, 232-235.
45. Haberkorn, I.; Buchmann, L.; Hiestand, M.; Mathys, A. Continuous nanosecond pulsed electric field treatments foster the upstream performance of Chlorella vulgaris-based biorefinery concepts. *Bioresource technology* **2019**, 293, 122029.
46. Buchmann, L.; Mathys, A. Perspective on pulsed electric field treatment in the bio-based industry. *Frontiers in bioengineering and biotechnology* **2019**, 265.
47. Sharma, A.; Kaur, T.; Singh, H.; Kaur, G. Intermittent Fasting–Dietary Restriction as a Biological Hormetin for Health Benefits. *In The Science of Hormesis in Health and Longevity; Elsevier*: **2019**; pp. 99-104.
48. Zong, E.; Wei, D.; Wan, H.; Zheng, S.; Xu, Z.; Zhu, D. Adsorptive removal of phosphate ions from aqueous solution using zirconia-functionalized graphite oxide. *Chemical engineering journal* **2013**, 221, 193-203.
49. Wei, C. Nutrient removal and fouling reduction in electrokinetic membrane bioreactor at various temperatures. University of Manitoba, **2009**.
50. Guo, M.; Feng, L.; Liu, Y.; Zhang, L. Electrochemical simultaneous denitrification and removal of phosphorus from the effluent of a municipal wastewater treatment plant using cheap metal electrodes. Environmental Science: *Water research and technology* **2020**, 6, 1095-1105.
51. Bani-Melhem, K.; Smith, E. Grey water treatment by a continuous process of an electrocoagulation unit and a submerged membrane bioreactor system. *Chemical engineering journal* **2012**, 198, 201-210.
52. Liu, L.; Liu, J.; Gao, B.; Yang, F. Minute electric field reduced membrane fouling and improved performance of membrane bioreactor. *Separation and purification technology* **2012**, 86, 106-112.

53. Akamatsu, K.; Lu, W.; Sugawara, T.; Nakao, S.-i. Development of a novel fouling suppression system in membrane bioreactors using an intermittent electric field. *Water research* **2010**, 44, 825-830.
54. Choi, H.J.; Lee, S.M. Effect of the N/P ratio on biomass productivity and nutrient removal from municipal wastewater. *Bioprocess and biosystems engineering* **2015**, 38, 761-766.
55. Wu, J.; Chen, F.; Huang, X.; Geng, W.; Wen, X. Using inorganic coagulants to control membrane fouling in a submerged membrane bioreactor. *Desalination* **2006**, 197, 124-136.
56. Fan, F.; Zhou, H.; Husain, H. Use of chemical coagulants to control fouling potential for wastewater membrane bioreactor processes. *Water environment research* **2007**, 79, 952-957.
57. Liu, L.; Liu, J.; Gao, B.; Yang, F.; Chellam, S. Fouling reductions in a membrane bioreactor using an intermittent electric field and cathodic membrane modified by vapor phase polymerized pyrrole. *Journal of membrane science* **2012**, 394, 202-208.
58. Bani-Melhem, K.; Elektorowicz, M. Performance of the submerged membrane electro-bioreactor (SMEBR) with iron electrodes for wastewater treatment and fouling reduction. *Journal of membrane science* **2011**, 379, 434-439.
59. Marbelia, L.; Bilad, M.R.; Passaris, I.; Discart, V.; Vandamme, D.; Beuckels, A.; Muylaert, K.; Vankelecom, I.F. Membrane photobioreactors for integrated microalgae cultivation and nutrient remediation of membrane bioreactors effluent. *Bioresource technology* **2014**, 163, 228-235.
60. Matho, C.; Schwarzenberger, K.; Eckert, K.; Keshavarzi, B.; Walther, T.; Steingroewer, J.; Krujatz, F. Bio-compatible flotation of Chlorella vulgaris: Study of zeta potential and flotation efficiency. *Algal research* **2019**, 44, 101705.
61. Abt, V.; Gringel, F.; Han, A.; Neubauer, P.; Birkholz, M. Separation, characterization, and handling of microalgae by dielectrophoresis. *Microorganisms* **2020**, 8, 540.
62. Wei, C.; Huang, Y.; Liao, Q.; Xia, A.; Zhu, X.; Zhu, X. Analysis of the energy barrier between Chlorella vulgaris cells and their interfacial interactions with cationic starch under different pH and ionic strength. *Bioresource technology* **2020**, 304, 123012.

63. Rashid, M.; Price, N.T.; Pinilla, M.Á.G.; O'Shea, K.E. Effective removal of phosphate from aqueous solution using humic acid coated magnetite nanoparticles. *Water research* **2017**, 123, 353-360.
64. Gizaw, A.; Zewge, F.; Kumar, A.; Mekonnen, A.; Tesfaye, M. A comprehensive review on nitrate and phosphate removal and recovery from aqueous solutions by adsorption. AQUA—*Water Infrastructure, Ecosystems and society* **2021**, 70, 921-947.
65. Markou, G.; Depraetere, O.; Vandamme, D.; Muylaert, K. Cultivation of Chlorella vulgaris and Arthrospira platensis with recovered phosphorus from wastewater by means of zeolite sorption. *International journal of molecular sciences* **2015**, 16, 4250-4264.
66. González, L.E.; Cañizares, R.O.; Baena, S. Efficiency of ammonia and phosphorus removal from a Colombian agroindustrial wastewater by the microalgae Chlorella vulgaris and Scenedesmus dimorphus. *Bioresource technology* **1997**, 60, 259-262.
67. Hu, B.; Min, M.; Zhou, W.; Li, Y.; Mohr, M.; Cheng, Y.; Lei, H.; Liu, Y.; Lin, X.; Chen, P. Influence of exogenous CO2 on biomass and lipid accumulation of microalgae Auxenochlorella protothecoides cultivated in concentrated municipal wastewater. *Applied biochemistry and biotechnology* **2012**, 166, 1661-1673.
68. Sakakibara, Y.; Kuroda, M. Electric prompting and control of denitrification. *Biotechnology and bioengineering* **1993**, 42, 535-537.
69. Ibeid, S.; Elektorowicz, M.; Oleszkiewicz, J. Modification of activated sludge properties caused by application of continuous and intermittent current. *Water research* **2013**, 47, 903-910.
70. Luo, S.; Griffith, R.; Li, W.; Peng, P.; Cheng, Y.; Chen, P.; Addy, M.M.; Liu, Y.; Ruan, R. A continuous flocculants-free electrolytic flotation system for microalgae harvesting. *Bioresource technology* **2017**, 238, 439-449.
71. Chojnacka, K.; Marquez-Rocha, F.-J. Kinetic and stoichiometric relationships of the energy and carbon metabolism in the culture of microalgae. *Biotechnology* **2004**, 3, 21-34.

Chapter 4 Comparison of sludge properties and membrane performance of membrane photobioreactors with/without electric field

Abstract

A novel low-voltage DC electrokinetic membrane photobioreactor (EK-MPBR) was operated in parallel to a control MPBR without an electric field for 57 days to study membrane fouling and sludge properties for synthetic municipal wastewater treatment. Stainless steel mesh and graphite sheet were used as cathode and anode, respectively, with a novel design of electrode configuration. Less fouling and better sludge settleability were observed under the steady current of 4 mA in the EK-MPBR. The backwash flux induced by electrophoresis and the electric field was 6.5 % of the water flux (0.57 LMH). The fouling precursors were found to have a correlation with the applied electric field. Soluble microbial product (SMP) was reduced by 30 to 43 % in EK-MPBR as compared to MPBR over the experimental period and was found to have a positive correlation with fouling depression. Extra polymeric substances (EPS), however, were higher in EK-MPBR. The cake layer resistance was consistently less in the EK-MPBR than in the control MPBR indicating that the electric field reduced the accumulation of the particles on the surface of the membrane. The pore blocking resistance, however, was higher in EK-MPBR due to the presence of smaller colloidal particles. Particle size distribution (PSD) results showed a greater fraction of smaller floc size under the electric field effect. Sludge volume index (SVI) measurements showed improved settleability of the flocs in EK-MPBR. The electric field showed multiple effects leading to 50 percent less fouling frequency compared to the control MPBR.

4.1 Introduction

Membrane photobioreactors (MPBRs) have become an established technology for simultaneous microalgae growth and wastewater treatment [1,2]. Wastewater contains nutrients such as nitrogen and phosphorus and other organic compounds that can reduce dissolved oxygen in the water [3]. The nutrients in wastewater are a good source of algae growth and are removed by algae. Therefore, MPBRs that incorporate phycoremediation with the production of concentrated microalgae, has become an emerging technology in recent years[4,5].

The membrane, as the central part of this process, would have a reduced lifetime as a result of membrane fouling in the suspension. The presence of organic and inorganic materials from microorganisms and the contaminants in wastewater can cause fouling of the membrane. Membrane fouling increases the operation and maintenance cost and decreases the performance of MPBR [6]. Standard methods for combating fouling in membrane technologies include physical fouling control such as backwash and air sparging [7], chemical cleaning[8,9], electrical[10], biological[11], and operational approaches [12]. Among these methods, electrically assisted fouling control shows great potential and is preferred over other traditional methods due to its low environmental footprint and high durability [13,14]. With the addition of a cathode and an anode, the charged particles and the liquid move due to the produced electrokinetic phenomena. This movement can lower the fouling rate and improve membrane permeability by preventing the precipitation and accumulation of particles on the surface of the membrane. Moreover, the electro-generated gases around the electrodes improve membrane cleaning [15]. Hence, applying the electric field leads to control of the movement and deposition of the foulants. In recent years, electrically-assisted fouling control has made some progress in addressing fouling [16]. Some studies have tried different electrode materials to improve electrooxidation and filterability in membrane bioreactors (MBR)[17-19]. Corpuz et al. studied the implication of applied electric field in MBR with the combination of activated sludge and algae [20]. Even though there are excellent established electrically-assisted fouling controls in conventional activated sludge membrane bioreactors [13,20,21], the utilization of electric current in MPBRs is not investigated yet.

The use of the electric field and the electrode material could raise the cost of MPBRs. Hence, this study aims to alleviate fouling, while maintaining low cost by using a low-voltage DC electric

field with a modified design to improve the lifetime of the membrane. Our EK-MPBR design incorporated a graphite sheet and a stainless-steel mesh as anode and cathode, respectively. This EK-MPBR was run parallel with a control MPBR to investigate the effect of a low-voltage DC electric field on the sludge properties, membrane performance, and fouling.

4.2 Materials and methods

4.2.1 MPBR and EK-MPBR set-up and operation

Synthetic municipal wastewater (Table 4.1) was prepared and treated using a lab-scale membrane photobioreactor (MPBR) and an electric field-assisted membrane photobioreactor (EK-MPBR). The wastewater contained 25 mg/L of total nitrogen, 3.5 mg/L of total phosphorus, and 20 mg/L of chemical oxygen demand (COD). A membrane module was immersed in an effective volume of 10 L of the reactors with two configurations. In order to apply an electric field in EK-MPBR, the conventional membrane module was modified (Figure 4.1). The Figure shows that a stainless-steel mesh was used as a membrane as a support and cathode. Graphite anodes were positioned at 0.03 m facing the membranes. DC electric field was applied with a current of 4 mA. Other parameters regarding the membrane modules in EK-MPBR and MPBR were identical in both MPBRs. The membrane with a pore size of 0.4 μm was purchased from SINAP Co. Ltd, Shanghai, China. The pre-cultivated *Chlorella Vulgaris* microalgae were used to treat the wastewater. The aeration intensity at the bottom of the membrane module was 2.2 ± 0.05 L/min in each MPBR for CO_2 delivery and membrane fouling control. The permeate flux of both reactors was kept constant at approximately 8.5 L/m^2h. The reactors were operated for almost 57 days, and hydraulic retention time (HRT) and solid retention time (SRT) were maintained at approximately 2.5 days and 30 days, respectively. The temperature of the algal suspension remained relatively unchanged at around room temperature and was monitored daily. Physical cleaning was conducted to maintain the flux and remove the foulants when the transmembrane pressure (TMP) reached at about 45 kPa. Chemical cleaning was performed at the end of the phase to study the contribution of each filtration resistance. NaOCl solution (1 %) followed by Citric acid solution (2 g/L) were used for chemical cleaning. The membrane was soaked for 2 hours in each solution and the permeability test was performed afterward.

Table 4-1 Characteristics of the synthetic wastewater

Water Quality Index	Average Value (g/L)
Nitrogen	0.025
Phosphorus	0.0035
COD	0.020
Compounds	
NaCl	0.0025
$MgSO_4.7H_2O$	0.082
$CaCl_2.2H_2O$	0.005
$FeSO_4.7H_2O$	0.02490
$ZnSO_4.7H_2O$	0.00044
$MnCl_2.4H_2O$	0.00022
$Na_2MoO_4.2H_2O$	0.00126
$CuSO_4.5H_2O$	0.00039
$CoCl_2.6H_2O$	0.00041
NH_4Cl	0.09553
KH_2PO_4	0.01537
$NaHCO_3$	0.3

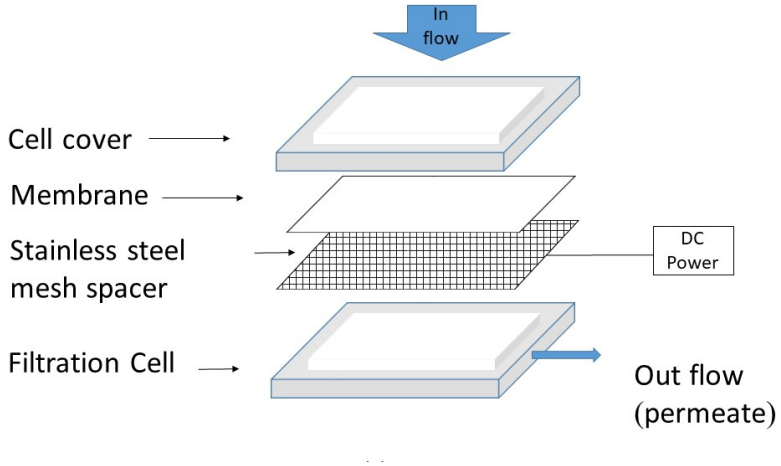

Figure 4-1 Schematic of a membrane module (on one-side of the module) in an EK-MPBR.

4.2.2 Evaluation of membrane filtration resistance

According to Darcy's law, the filtration resistance of the membrane can be calculated as follow [22]:

$$R = \frac{\Delta P}{J\mu} \tag{4.1}$$

$$R_t = R_m + R_p + R_c \tag{4.2}$$

Where, ΔP is the trans-membrane pressure difference (kPa); J implies the permeate flux (L/m^2.h); μ is the dynamic viscosity of the permeate (Pa.s); R represents the filtration resistance (m^{-1}); $R_t, R_m, R_p,$ and R_c are the total filtration resistance, virgin membrane filtration resistance, pore-clogging resistance and cake layer resistance, respectively.

These values were obtained according to the following procedure: R_m was measured using tap water and the permeability test of the virgin membrane before starting the runs. R_c and R_p can be calculated by measuring the permeability of the fouled membrane after the physical and chemical cleaning, respectively [22]. R_t, the total resistance can be obtained from the final permeability and TMP at the end of the experiment.

4.2.3 Particle size distribution (PSD)

Particle size distribution was determined by Malven Mastersize 2000 instrument (Worcestershire, UK) with a detection range of 0.02-2000 µm. The samples were automatically measured in triplicate.

4.2.4 Extracellular polymeric substances (EPS) and soluble microbial products (SMP) extraction and measurement

Soluble microbial product (SMP) was extracted by centrifuging the suspension at 4000 × g for 10 min. The supernatant was filtered through 0.45 µ filter paper. Extracellular polymeric substances (EPS) extraction was measured using the method mentioned by Tong et al. for algal suspension [23]. The suspension was added to 25 ml of 1.5 M NaCl at 30°C for one hour, followed by centrifugation at 2504 g for 15 min. The supernatant was then filtered through a 0.45 µ Nitrocellulose filter paper (Merk, Ireland). The EPS and the SMP were then normalized as the sum of protein and carbohydrates according to Lowry's and Gaudy's methods, respectively. Based on these methods, colorimetric analysis using bovine serum albumin (BSA) and glucose as standards can determine the contents of protein using Lowry's method and carbohydrates using Gaudy's method and Anthrone reagent in the solution [24,25].

4.2.5 *Capillary suction time (CST) and sludge volume index (SVI)*

The harvesting potential of microalgae suspension was undertaken by measuring CST using a Triton Type 319 Multi-purpose CST (Triton Electronics Limited., UK), and the method described by the literature [26]. CST is the rate that water is released from the biomass. A lower CST generally suggests a longer water release time and better dewaterability/filterability [27]. All the measurements were performed in triplicate. In the case of different MLSS concentrations in the reactors, the dilution or concentration was performed to exclude the effect of biomass concentration from harvesting potential. SVI was tested according to APHA 21st Edition [28].

4.2.6 Statistical analysis

The parameters of MPBR and EK-MPBR were subjected to paired two samples t-tests to differentiate data statistically. Data is considered significantly different if the p-value is lower than 0.05.

4.3 Results

4.3.1 Novel Design of the Electrodes Configuration

As shown in Figure 4.1, a novel design of the electrode's configuration was presented. For the first time, the stainless steel mesh cathode was embedded on flat membrane module support and underneath the flat-sheet membrane. This novel design is totally different from that found in the literature [17,19,20,29] and is anticipated to generate a direct and strong repulsive force from the membrane surface to prevent the deposition and adhesion of negatively charged cells and colloids polymers on the membrane surface for fouling control. This concept was verified in this study and would be elaborated on in later sections.

4.3.2 Membrane fouling performance

Figure 4.2 shows the flux of the EK-MPBR and MPBR that was monitored and recorded daily during the experimental period. Under the same operating conditions, the fouling of the

membranes was monitored by transmembrane pressure (TMP). Both reactors exhibited the same TMP during the first ten days, and the membranes could maintain the flux. Between days 10 to 29, the reactors showed different membrane fouling rates during which EK-MPBR showed an earlier TMP increase starting at around day 11 while the conventional MPBR had a delayed but sharper TMP increase from day 23. After the first phase of operation and membrane physical cleaning, as represented in Figure 4.2, the physical cleaning cycle in MPBR was shortened from 29 days to 7 days for the conventional MPBR, while in EK-MPBR, the same cleaning cycle of 29 days was sufficient. The less frequent cleaning in EK-MPBR suggests better and more persistent fouling repression and TMP evolution. This could be explained by the changes in sludge properties and the effect of the applied electric field, which will be explored in later sections.

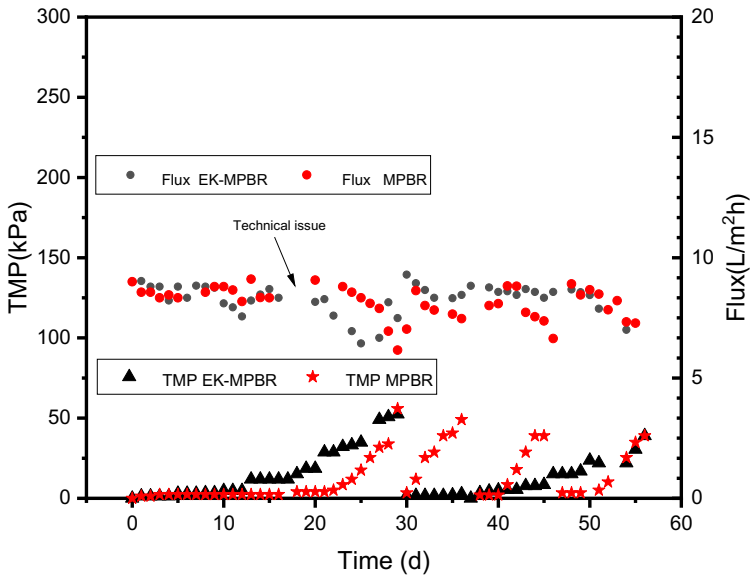

Figure 4-2 Membrane flux and TMP over the experimental period.

4.3.3 Optical image of the cake layer

Figure 4.3 shows the optical image of the fouled membranes at the end of each operation cycle and before each physical cleaning. Visual observation of the images shows different colours and thicknesses of the cake layers formed on the membranes' surface. The EK-MPBR first cake layer

on Day 29 (Figure 4.3 a) was similar to Day 57 (Figure 4.3 b). Images of the MPBR cake layers taken on Days 29, 36, 45 and 57 (Figure 4.3 c, d, e, and f respectively) all showed a thicker greenish cake layer as compared to the thinner, more yellow cake layers of the EK-MPBR.

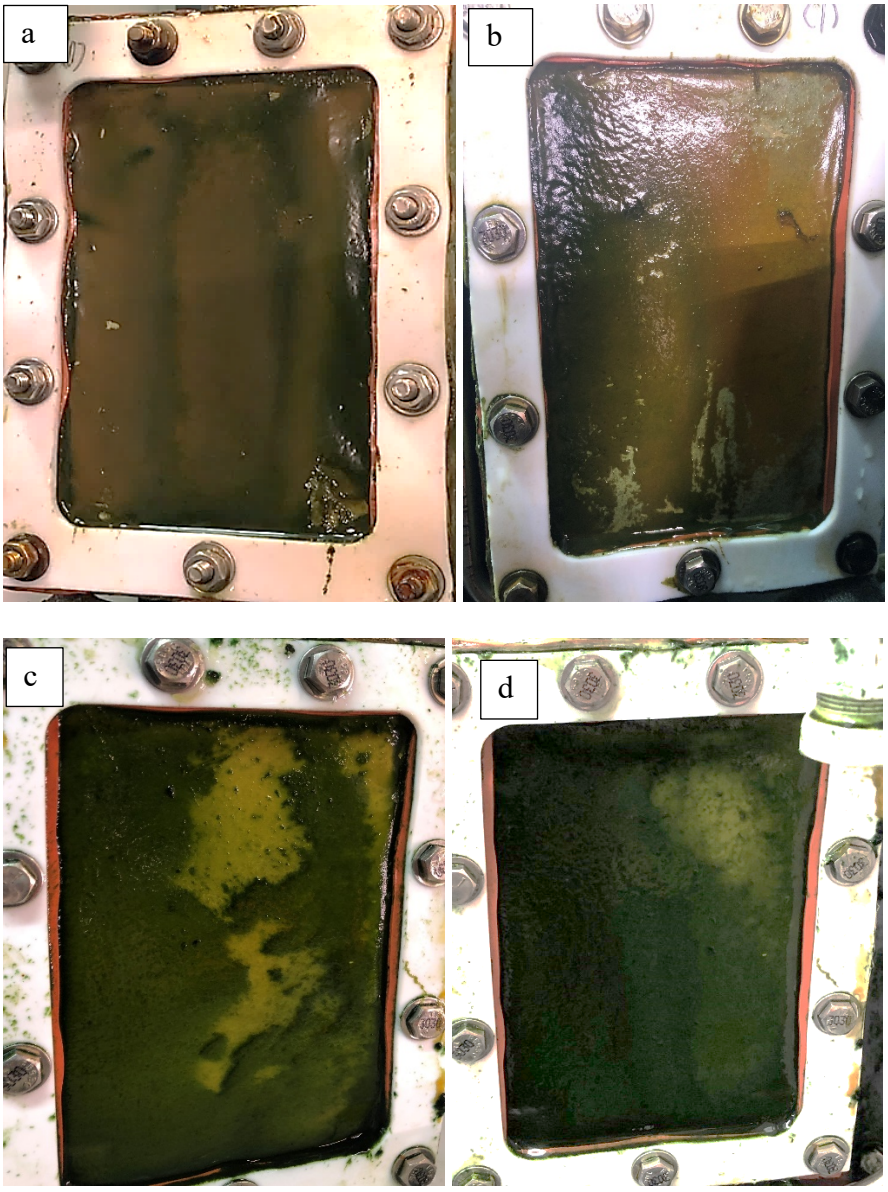

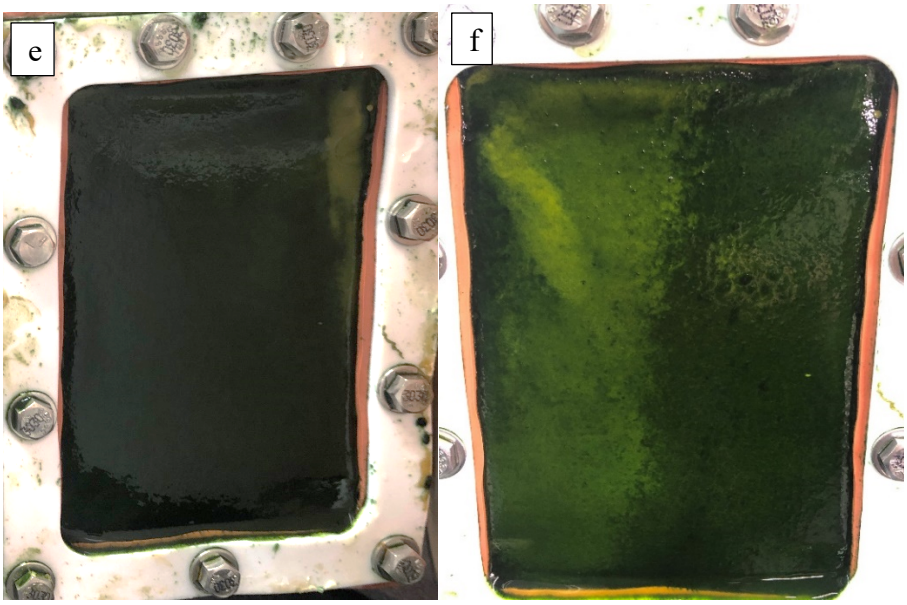

Figure 4-3 Optical image of the cake layer formed on the surface of the membrane. a) EK-MPBR first cake layer, Day 29; b) EK-MPBR second cake layer, Day 57; c) MPBR first cake layer, Day 29; d) MPBR second cake layer, Day 36; e) MPBR third layer, Day 45; f) MPBR forth cake layer, Day 57.

4.3.4 Membrane Filtration Resistances

At the end of the run, the permeability of the membranes was measured after physical and chemical cleaning. Table 4.2 summarizes the filtration resistances in MPBR and EK-MPBR. This measurement can help identify the dominant fouling mechanism and the contribution of different mechanisms in MPBRs. The membrane filtration resistances did not differ greatly between MPBR and EK-MPBR, with the exception of R_p, which was only 0.34% in MPBR and 7.99% in EK-MPBR.

Table 4-2 Compositions of membrane filtration resistances

	$R_m(\times 10^{12}\ m^{-1})$	$R_p(\times 10^{12}\ m^{-1})$	$R_c(\times 10^{12}\ m^{-1})$	$R_t(\times 10^{12}\ m^{-1})$
MPBR	0.176 (0.93%)	0.641(0.34%)	18.765 (98.73%)	19.01 (100%)
EK-MPBR	0.183 (1.12%)	1.315 (7.99%)	14.955 (90.89%)	16.45 (100%)

4.3.4 Floc size distribution during the experimental period

4.3.4.1 Floc size distribution of biomass in the suspension

Particle size distribution is one of the factors affecting membrane fouling [30,31]. Figure 4.4 shows the changes in the size distribution of the biomass in EK-MPBR and MPBR over the experimental period. The particle size distribution indicates that under the electric field effect, a larger portion of small flocs in size range from 1 to 5-50 µm was observed in EK-MPBR, while in the conventional MPBR, there were limited and very small fractions of small flocs less than 5-50 µm. According to Figure 4.4 (a), the portion of smaller flocs increases over time to day 45 in EK-MPBR. By day 59, a unimodal PSD was observed. This might indicate that the change in trend may be observed over a longer operation time with a more significant effect on fouling. In the conventional MPBR, however, biomass's steady-state particle size distribution was observed.

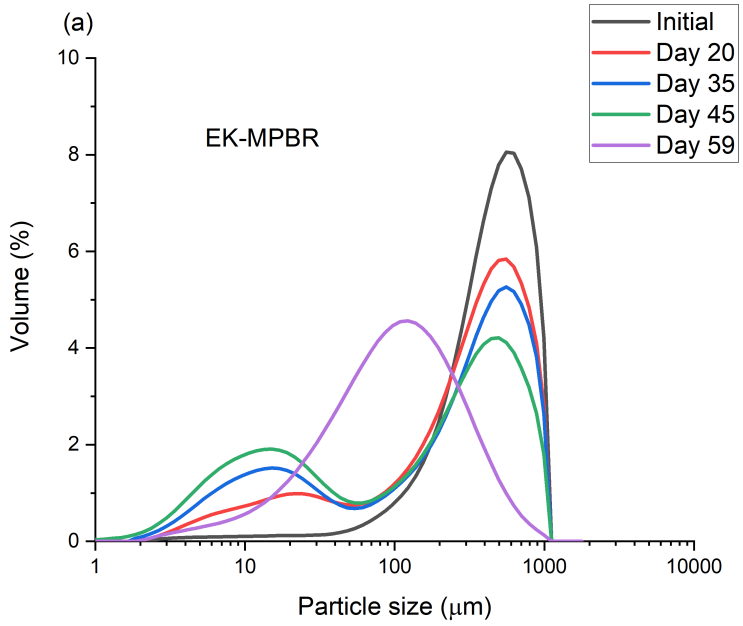

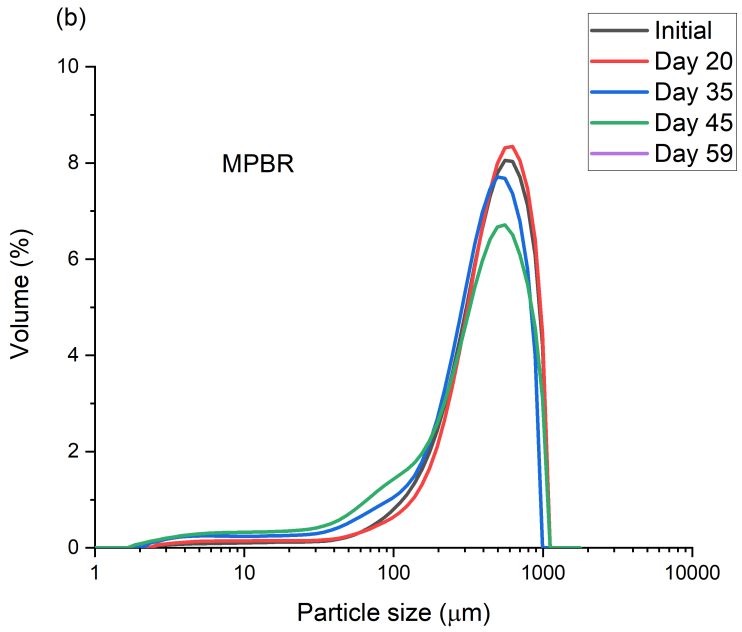

Figure 4-4 Particle size distribution of a) EK-MPBR, b) MPBR.

4.3.4.2 Floc size distribution of the cake layer

Figure 4.5 presents the PSD of the cake layer formed in EK-MPBR and MPBR. While in MPBR, a bimodal distribution was observed, the EK-MPBR showed polymodal distribution with a lower portion of larger flocs between 100-1000 μm. The volume of smaller particles (1-100 μm) in the cake layer of both MPBR showed a significant difference with a larger fraction of these smaller flocs in the cake layer of EK-MPBR. This was consistent with the observation of a larger fraction of small flocs in EK-MPBR biomass suspension.

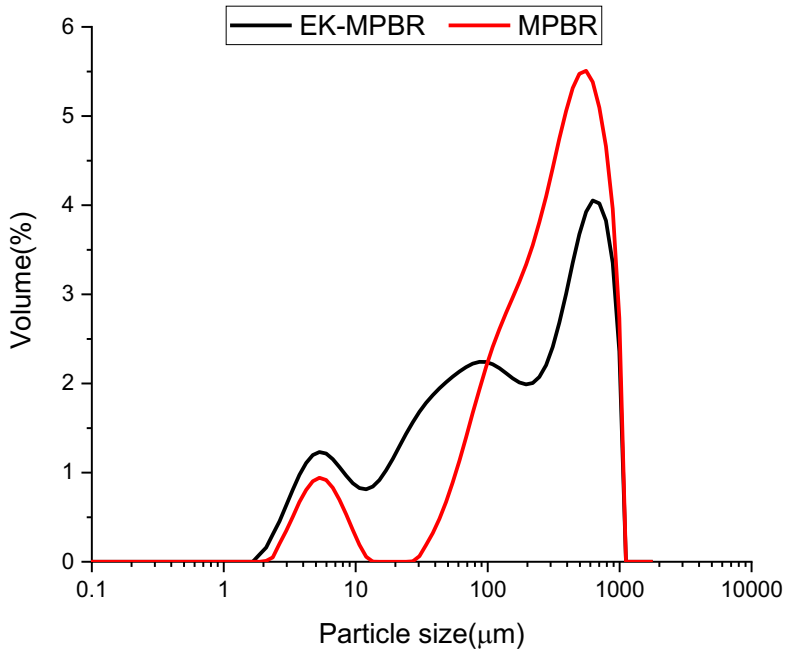

Figure 4-5 Floc size of the cake layer

4.3.5 Extracellular polymeric substances (EPS) and soluble microbial products (SMP) content

Figure 4.6 shows the comparative study of SMP and EPS components with and without the applied electric field. The t-tests showed that the overall average of total SMP, protein and carbohydrate concentrations were comparable in the two reactors ($p>0.05$) (Figure 4.6 (a) vs. Figure 4.6 (b)). However, a significant difference in the total SMP was observed on the same operating day for different MBPRs. The total SMP content in the EK-MPBR was lower than that of the conventional MPBR at the same operating day ($p <0.05$) except for Day 37. As shown in Figure 4.6 (a) and (b), the electric field could lower the total SMP in EK-MPBR. Furthermore, the composition of the SMP with regards to the protein to polysaccharide ratio (PN/PS) was lower and remained relatively unchanged over the experimental period (25 ± 5 %) in EK-MPBR compared to MPBR. Unlike SMP, EPS was not alleviated by the electric field, as shown in Figure 4.6. (c) and (d). EPS is a key

factor for binding cells and enables them to attach to the surface [32]. The composition and the total amount of EPS were used as indicators of the membrane fouling potential [33,34]. The average of the total EPS in MPBR was comparable to EK-MPBR ($p > 0.05$), with proteins being the largest component of EPS in both MPBR and EK-MPBR over the whole experimental period. However, a relatively larger amount of total EPS was observed in the EK-MPBR, as compared to that of the conventional MPBR, on the same day (except for day 37 and 47, which had a similar amount of total EPS) (t-test, $p < 0.05$). Furthermore, the PN/PS ratio in the EPS had a general trend of increase from 1.18 to 1.95 with experimental time in the EK-MPBR, while the PN/PS ratio in the EPS showed an opposite trend of change and decreased from 1.98 to about 1.4 over the experimental period.

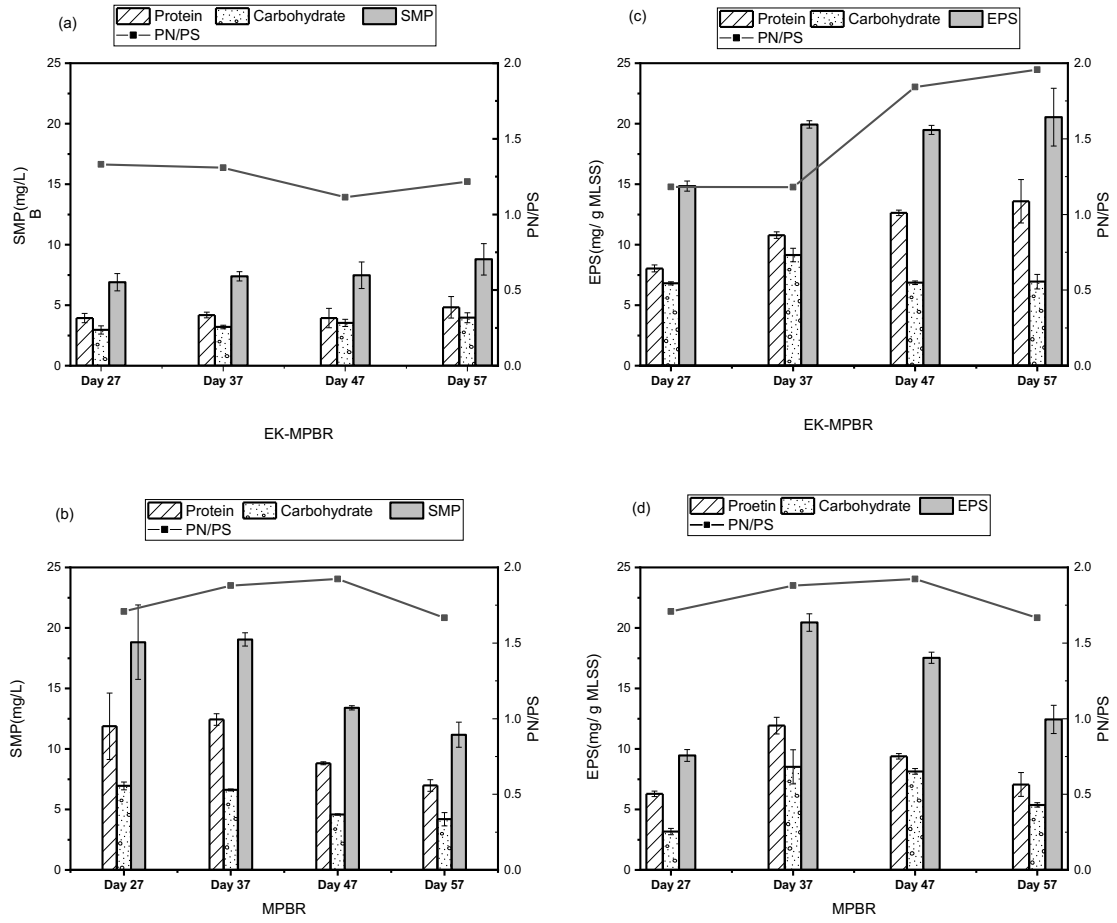

Figure 4-6 Comparison of SMP and EPS components in EK-MPBR and MPBR. Values and error bars represent average and standard deviation from two technical replicate measurements (n = 2), respectively.

4.3.6 The voltage changes vs. transmembrane pressure (TMP)

To further study the effect of the electric field on the cake layer's formation, simultaneous monitoring of transmembrane pressure and voltage was monitored, as illustrated in Figure 4.7.

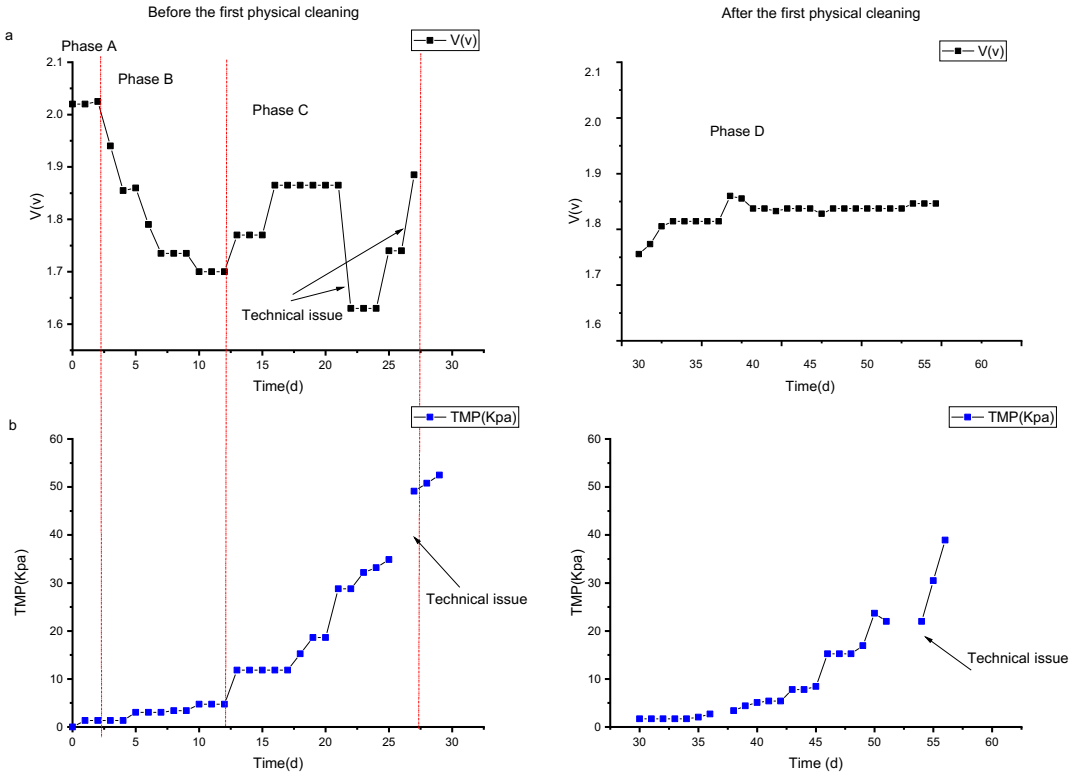

Figure 4-7 Electrical potential and transmembrane pressure changes in EK-MPBR before and after cleaning on day 29.

Phase A is the equilibrium phase between the electrolyte and the membrane. In this phase, the transmembrane pressure is almost constant (Figure 4.7 b). During phase B, the particles in the

suspension start to form a cake layer and the transmembrane pressure increases. In phase C, the voltage shows a stable trend (V=1.85 v). The transition between phases C and D was interrupted by technical issues with the power supply during the operation. Phase D demonstrates the voltage variation after the first physical cleaning (Day 29).

4.3.7 Effect of electric field force

In this study, DC electric field was applied continuously from the start of the experiment. Therefore, its influence on the attached particle and the membrane fouling was worth considering. Furthermore, the design of the membrane module aimed to improve the repulsion introduced by the cathode placed under the membrane. The cathode was placed inside the membrane module so that it could induce a repulsive force from the membrane toward the suspension. The algae biomass has a negative charge and will be repelled from the cathode and move toward suspension under the electric field effect. The movement of the particles toward the anode is in the opposite direction to the water pumped out through the membrane. This repulsive force caused by electrophoresis may have a similar effect to backwash. The equivalent backwash flux caused by the electrophoresis could be calculated below

$$J_{backwash} = \frac{Q_p}{A} = 3.6 \times 10^6 . v_p \quad (4.3)$$

$$v_p = \frac{\varepsilon \zeta}{\mu} E \quad (4.4)$$

$$E = \frac{\Delta U}{d} = \frac{I}{\sigma A} \quad (4.5)$$

Where $J_{backwash}$ is the electric force induced flux and equivalent backwash flux ($^{L}/_{(m^2 . h)}$), Q_p is the flow rate of permeate water ($^{m^3}/_{s}$), A is the effective surface area of the membrane (m^2), v_p is the electrophoretic velocity of charged particles ($^{m}/_{s}$), E is the electric field strength ($^{v}/_{m}$), ζ is the zeta potential of the particles (v), ε is the permittivity of the electrolyte($^{F}/_{m}$), μ is the viscosity of the permeate ($Pa.s$), ΔU is the applied voltage (V), d is the distance between the electrodes (m), I is the applied current (A), and σ is the conductivity of the bulk solution ($^{S}/_{m}$) [35,36].

In the current study, the current was fixed at 0.004 A and the zeta potential in EK-MPBR was -27 ± 3.2 mv. The electrophoresis velocity in EK-MPBR was $(1.45 \pm 0.2) \times 10^{-7}$ $^{m}/_{s}$, resulting in the equivalent backwash flux of (0.52 ± 0.072) $^{L}/_{(m^2h)}$. Given the permeation flux of (8.6 ± 0.5) $^{L}/_{(m^2h)}$, the equivalent backwash flux was approximately 6.5 % of the water flux.

4.3.8 SVI and CST of the microalgae suspension

The SVI is widely used to measure the MLSS settleability in wastewater treatment as an indicator of membrane fouling. At the average temperature of 25.7 ± 0.7 ° C for both reactors, EK-MPBR showed better settleability (SVI ≤ 100 ml/g) (Figure 4.8). The SVI decreased by 95% in EK-MPBR.

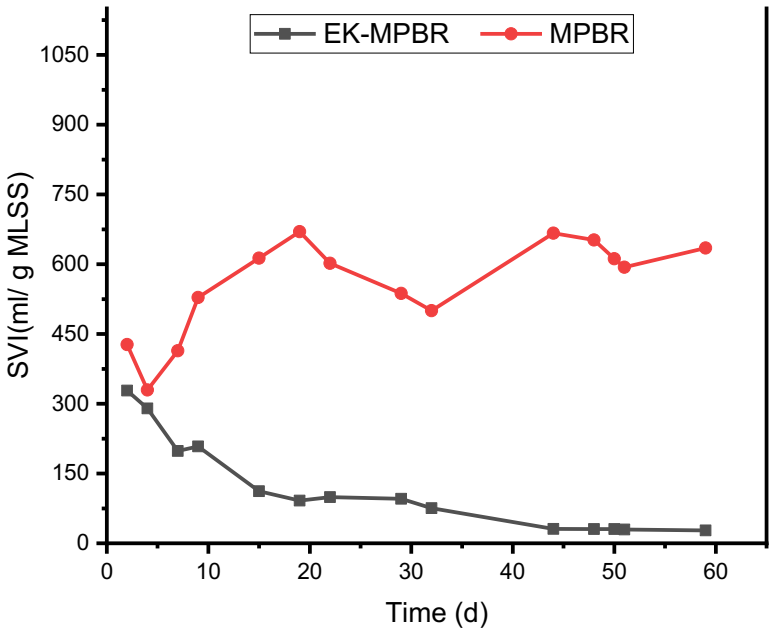

Figure 4-8 SVI over the experimental period

CST is an indicator of the dewaterability of the floc and the filterability potential and a routine quantifying parameter in wastewater treatments and has recently been used in MPBRs as harvesting potential [37,38]. The factors affecting CST are floc size, the concentration of EPS and

its composition [39]. The other factor affecting CST is MLSS concentration. In order to exclude this factor, the CST of both reactors was measured at the MLSS range of 0.9-1.1 g/L and samples were diluted if necessary. According to Figure 4.9, the CST had a higher value in the conventional MPBR at the beginning of this study and then decreased to a lower value after day 7, as compared to that in the EK-MPBR. Under stable operation (after day 29), the CST had a significant higher value, as compared to that in MPBR (t-test, $p < 0.05$, $P = 0.007$), implying that the filterability of sludge in the EK-MPBR was poorer than that of the MPBR, under stable operation.

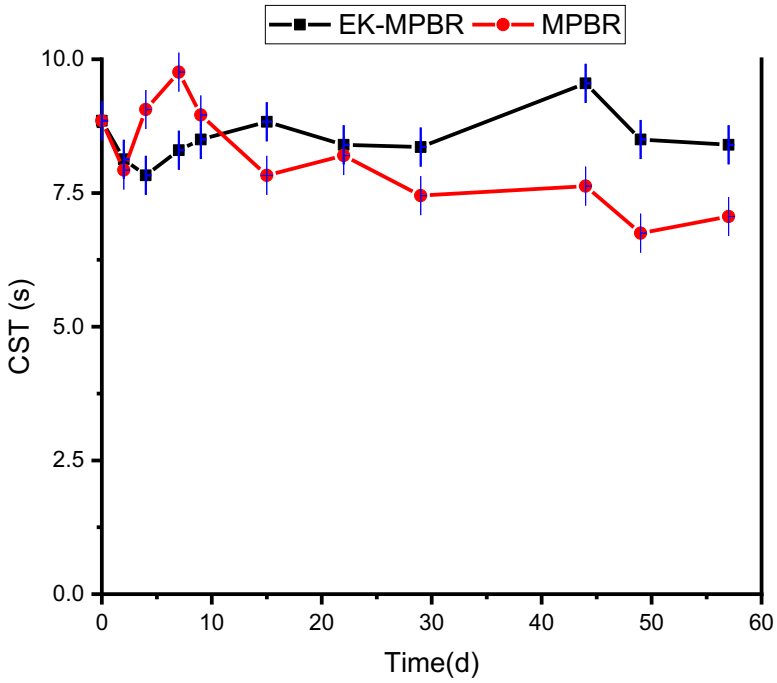

Figure 4-9 Capillary suction time of the algal suspension in MPBRs. Values and error bars represent average and standard deviation from three technical replicate measurements (n = 3), respectively.

4.4 Discussion

4.4.1 Sludge properties

A comparison between Figure 4.4 a and b shows a higher portion of smaller flocs, highlighting the presence of a bimodal distribution in EK-MPBR, in which another peak between 0.1 to 40 μm is seen. This is likely due to the deactivation of bacteria in the presence of an electric field and prevented agglomeration of the cells. With longer exposure and a unimodal particle size distribution could be a result of aggregation of small cells to form larger flocs. This cell agglomeration can be due to the increased total EPS over experimental time in EK-MPBR. By comparing Figure 4.9 and Figure 4.4 a, it can be concluded that with the increase in the size floc in EK-MPBR, the CST increased. This finding is in agreement with the earlier study that indicates that larger flocs correspond to long CST [26]. Generally, the larger flocs contain more bound water and longer CST value. Furthermore, the decreased dewaterability with the decreased floc size could show the effect of electroosmosis induced by the electric field in reducing the bound water from the flocs and, therefore, reducing CST value in EK-MPBR [20,40]. By comparing the floc size of EK-MPBR and that of the control, higher CST in the control MPBR could be expected as the portion of larger algal flocs is higher in MPBR compared to EK-MPBR. However, the contradictory trend observed from comparing CST and floc size can highlight the other contributors to CST value, which are MLSS concentration and total EPS in the two MPBRs. These controlling contributors support the declined dewaterability in EK-MPBR compared to MPBR. There has been also a relation between the lower protein content in MPBR compared to EK-MPBR which is in agreement with the study that indicates the lower humic acid substances and protein contribute to better filterability of algal flocs [41].

As illustrated in Figure 4.8, the settleability of the algae was significantly improved in EK-MPBR ($P < 0.05$). This could be due to the decreased bound water resulting in smaller and denser flocs under the electric field effect. With graphite sheet as an inactivate anode, the dominant electrochemical process involved in the settleability is electroflotation where the released oxygen gas around the anode carries the algal cells to the surface, which would interfere the settleability caused by gravity [42,43]. However, the decreased negatively charged polysaccharides in SMP

content seems to be a governing factor in neutralizing the algal flocs and better settleability of the algal flocs in EK-MPBR [20].

4.4.2 Membrane fouling performance

The membrane fouling in algal-related systems is affected by biomass characteristics such as particle size distribution and organic matter, such as SMP and EPS [44,45]. In EK-MPBR, however, the electric force is an additional contributor to the factors governing fouling. In order to better identify the membrane fouling performance in MPBRs, this discussion focuses on different periods of the cleaning frequency in each reactor. As represented in Figure 4.2, in EK-MPBR a physical cleaning cycle of 29 days was sufficient as opposed to in the MPBR without electricity, cleaning was required every 7 days. The less frequent cleaning in EK-MPBR suggests better and more persistent fouling repression and TMP evolution. It has been argued before that particle size distribution is one of the factors affecting fouling behaviour, with smaller particles leading to more fouling in membrane filtration systems [6,46]. The present study, however, partially confirmed the similar correlation between the size of the particles and fouling which is only seen in the first 29 days of the experiment. From Day 1 to Day 29, before the first cleaning cycle, the increased TMP and its slightly steepened slope in the EK-MPBR corresponded with a higher percentage of smaller particles than in the control MPBR (Figure 4.4). This suggests that the smaller flocs and particles in EK-MPBR could be one of the main contributors to the greater TMP, as discussed earlier. The data in Table 4.1 also support the idea that the larger contribution of the pore blocking resistance is a result of smaller particles in EK-MPBR compared to those in MPBR. As such, it could be predicted that from Day 29 to the end of the experimental period, with increased portion of the smaller particles (Figure 4.4 (a)), the fouling in EK-MPBR may happen faster. The monitored lower TMP in EK-MPBR and simultaneously increased smaller particles, however, is in direct contrast to this prediction and, therefore, other factors such as SMP are involved in observing this behaviour.

As shown in Figure 4.6 (a) and (b), the SMP component in the suspension was lower under the effect of the electric field, corresponding to less fouling frequency in EK-MPBR. The relatively constant SMP contents in the EK-MPBR could further explain the unchanged fouling trend and relatively unchanged cleaning cycle in EK-MPBR. Therefore, a positive correlation between the

fouling behaviour and the SMP was observed in this study. This agrees with other literature that SMP was highly correlated to the fouling rate [47-49]. It also may indicate that the electric field did not stimulate SMP production in EK-MPBR. This is in line with the results observed in the literature [50]. By comparing the protein and carbohydrate content in EK-MPBR and MPBR, it can be concluded that the protein content of the SMP was more affected by the electric field. This agrees with the observation of Corpuz et al. and Ding et al. [20,47] that the applied electric field lowered the protein content of the SMP [20]. The reduced protein content of SMP could be explained by the released oxidant in the biomass suspension, causing degradation and lower concentration of SMP.

As mentioned earlier, EPS is one of the fouling precursors in MPBRs and determining cell-membrane surface and cell-cell interactions (i.e., cake layer formation). According to Figure 4.6 (c), on Day 27, EPS content in EK-MPBR was higher than MPBR, suggesting that the partially higher TMP in the first period (Day 0 - Day 29) is associated with the EPS content. The results for Day 37, Day 47, and Day 57 suggest that the relatively constant EPS resulted in the unchanged rate of fouling in EK-MPBR over the experimental period. However, in MPBR, fluctuation in EPS levels may cause different fouling rates related to higher EPS, resulting in faster cake layer formation on the surface of the membrane and, therefore, increased TMP (see Figure 4.6 (d) and Figure 4.2). The lower EPS content in MPBR may be due to contamination and the presence of bacteria in MPBR and, therefore, degradation of EPS by their activity [20]. On the other hand, the produced oxidant ions in EK-MPBR may have reduced the growth of bacteria in the contaminated suspension.

Many studies have mentioned that the ratio of protein to carbohydrate (PN/PS) can be one of the main factors determining the rate of membrane fouling [20,51,52]. It is assumed that the higher PN/PS ratio of EPS corresponds to a faster fouling rate. In this study, however, the periods of higher PN/PS in EK-MPBR and MPBR were not in accordance with the higher fouling rate. This agrees with a study that PN/PS was not the main contributor to the fouling in MPBRs [53]. Furthermore, the composition of the SMP with regards to the protein to polysaccharide ratio (PN/PS) was lower and remained relatively unchanged over the experimental period (25 ± 5 %) in EK-MPBR compared to MPBR. Thus, the study of the fouling precursors when a low voltage electric field is applied is speculative and complex and requires further investigations [54].

4.4.3 EF contribution to the fouling behaviour

The electric field can contribute to fouling via different mechanisms throughout the experimental run. Electroosmosis can be one of the mechanisms ascribed to reduce filtration resistance and better floc dewaterability [40]. Electroosmosis could be related to the formation of smaller flocs [27]. It has been argued before that the movement of bound water from the flocs due to electroosmosis can lead to decreased floc size and improved dewaterability of the flocs, which in turn can reduce the extent of fouling [55].The present study has confirmed this assumption and is in agreement with findings of others (e.g.[55]) in terms of floc shrinkage. Figure 4.4 indicates that the electroosmosis and applied electric field are related to the floc size distribution changes and comparably higher portion of smaller particles in EK-MPBR compared to the control MPBR. However, as shown in Figure 4.9, the induced electrophoresis adversely affected the dewaterability potential of the flocs and increased CST in EK-MPBR. The presence of large EPS and higher MLSS, on the other hand, contributes to different extents to the dewaterability and fluctuation during the experiment [20,40]. It appears that both EPS and MLSS concentration had a positive correlation with the increased CST and reduced dewaterability potential. Therefore, it seems that the effect of electrophoresis on dewaterability was complex and changed over the experimental period.

Another possible electrokinetic phenomenon accounting for the reduced TMP is electrophoresis. The movement of charged particles towards the opposite electrode can repel the flocs from the surface of the membrane [56]. The electrostatic repulsion of the charged particles and possibly increased hydrophobicity due to lower PN/PS of SMP in EK-MPBR would cause changes in the movement of the particles [56]. Therefore, it is expected that the electrophoresis phenomena induced by the electric field can contribute largely to the fouling mitigation by preventing the initial cell adhesion to the membrane surface and then cake layer surface. The results indicate that the accumulation of the particles on the surface of the membrane and, therefore, TMP was reduced as result of this electrophoretic phenomena. The finding of this study confirms the observation of other groups [20,56]. The observation of smaller flocs on the surface of the membrane (in the cake layer) can also be attributed to this phenomenon (Figure 4.5). The visual observation of the cake

layer shown in Figure 4.3 can further verify the difference between the cake layer formed in EK-MPBR (thinner cake layer) and MPBR (thicker cake layer).

The backwash flux was calculated as an electrophoresis induced flux as explained in section 4.3.8 and is a governing electrophoretic phenomenon. While the equivalent backwash flux was not significant (6.5 % of the water flux), the continuous electrophoretic force and its effect on membrane fouling should not be ignored. The lower TMP in EK-MPBR especially after the first physical cleaning on Day 29, and the relatively constant voltage during the operation can suggest that the induced backwash (back movement of colloids and sludge flocs) could lower the fouling rate in EK-MPBR.

The cake layer, as a result of the backwash, could be loosely bound to the surface of the membrane and could be removed easily by the shear force of aeration [36]. While the contribution of electrophoresis is small compared to aeration, studies show that its effect on the formation of the thin and loosely attached cake layer and therefore lower TMP is one of the main mechanisms in electric field assisted fouling control [35,36]. Thus, it seems likely that the stabilizing effect of the electric field on TMP trend can be related to the backwash flux. Furthermore, the trend in observed voltage change after the first physical cleaning in EK-MPBR may be may align with these observations(Figure 4.7). It can be seen that a stable voltage in phase D was reached faster than in the previous phases. The shortened duration of reaching this stable voltage can suggest that the cake layer was largely removed by the physical cleaning and loosely attached to the membrane. This agrees with the finding of other laboratory investigations [36].

Although these electrokinetic phenomena associated with mitigated fouling in this study agree with other studies in electro-assisted MPBRs [20,57], further investigation by measuring the mass accumulated on the surface of the electrodes and in-situ monitoring of the cake layer formation could reveal more information.

4.4.4 Fouling development

As outlined in Table 4.1, the dominant resistance in both MPBR and EK-MPBR is attributed to the formation of the cake layer, among which EK-MPBR had lower cake resistance by 7.84 %. As shown in Figure 4.4, in EK-MPBR the portion of smaller particles (in a size range from 1 to 100 μm) is higher than in MPBR. Furthermore, the particle size distribution of the cake layer presents

the smaller flocs formed in the cake layer. This can suggest the role of electrostatic repulsion between the particles that may have an inhibitory effect on the accumulation of the flocs on the surface of the membrane and the development of larger flocs in the cake layer (Figure 4.4 PSD of the cake layer). This inhibitory effect of electrostatic repulsion on the cake layer formation agrees with the observation of other studies [58,59].

In EK-MPBR, the pore blocking resistance was more significant than MPBR and was the second contributor to the membrane resistance (Table 4.1). This could also be attributed to the higher portion of smaller flocs during the experimental period (Figure 4.4 (a)). Pore blocking is generally the initial stage of fouling in membrane systems. Instantaneous reduction in particle size and faster TMP increase over the first 29 days may explain the faster fouling development in EK-MPBR compared to MPBR.

The lower fouling rate in EK-MPBR can also be attributed to the inhibitory effect of the electric field on the excess growth of bacteria in the algal suspension [20]. This lowered bacterial contamination under the effect of the electric field can lead to less floc formation and slow down the cake layer formation on the surface of the membrane. Figure 4.4 and Figure 4.5 provide evidence of the smaller floc formed in EK-MPBR both in the suspension and on the surface of the membrane. Furthermore, the lower SVI and enhanced settleability can also contribute to the lower fouling rate in EK-MPBR (Figure 4.8).This agrees with the result reported by Shadi Hassan that argues that electrokinetic process reduced the fouling rate by improving floc settleability and changing the density [60].

4.5 Conclusion

The addition of a low-voltage electric field as a fouling mitigation technique could lower the cleaning frequency by 50% in EK-MPBR compared to MPBR. The physical cleaning cycle was of 29 days was sufficient in EK-MPBR whereas shortened cleaning cycle of 7 days was needed in the control MPBR. The results also highlight that the electric field contributed broadly to reduced fouling, spanning from affecting particle size distribution to the concentration of fouling precursors (EPS and SMP). Electrophoresis, electroosmosis and electrochemical reaction are possible mechanisms to explain the reduced fouling potential in EK-MPBR. The reduced total SMP and its protein content resulted from the applied electric field contributed greatly to the less fouling in

EK-MPBR. The electrophoresis induced flux was another contributor to the fouling mitigation in EK-MPBR. Furthermore, the properties of the cake layer, such as thickness and filterability, differed in EK-MPBR and MPBR. Less cake layer resistance and the formation of smaller flocs in EK-MPBR improved the filterability of the cake layer. Overall, the results suggest that the low-voltage electric field was effective for fouling alleviation. The electrically-assisted fouling control developed in this study is expected lower the operational cost of MPBR as a result of controlled fouling that is a major cost of MPBRs operation and can have implication in treating real municipal wastewater.

4.6 References

1. Bilad, M.; Discart, V.; Vandamme, D.; Foubert, I.; Muylaert, K.; Vankelecom, I.F. Coupled cultivation and pre-harvesting of microalgae in a membrane photobioreactor (MPBR). *Bioresource technology* **2014**, *155*, 410-417.
2. Gao, F.; Li, C.; Yang, Z.-H.; Zeng, G.-M.; Feng, L.-J.; Liu, J.-z.; Liu, M.; Cai, H.-w. Continuous microalgae cultivation in aquaculture wastewater by a membrane photobioreactor for biomass production and nutrients removal. *Ecological engineering* **2016**, *92*, 55-61.
3. Sweity, A.; Ying, W.; Ali-Shtayeh, M.S.; Yang, F.; Bick, A.; Oron, G.; Herzberg, M. Relation between EPS adherence, viscoelastic properties, and MBR operation: Biofouling study with QCM-D. *Water research* **2011**, *45*, 6430-6440.
4. Ye, Y.; Ngo, H.H.; Guo, W.; Chang, S.W.; Nguyen, D.D.; Varjani, S.; Ding, A.; Bui, X.-T.; Nguyen, D.P. Bio-membrane based integrated systems for nitrogen recovery in wastewater treatment: Current applications and future perspectives. *Chemosphere* **2021**, *265*, 129076.
5. Sirohi, R.; Pandey, A.K.; Ranganathan, P.; Singh, S.; Udayan, A.; Awasthi, M.K.; Hoang, A.T.; Chilakamarry, C.R.; Kim, S.H.; Sim, S.J. Design and applications of photobioreactors-A review. *Bioresource technology* **2022**, 126858.
6. Liao, Y.; Bokhary, A.; Maleki, E.; Liao, B. A review of membrane fouling and its control in algal-related membrane processes. *Bioresource technology* **2018**, *264*, 343-358.

7. Javadi, N.; Ashtiani, F.Z.; Fouladitajar, A.; Zenooz, A.M. Experimental studies and statistical analysis of membrane fouling behavior and performance in microfiltration of microalgae by a gas sparging assisted process. *Bioresource technology* **2014**, *162*, 350-357.
8. Zhang, Y.; Tian, J.; Liang, H.; Nan, J.; Chen, Z.; Li, G. Chemical cleaning of fouled PVC membrane during ultrafiltration of algal-rich water. *Journal of environmental sciences* **2011**, *23*, 529-536.
9. Liu, B.; Qu, F.; Liang, H.; Gan, Z.; Yu, H.; Li, G.; Van der Bruggen, B. Algae-laden water treatment using ultrafiltration: Individual and combined fouling effects of cells, debris, extracellular and intracellular organic matter. *Journal of membrane science* **2017**, *528*, 178-186.
10. Jiang, B.; Zeng, Q.; Hou, Y.; Li, H.; Liu, J.; Xu, J.; Shi, S.; Ma, F. Impacts of long-term electric field applied on the membrane fouling mitigation and shifts of microbial communities in EMBR for treating phenol wastewater. *Science of the total environment* **2020**, *716*, 137139.
11. Lade, H.; Paul, D.; Kweon, J.H. Quorum quenching mediated approaches for control of membrane biofouling. *International journal of biological sciences* **2014**, *10*, 550.
12. Zhang, Y.; Fu, Q. Algal fouling of microfiltration and ultrafiltration membranes and control strategies: A review. *Separation and purification technology* **2018**, *203*, 193-208.
13. Souza, E.; Follmann, H.V.D.M.; Dalri-Cecato, L.; Battistelli, A.A.; Lobo-Recio, M.A.; Belli, T.J.; Lapolli, F.R. Membrane fouling suppression using intermittent electric current with low exposure time in a sequencing batch membrane bioreactor. *Journal of environmental chemical engineering* **2020**, *8*, 104018.
14. Yin, X.; Li, J.; Li, X.; Hua, Z.; Wang, X.; Ren, Y. Self-generated electric field to suppress sludge production and fouling development in a membrane bioreactor for wastewater treatment. *Chemosphere* **2020**, *261*, 128046.
15. Wang, B.; Zhang, K.; Field, R.W. Optimization of aeration variables in a commercial large-scale flat-sheet MBR operated with slug bubbling. *Journal of membrane science* **2018**, *567*, 181-190.

16. Meng, F.; Zhang, S.; Oh, Y.; Zhou, Z.; Shin, H.-S.; Chae, S.-R. Fouling in membrane bioreactors: An updated review. *Water research* **2017**, *114*, 151-180.
17. El Kateb, M.; Trellu, C.; Darwich, A.; Rivallin, M.; Bechelany, M.; Nagarajan, S.; Lacour, S.; Bellakhal, N.; Lesage, G.; Heran, M. Electrochemical advanced oxidation processes using novel electrode materials for mineralization and biodegradability enhancement of nanofiltration concentrate of landfill leachates. *Water research* **2019**, *162*, 446-455.
18. Gurung, K.; Ncibi, M.C.; Shestakova, M.; Sillanpää, M. Removal of carbamazepine from MBR effluent by electrochemical oxidation (EO) using a Ti/Ta2O5-SnO2 electrode. *Applied Catalysis B: Environmental* **2018**, *221*, 329-338.
19. Karimi, L.; Hazrati, H.; Gharibian, S.; Shokrkar, H. Investigation of various anode and cathode materials in electrochemical membrane bioreactors for mitigation of membrane fouling. *Journal of environmental chemical engineering* **2021**, *9*, 104857.
20. Corpuz, M.V.A.; Borea, L.; Senatore, V.; Castrogiovanni, F.; Buonerba, A.; Oliva, G.; Ballesteros Jr, F.; Zarra, T.; Belgiorno, V.; Choo, K.-H. Wastewater treatment and fouling control in an electro algae-activated sludge membrane bioreactor. *Science of the total environment* **2021**, *786*, 147475.
21. Huang, L.; Lee, D.-J. Membrane bioreactor: a mini review on recent R&D works. *Bioresource technology* **2015**, *194*, 383-388.
22. Lin, H.; Xie, K.; Mahendran, B.; Bagley, D.; Leung, K.; Liss, S.; Liao, B. Sludge properties and their effects on membrane fouling in submerged anaerobic membrane bioreactors (SAnMBRs). *Water research* **2009**, *43*, 3827-3837.
23. Tong, C.; Derek, C. Biofilm formation of benthic diatoms on commercial polyvinylidene fluoride membrane. *Algal research* **2021**, *55*, 102260.
24. Lowry, O.H.; Rosebrough, N.J.; Farr, A.L.; Randall, R.J. Protein measurement with the Folin phenol reagent. *Journal of biological chemistry* **1951**, *193*, 265-275.
25. Gaudy, A. Colorimetric determination of protein and carbohydrate. *Industrial water and wastes.* **1962**, *7*, 17-22.
26. Jin, B.; Wilén, B.-M.; Lant, P. Impacts of morphological, physical and chemical properties of sludge flocs on dewaterability of activated sludge. *Chemical engineering journal* **2004**, *98*, 115-126.

27. Luo, Y.; Le-Clech, P.; Henderson, R.K. Characterisation of microalgae-based monocultures and mixed cultures for biomass production and wastewater treatment. *Algal research* **2020**, *49*, 101963.
28. Federation, W.E.; Association, A. Standard methods for the examination of water and wastewater. *American Public Health Association (APHA): Washington, DC, USA* **2005**, *21*.
29. Asif, M.B.; Maqbool, T.; Zhang, Z. Electrochemical membrane bioreactors: state-of-the-art and future prospects. *Science of the total environment* **2020**, *741*, 140233.
30. Isma, M.A.; Idris, A.; Omar, R.; Razreena, A.P. Effects of SRT and HRT on treatment performance of MBR and membrane fouling. *International Journal of Chemistry and Molecular and Nuclear Material Metallurgy Engineering* **2014**, *8*, 485-489.
31. Low, S.L.; Ong, S.L.; Ng, H.Y. Characterization of membrane fouling in submerged ceramic membrane photobioreactors fed with effluent from membrane bioreactors. *Chemical engineering journal* **2016**, *290*, 91-102.
32. Nouha, K.; Kumar, R.S.; Balasubramanian, S.; Tyagi, R.D. Critical review of EPS production, synthesis and composition for sludge flocculation. *Journal of environmental sciences* **2018**, *66*, 225-245.
33. Lin, H.; Peng, W.; Zhang, M.; Chen, J.; Hong, H.; Zhang, Y. A review on anaerobic membrane bioreactors: applications, membrane fouling and future perspectives. *Desalination* **2013**, *314*, 169-188.
34. Lin, H.; Zhang, M.; Wang, F.; Meng, F.; Liao, B.-Q.; Hong, H.; Chen, J.; Gao, W. A critical review of extracellular polymeric substances (EPSs) in membrane bioreactors: characteristics, roles in membrane fouling and control strategies. *Journal of membrane science* **2014**, *460*, 110-125.
35. Zhang, S.; Yang, K.; Liu, W.; Xu, Y.; Hei, S.; Zhang, J.; Chen, C.; Zhu, X.; Liang, P.; Zhang, X. Understanding the mechanism of membrane fouling suppression in electro-anaerobic membrane bioreactor. *Chemical engineering journal* **2021**, *418*, 129384.
36. Zhang, J.; Satti, A.; Chen, X.; Xiao, K.; Sun, J.; Yan, X.; Liang, P.; Zhang, X.; Huang, X. Low-voltage electric field applied into MBR for fouling suppression: Performance and mechanisms. *Chemical engineering journal* **2015**, *273*, 223-230.

37. Daigger, G.; Roper Jr, R. The relationship between SVI and activated sludge settling characteristics. *Journal (Water Pollution Control Federation)* **1985**, 859-866.
38. Luo, Y.; Le-Clech, P.; Henderson, R.K. Assessment of membrane photobioreactor (MPBR) performance parameters and operating conditions. *Water research* **2018**, *138*, 169-180.
39. Dentel, S.K.; Abu-Orf, M.M. Laboratory and full-scale studies of liquid stream viscosity and streaming current for characterization and monitoring of dewaterability. *Water research* **1995**, *29*, 2663-2672.
40. Ibeid, S.; Elektorowicz, M.; Oleszkiewicz, J. Modification of activated sludge properties caused by application of continuous and intermittent current. *Water research* **2013**, *47*, 903-910.
41. Zhang, W.; Song, R.; Cao, B.; Yang, X.; Wang, D.; Fu, X.; Song, Y. Variations of floc morphology and extracellular organic matters (EOM) in relation to floc filterability under algae flocculation harvesting using polymeric titanium coagulants (PTCs). *Bioresource technology* **2018**, *256*, 350-357.
42. Visigalli, S.; Barberis, M.G.; Turolla, A.; Canziani, R.; Zrimec, M.B.; Reinhardt, R.; Ficara, E. Electrocoagulation–flotation (ECF) for microalgae harvesting–A review. *Separation and purification technology* **2021**, *271*, 118684.
43. Krishnamoorthy, N.; Unpaprom, Y.; Ramaraj, R.; Maniam, G.P.; Govindan, N.; Arunachalam, T.; Paramasivan, B. Recent advances and future prospects of electrochemical processes for microalgae harvesting. *Journal of environmental chemical engineering* **2021**, *9*, 105875.
44. Wang, Z.; Wu, Z.; Tang, S. Extracellular polymeric substances (EPS) properties and their effects on membrane fouling in a submerged membrane bioreactor. *Water research* **2009**, *43*, 2504-2512.
45. Azizi, S.; Hashemi, A.; Shariati, F.P.; Tayebati, H.; Keramati, A.; Bonakdarpour, B.; Shirazi, M.M.A. Effect of different light-dark cycles on the membrane fouling, EPS and SMP production in a novel reciprocal membrane photobioreactor (RMPBR) by C. vulgaris species. *Journal of water process engineering* **2021**, *43*, 102256.

46. Marbelia, L.; Mulier, M.; Vandamme, D.; Muylaert, K.; Szymczyk, A.; Vankelecom, I.F. Polyacrylonitrile membranes for microalgae filtration: Influence of porosity, surface charge and microalgae species on membrane fouling. *Algal research* **2016**, *19*, 128-137.
47. Ding, A.; Fan, Q.; Cheng, R.; Sun, G.; Zhang, M.; Wu, D. Impacts of applied voltage on microbial electrolysis cell-anaerobic membrane bioreactor (MEC-AnMBR) and its membrane fouling mitigation mechanism. *Chemical engineering journal* **2018**, *333*, 630-635.
48. Cho, B.; Fane, A. Fouling transients in nominally sub-critical flux operation of a membrane bioreactor. *Journal of membrane science* **2002**, *209*, 391-403.
49. Zhang, J.; Chua, H.C.; Zhou, J.; Fane, A. Factors affecting the membrane performance in submerged membrane bioreactors. *Journal of membrane science* **2006**, *284*, 54-66.
50. Wei, C. Nutrient removal and fouling reduction in electrokinetic membrane bioreactor at various temperatures. **2009**.
51. Hao, L.; Liss, S.; Liao, B. Influence of COD: N ratio on sludge properties and their role in membrane fouling of a submerged membrane bioreactor. *Water research* **2016**, *89*, 132-141.
52. Lee, W.; Kang, S.; Shin, H. Sludge characteristics and their contribution to microfiltration in submerged membrane bioreactors. *Journal of membrane science* **2003**, *216*, 217-227.
53. Zhang, M.; Leung, K.-T.; Lin, H.; Liao, B. Effects of solids retention time on the biological performance of a novel microalgal-bacterial membrane photobioreactor for industrial wastewater treatment. *Journal of environmental chemical engineering* **2021**, *9*, 105500.
54. Seviour, T.; Derlon, N.; Dueholm, M.S.; Flemming, H.-C.; Girbal-Neuhauser, E.; Horn, H.; Kjelleberg, S.; van Loosdrecht, M.C.; Lotti, T.; Malpei, M.F. Extracellular polymeric substances of biofilms: Suffering from an identity crisis. *Water research* **2019**, *151*, 1-7.
55. Ibeid, S.; Elektorowicz, M.; Oleszkiewicz, J.A. Electro-conditioning of activated sludge in a membrane electro-bioreactor for improved dewatering and reduced membrane fouling. *Journal of membrane science* **2015**, *494*, 136-142.
56. Bayar, S.; Karagunduz, A.; Keskinler, B. Influences of electroosmosis and electrophoresis on permeate flux and membrane fouling in submerged membrane bioreactors (SMBRs). *Water science and technology* **2016**, *74*, 766-776.

57. Giwa, A.; Ahmed, I.; Hasan, S.W. Enhanced sludge properties and distribution study of sludge components in electrically-enhanced membrane bioreactor. *Journal of environmental management* **2015**, *159*, 78-85.
58. Xu, X.; Zhang, H.; Gao, T.; Wang, Y.; Teng, J.; Lu, M. Customized thin and loose cake layer to mitigate membrane fouling in an electro-assisted anaerobic forward osmosis membrane bioreactor (AnOMEBR). *Science of the total environment* **2020**, *729*, 138663.
59. Yin, X.; Li, X.; Hua, Z.; Ren, Y. The growth process of the cake layer and membrane fouling alleviation mechanism in a MBR assisted with the self-generated electric field. *Water research* **2020**, *171*, 115452.
60. Hasan, S.W.; Elektorowicz, M.; Oleszkiewicz, J.A. Start-up period investigation of pilot-scale submerged membrane electro-bioreactor (SMEBR) treating raw municipal wastewater. *Chemosphere* **2014**, *97*, 71-77.

Chapter 5 Effects of solid retention time on the biological performance of a novel electrokinetic-assisted membrane photobioreactors (EK-MPBR)

Abstract

Electro-phycoremediation is a relatively novel approach to control eutrophication and water pollution. This study aims to investigate the effect of solid retention time (SRT) on the biological performance of novel electrokinetic-assisted membrane photobioreactor (EK-MPBRs) in treating synthetic municipal wastewater using microalgae *Chlorella vulgaris.* The influence of SRT variation, 40, 20, and 10 days, has been studied on microalgae properties and its nutrients (N and P) removal efficiencies by utilizing three lab-scale EK-MPBR. Two EK-MPBRs operating with SRTs of 40 and 20 days were run in parallel for 80 days, followed by another EK-MPBR operating at SRT of 10 days for 45 days. A low voltage direct current (current density: 0.261 A/m2) was supplied continuously throughout the operation. Mixed liquor suspended solids (MLSS) concentration, productivity, chemical oxygen demand (COD), floc morphology, and total phosphorus (TP) and total nitrogen (TN) removals were measured during the experimental periods. The comparison of the results revealed that SRT of 10 days had superior performance in terms of nutrient removal along with having the highest biomass productivity (0.055±0.02 g/L.d). All three EK-MPBRs showed relatively similar phosphorus removal (>96.7 %). Shortened SRT improved TN removal efficiency by approximately 10 % and 7 % for SRT of 10 days compared to SRT of 40 and 20 days, respectively. In conclusion, the SRT of 10 days was the optimum SRT among 10, 20, and 40 days of SRTs.

Keywords: Membrane photobioreactor, Solid retention time, Phycoremediation, Nutrient removal, Electrokinetic

5.1 Introduction

Water eutrophication is a problem which is gaining global attention as it adversely affects the ecosystem and is defined as excessive nutrients in water caused by water bodies [1]. The application of algae and biological treatment has become a promising technique for water and wastewater treatment due to its low environmental impact and cost [2,3] This technique, which is called phycoremediation, has been investigated by researchers in treating a wide range of wastewaters [3,4]. The Membrane photobioreactor (MPBR), as a subset and an advanced technique of phycoremediation, has been widely studied in terms of nutrient removal efficiency and simultaneous microalgae cultivation [5]. The produced biomass can be used as biofuel as well as in food and other industries [6-9]. Some studies on MPBRs focused on enhancing biomass production [10,11]. Operational parameters such as hydraulic retention time (HRT) have been found to be effective in improving biomass production. A relatively new approach for growth stimulation uses electric field and has been studied mostly in batch experiments[12]. A pulse electric field applied could increase the growth rate of the microalgae and biomass production[6,13]. Electrotechnology has also been effective in microalgae downstream processing such as harvesting and protein extraction [14-16]. There are few studies, however, that examined the effect of a continuous electric field on microalgae production in a MPBR [17].

Membrane performance is the other determining factor of MPBR efficiency. Membrane fouling is a bottleneck and a major limitation in the application of MPBRs. There are some studies investigating the influence of factors in fouling mitigation in MPBRs. The ratio of nutrients in the feed, such as nitrogen and phosphorus, was found to influence membrane fouling[18]. Integrating cold plasma and biological approaches such as quorum quenching have also been investigated to remedy the fouling in MPBRs [19,20]. Another recent approach in fouling mitigation in biological wastewater treatment is electro-phycoremediation. Combining electrochemical processes and biological wastewater treatment has shown to be effective in mitigating membrane fouling [21-23]. However, as of writing this paper, there is only one published study examining electro-phycoremediation in MPBRs [23]. Moreover, that MPBR was utilized both bacteria and algae as their biomass. To the best of our knowledge, this is the first study focusing on microalgae production and electro-phycoremediation in an MPBR.

Other factors affecting MPBR performance, such as membrane configuration and type, temperature, wastewater type and operational parameters, including solid retention time (SRT), have been investigated and reported [24,25]. However, the combined effect of SRT with electrokinetic-assisted MPBR has remained a gap in this area and is the focus of this study.

The present research aims to investigate the effect of SRT on biological performance and nutrient removal of electrified membrane photobioreactors (EK-MPBR). Three EK-MPBRs were run with corresponding SRTs of 10, 20, and 40 days using the microalgae *C. vulgaris*. Over the experimental period of 80 days for SRTs of 20 and 40 and 45 days for the SRT of 10, nitrogen and phosphorus removal from synthetic municipal wastewater in conjunction with biomass productivity were analyzed and compared. The performance of these relatively novel MPBRs is compared with other few studies in EK-MPBRs and other conventional MPBRs without electric field [17,23].

5.2 Materials and Methods

5.2.1 Chemicals and microalgae

The chemicals were purchased from Sigma-Aldrich (Merck, Germany). Synthetic municipal wastewater was prepared based on the composition reported in the previous procedure and is summarized in Table 5.1 [17].

Table 5-1 Composition of synthetic municipal wastewater

Water Quality Index	**Average value (g/L)**
Nitrogen	0.025±0.002
Phosphorus	0.0035±0.0003
COD	< 0.01
Compound	
NaCl	0.0025
$MgSO_4.7H_2O$	0.082
$CaCl_2.2H_2O$	0.005
$FeSO_4.7H_2O$	0.02490
$ZnSO_4.7H_2O$	0.00044
$MnCl_2.4H_2O$	0.00022
$Na_2MoO_4.2H_2O$	0.00126
$CuSO_4.5H_2O$	0.00039
$CoCl_2.6H_2O$	0.00041
NH_4Cl	0.09553
KH_2PO_4	0.01537
$NaHCO_3$	0.3

Pre-culture microalgae *Chlorella vulgaris* was performed by continuous aeration and photoautotrophically at room temperature. The microalgae strain (CPCC 90) was purchased from the Canadian Phycological Culture Centre (University of Waterloo, ON, Canada). The modified mineral salt medium (MSM) with the following concentration and composition in 1 litre of solution was used to cultivate the microalgae: 0.66 g NH_4 Cl, 0.625g Mg SO_4, 0.1105 g $CaCl_2$.2H2O, 0.1142 g H_3BO_3, 0.0498 g $FeSO_4.7H_2O$, 0.0882 $ZnSO_4.7H_2O$, 0.0144 g $MnCl_2.4H_2O$, 0.0118 g $Na_2MoO_4.2H_2O$, 0.0157 g $CuSO_4.5H_2O$, 0.004 g $CoCl_2.6H_2O$, 0.64 g EDTA-2 $Na.2H_2O$, 0.6247 g KH_2PO_4, 1.3251 g K_2HPO_4. The chemicals were added to the DI water prepared in the lab. The cultivation continued for 45 days to reach the desired concentration of 1.7 g/L of dried biomass.

5.2.2 Configuration and operational parameters

One configuration of EK-MPBR was used for all three bioreactors in this study: The MPBRs were composed of a transparent cylindrical poly (methyl methacrylate) tank. The working volume of the reactors was 10 L each and two flat sheet polyvinylidene fluoride (PVDF) membranes (one on each side of the membrane module) with a nominal pore size of 0.1 μm. Stainless steel meshes were placed inside the membrane module and as a support of the membranes. The graphite sheet cathodes were placed outside the module facing the membranes. A continuous DC electric field was applied to the microalgae over the experimental period in all three EK-MPBRs at the current density of 0.261 A/m^2 using a DC power supply (B & K precision's, 132 Taiwan). The influent was semi-continuously added the EK-MPBRs using peristaltic pump (Model 77122-12, Mas-110 Masterflex®C/L®PWR, Cole-Parmer, USA). A level sensor 109 (LC40, Flowline Inc., USA) was used in each MPBR to maintain the level of the suspension. The permeation pumps were operated with the intervals of 3-min-on and 2-min-off modes for permeation and relaxation, respectively, to control membrane fouling. The reactors EK-MPBR 40 and 20 were operated for 80 days, and the SRT of 10 was operated for 45 days. Hydraulic retention time (HRT) was kept constant for all three EK-MPBRs. Over the experimental periods, HRT was kept constant by controlling the flux (8.5 L/m^2h). Off-line cleaning was performed when the transmembrane pressure (TMP) reached 30 kPa using tap water to remove the fouling layer. The basic parameters of the membrane module and the operating conditions are summarized in Table 5.2.

Table 5-2 Operating conditions of EK-MPBRs

Membrane module	$EkMPBR_{10}$	$EK\text{-}MPBR_{20}$	$EK\text{-}MPBR_{40}$
Total membrane surface area (m^2)	0.03	0.03	0.03
Membrane materials	Polyvinylidene fluoride (PVDF)	Polyvinylidene fluoride (PVDF)	Polyvinylidene fluoride (PVDF)
Membrane type	Flat sheet	Flat sheet	Flat sheet
Mean membrane pore size (μm)	0.1	0.1	0.1
Operational Parameter			
Working volume (L)	10	10	10
Temperature (°C)	25.93 ± 0.4	25.32 ± 0.96	24.81 ± 1.15
pH	8.76 ± 0.87	7.55 ± 0.95	7.72 ± 0.94
Aeration rate (L/min)	2.16±0.10	2.16±0.10	2.16±0.10
Illumination intensity (lux)	8400	8400	8400
Voltage gradient (V/cm)	0.62±0.02	0.62±0.02	0.62±0.02
Current density (A/m^2)	0.261	0.261	0.261
Electrodes surface area (m^2)	0.015 ± 0.008	0.015 ± 0.008	0.015 ± 0.008
Electrodes distance (m)	0.03	0.03	0.03
HRT (d)	2.5	2.5	2.5
SRT (d)	10	20	40

5.2.3 Instrumentation and methods

TMP was continuously monitored by a pressure gauge (Omega, Korea) installed in-line in the pathway of the pathway connected to the membrane. Daily measuring of dissolved oxygen (DO), pH and temperature were conducted using a DO meter (Model 407510, Extech, 142 USA), a pH meter (pH 700, Oakton, USA) and a thermometer, respectively.

The particle size distribution was determined by a Malvern Mastersize 2000 instrument (Worcestershire, UK) with a detention range of 0.02-2000 μm. Each sample was measured in triplicate with the constant laser obscuration range of 0.1-0.4 %. The structural observation of the algal cell was carried out by an Inverted microscope (Olympus IX51, 160 Japan). The samples

were dropped onto a slide, followed by dispersion with a cover slide, and the pictures were taken randomly using a digital camera.

Chemical oxygen demand (COD) was measured using the standard method [26], and total nitrogen (TN), and total phosphorus (TP) were measured by spectrophotometry using the alkaline potassium persulfate digestion-UV and ammonium molybdate spectroscopy method, respectively [27].

MLSS was determined using a standard method [28] and biomass productivity was calculated accordingly [29]:

$$r_x = X \times \frac{Q_{waste}}{V} = \frac{X}{SRT} \quad (5.1)$$

where, r_x indicates biomass productivity (mg/L.d); X is the average biomass concentration (g/L), Q waste is the reactor biomass wasting rate (L/d), and V is its working volume (L).

5.2.4 Statistical analysis

Determination of statistical difference between corresponding data was performed using a two-sample t-test, with a significance level of 0.05 (P=0.05). The null hypothesis is rejected if $P < 0.05$ and the values are considered statistically different in this case.

5.3 Results and discussion

5.3.1 Effects of SRT on biomass production of EK-MPBRs

Biomass concentration variations over the experimental period are illustrated in Figure 5.1. Two EK-MPBRs with SRT of 40 and 20 were run in parallel for 80 days, followed by another run of SRT of 10 for 45 days (phase 2). The initial MLSS concentration for all three EK-MPBRs was 1.7 ± 0.2 g/L and continued to decline toward stable condition. This decline is due to the lower biomass growth rate compared to the waste taken daily from the reactors. As SRT defines the amount of waste and therefore the concentration of biomass in the reactors, the longer SRT results in more biomass concentration in the reactors. As shown in Figure 5.1, SRT of 40 days exhibited more MLSS concentration than SRT of 20 and 10 days over the experimental period (1.62 ± 0.25, 0.84 ± 0.2, and 0.50 ± 0.07 g/L, respectively for SRTs of 40, 20, and 10 days).

Both reactors with SRT of 40 and 20 days reached a stable operation on Day 40, whereas the steady state was shortened to 15 days with SRT of 10 days. Although the stable condition was interrupted

by technical issues on days 42 and 53 in the reactors with SRT of 40 and 20 days, they were able to recover their concentration after two days. The other reason for MLSS fluctuation is the mixing condition, which was insufficient for the charged algal biomass, especially in higher MLSS concentrations. As the algal biomass acquires more charge under the applied electric field, they are prone to attach to the wall of the reactors, making the common mixing methods insufficient in the long run. For SRT of 10 days, however, the lower MLSS concentration and shortened SRT helped maintain the concentration consistent over the experimental period.

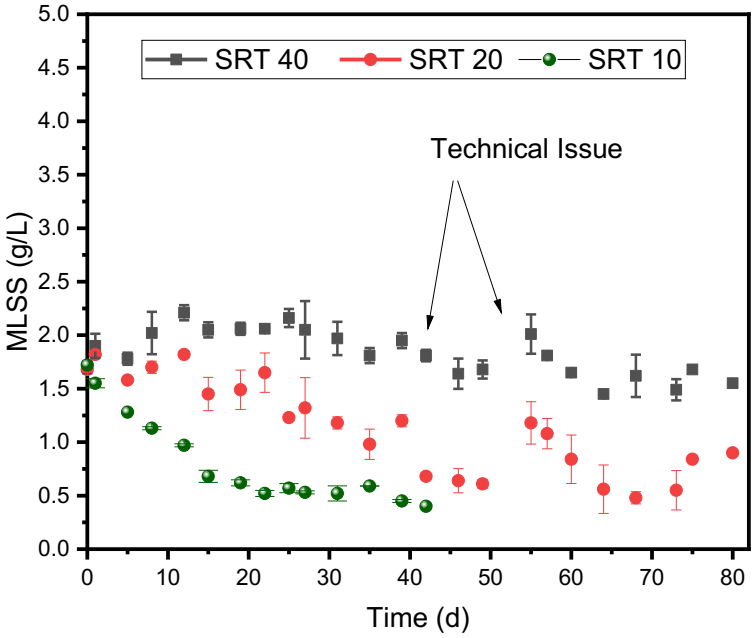

Figure 5-1 MLSS concentration of EK-MPBRs with SRTs of 40, 20, and 10 days over the experimental period. Values and error bars represent average and standard deviation from two technical replicate measurements (n = 2), respectively. pH value and temperature of the algal suspension was around 8 and 25 ° c, respectively.

In addition, the biomass productivity of MPBRs, when stable conditions are reached, is summarized in Table 5.3. According to this table, SRT of 20 and 40 showed comparable volumetric biomass productivity of 0.043 ± 0.017 g/L.d (P = 0.44). This value, however, is significantly higher for the SRT of 10 days and increased to 0.055 ± 0.02 g/L.d (P = 0.003). The results indicate that the productivity was adversely affected by the prolonged SRTs of 40 and 20 days, and the optimum SRT was found to be 10 days. This could be due to the self-shading

phenomena and lack of nutrients, both of which happen when the biomass concentration in the bioreactors increases [30,31]. High biomass accumulation inside the reactors with longer SRTs could inhibit microalgae growth by preventing them from receiving enough light. This agrees with a study investigating the role of SRT on the biomass productivity of *Scenedesmus obliquus* [32]. The other contributing factor to the higher productivity of SRT of 10 days could be the greater abundance of nutrients for algal biomass compared to SRT of 40 and 20 days. With the same feed concentration, the portion of the feed to algal cells is higher in SRT of 10 compared to SRT of 20 and 40 days.

Table 5-3 Comparison of the results of treating synthetic wastewater using *Chlorella Vulgaris*

SRT (d)	HRT (d)	MLSS (g/L)	Biomass productivity (g/Ld)	TN removal (%)	TP removal (%)	Type of reactor	Ref.
10	2.5	0.50 ± 0.07	0.055 ± 0.02	33.07 ± 4.13	98.29 ± 0.3	EK-MPBR	This study
20	2.5	0.84 ± 0.2	0.043 ± 0.017	21.44 ± 0.8	97.93 ± 0.1	EK-MPBR	This study
40	2.5	1.62 ± 0.25	0.043 ± 0.007	18.98 ± 1.12	96.70 ± 0.03	EK-MPBR	This study
30	2.5	0.97 ± 0.2	0.032 ± 0.025	43 ± 2	97.98 ± 0.02	EK-MPBR	[17]
-	-	0.60 ± 0.46	-	65.60	97.22	E-MPBR	[23]
21.1	2	1.524	0.06	80.6	89.2	MPBR	[10]

Note: The average values of MLSS and effluent pollutants (TN and TP) concentration, as well as the removal efficiency, were measured in duplicate and calculated from the data of the last two 10 days for each phase. The data are represented as mean ± standard deviation.

5.3.2 Effects of SRTs on nutrients removal of EK-MPBRs

The nutrients removal of MPBRs over the experimental periods is presented in Figures 5.2 and 5.3. The N and P concentrations in the feed were maintained constant at 25 ± 2 mg/L and 3.5 ± 0.3 mg/L, respectively. As illustrated in Figure 5.2, the nitrogen concentration in the effluent decreased initially in SRT of 40 and 20. Starting from day 11, however, both SRTs of 40 and 20 days showed higher TN concentration in the effluent with some fluctuation and stabilized gradually to an average value of about 20.25 ± 0.23 and 19.64 ± 0.6 mg/L on day 40, respectively. The initial lower nitrogen concentration in the effluent in the first 10 days of operation can be attributed to the higher MLSS concentration in these reactors. Similarly, at SRT of 10, the stabilized TN concentration of about 12.58 on day 21 indicated a relation between TN concentration in the

effluent and stabilized MLSS on the same day. The average TN removal efficiency of the last ten days of operation was 33.07 ± 4.13, 21.44 ± 0.8, and 18.98 ± 1.12 %, for SRT 10, 20 and 40 respectively. While the SRT of 20 and 40 days were comparable in terms of nitrogen removal efficiency (P = 0.3), SRT of 10 days showed significantly higher nitrogen removal compared to SRTs of 40 and 20 days (P<0.05). The highest TN removal in SRT of 10 might be attributed to higher cell growth and productivity in the reactor.

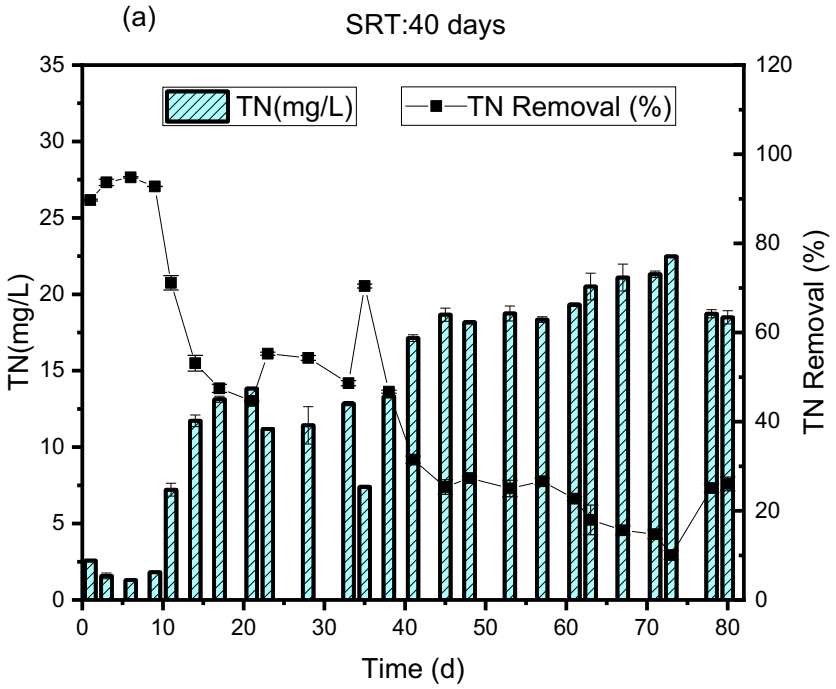

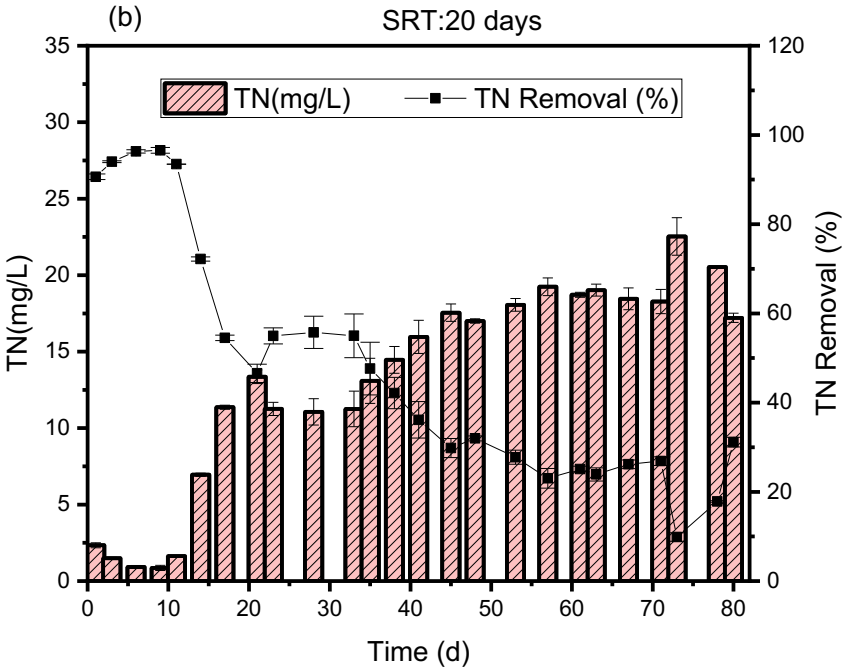
(b)
SRT:20 days
TN(mg/L)
TN Removal (%)
TN(mg/L)
TN Removal (%)
Time (d)

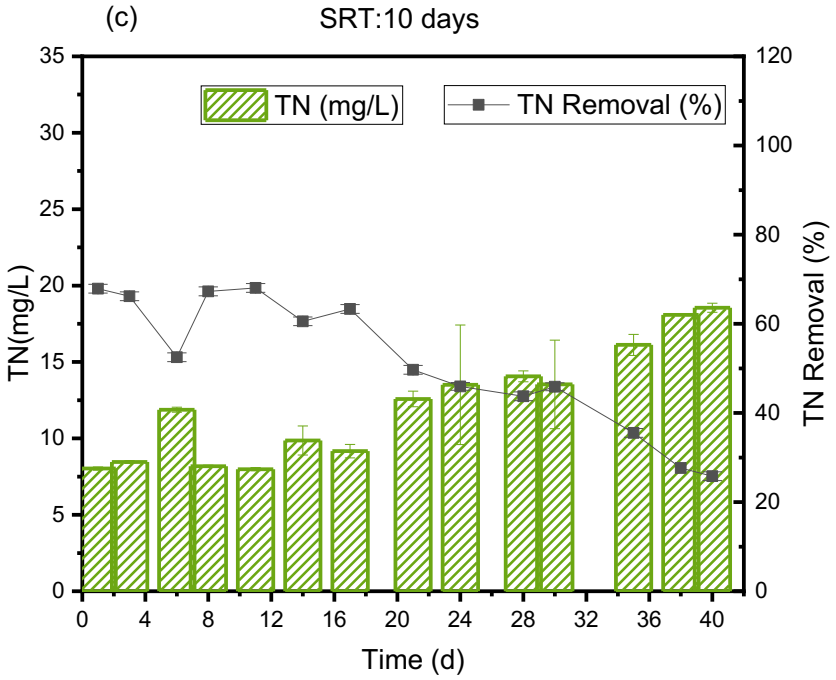
(c)
SRT:10 days
TN (mg/L)
TN Removal (%)
TN(mg/L)
TN Removal (%)
Time (d)

Figure 5-2 Total nitrogen concentration and removal efficiency of EK-MPBRs, (a) for SRT of 40 days (b) for SRT of 20 days (c) for SRT of 10 days. Values and error bars represent average and standard deviation from two technical replicate measurements (n = 2), respectively.

As shown in Figure 5.3, total phosphorus concentration in the effluent was stabilized on Days 53, 35, and 18 in MPBRs with SRTs of 40, 20, and 10, respectively. The average effluent TP concentration for the last ten days of the operation was 0.11 ± 0.003, 0.0723 ± 0.004, and 0.063 ± 0.01 mg/L for SRTs of 40, 20, and 10 days, respectively. Overall, all three SRTs showed a good phosphorus removal of about 97 %, in which the highest rate accounted for SRT of 10 days, as opposed to the lowest recorded for SRT of 40 days. The better removal efficiency seen in the SRT of 10 days, could be due to better biomass productivity and young cells that are metabolically more active than other cells [33].

However, this difference in phosphorus removal efficiency for the three EK-MPBRs was negligible and not statistically significant (P = 0.11), implying that SRT had little influence on total phosphorus removal. This agrees with the other studies claiming that SRT's influence on nutrient removal efficiency is weak compared to other operational parameters, such as HRT [29,34,35]. Moreover, the MLSS concentration in the reactors did not eliminate the phosphorus uptake. This could imply that other phosphorus removal mechanisms were possible contributors to phosphorus uptake. When the electric field is taken into consideration, the major assimilation is attributed to the electrochemical oxidation [23]. It is argued that under the electric field, electrochemical reactions around the electrodes are significant contributors to phosphorus removal in MPRBs [17,23]. As such, the phosphorus removal appeared independent of MLSS concentration and SRT. Elemental analysis further supports the nutrient removal efficiency of the EK-MPBRs. As summarized in Table 5.2, SRT of 10 days could assimilate more nitrogen and phosphorus in the feed and exhibited more nitrogen and phosphorus concentration in the biomass cells as compared to SRT of 20 and 40 days.

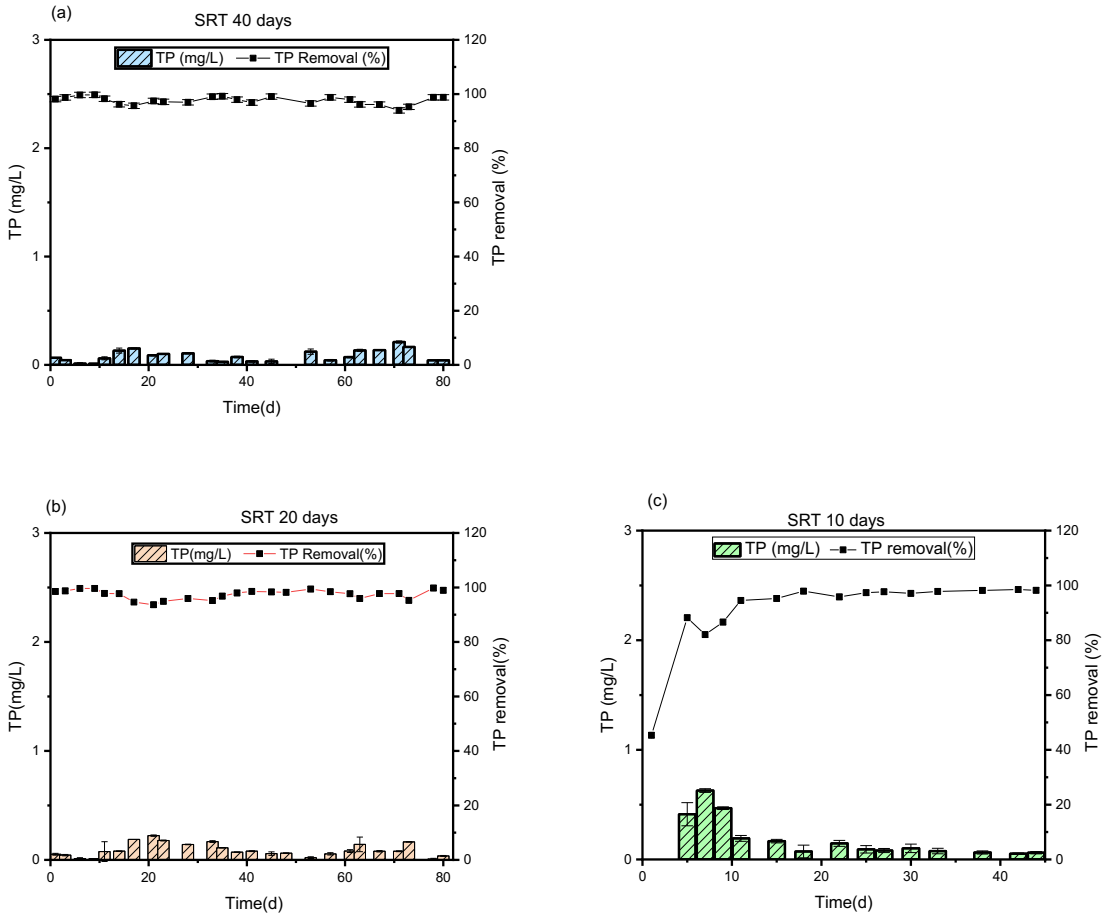

Figure 5-3 Total phosphorus concentration and removal efficiency of EK-MPBRs, (a) TP removal efficiency for SRT of 40 days (b) TP removal efficiency for SRT of 20 days (c) TP removal efficiency for SRT of 10 days. Values and error bars represent average and standard deviation from two technical replicate measurements (n = 2), respectively.

Table 5-4 Elemental compositions of biomass

	Carbon (%)	Nitrogen (%)	Sulphur (%)	Phosphorus (mg/g MLSS)
EK-MPBR, SRT 10	33.54±0.63	5.03±0.09	0.33±0.017	19.8 ± 0.47
EK-MPBR, SRT 20	30.1825±0.11	4.59±0.11	0.255±0.11	17.45 ± 0.41
EK-MPBR, SRT 40	31.5725±0.78	4.52±0.28	0.3575±0.07	14.32 ± 0.34

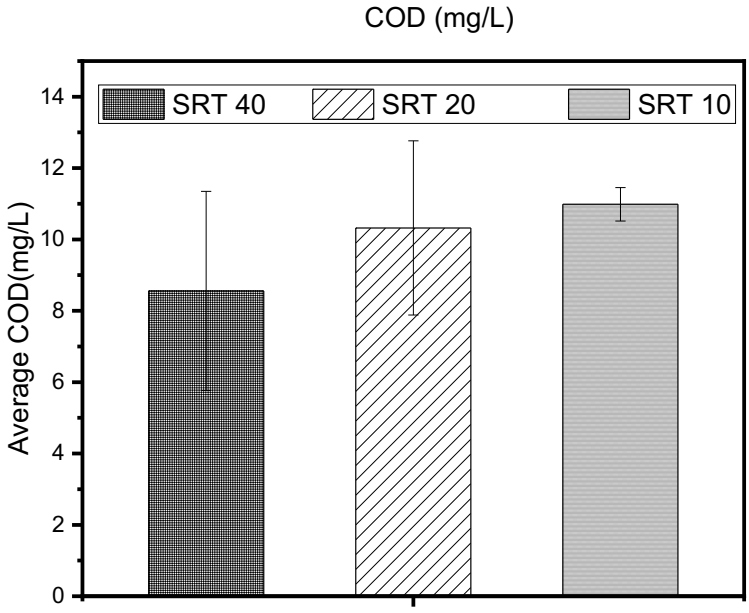

Figure 5-4 Average COD concentration of the EK-MPBRs in the last 10 days of the operation. Values and error bars represent average and standard deviation from three technical replicate measurements (n = 3), respectively.

Figure 5.4 shows the changes in COD concentration in the effluents of EK-MPBRs with different SRTs. Based on the results, it can be seen that COD was not affected by SRTs. This agrees with the study by Zhang et al. [36] that SRT was revealed to have little impact on COD removal. The COD reduction in the reactors can be attributed to other factors such as electrochemical reactions and released oxidants such as hydrogen peroxide and the thickness of the biofilm formed on the membrane surface [17,23]. All three EK-MPBRs successfully meet the effluent mg COD/L standard of discharge according to European Directive COD (<125 mg/L)[37].

In summary, EK-MPBRs were shown to be capable of removing COD and nutrients from synthetic municipal wastewater. The average TN removal of the last ten days of the experiments was calculated as 33.07 ± 4.13, 21.44 ± 0.8, and 18.98 ± 1.12 % for SRTs of 10, 20, and 40 days, respectively. Correspondingly, TP removal was found to be 98.29±0.3, 97.93 ±0.1, and 96.70±0.03

%) for SRTs of 10, 20, and 40 days, respectively. In comparison to conventional MPBRs, all three EK-MPBRs showed significantly higher phosphorus removal and lower nitrogen removal efficiency (Table 5.1). This is due to the different mechanisms of removal in regard to nitrogen and phosphorus suggesting the electric field had a negative effect on nitrogen adsorption by the algal cells [23].

5.3.3 Effects of SRTs on floc morphology

Figure 5.5 shows the microscopic images of the suspension in the EK-MPBRs taken on the last day of the run. The objective of this observation is to investigate the effect of SRT on the morphological aspects of the algal cells. As represented in Figure 5.5, the floc size of particles in SRT of 10 is smaller compared to SRT 20 and 40. The PSD distribution of the flocs further supports this difference in the floc sizes for the suspension in the EK-MPBRs (Figure 5.6). As shown in Figure 5.6, PSDs of all three EK-MPBRs were multimodal with different distributions. At SRT of 10 d, the algal flocs were distributed with a sharp peak, mainly ranging from 1 to 100 µm. At SRTs of 20 and 40, however, the main portion of flocs are in the range of 100 to 1000 µm. The images suggest that bacterial contamination is higher in SRTs of 40 and 20, as the larger flocs of 200 to 1000 µm could be evidence of the presence of the agglomerated algal cells by bacteria, due to microalgal-bacterial symbiosis. At SRT of 10, however, there were almost no bacteria (Figure 5.5 (c)). The higher portion of small flocs and young cells could also explain the greater biomass productivity compared to the longer SRTs.

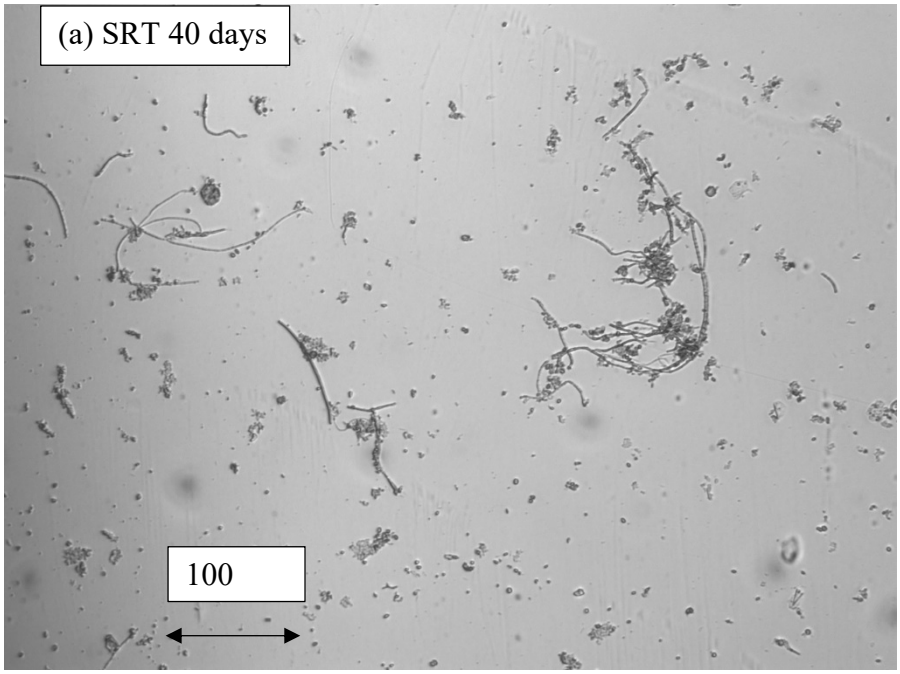
(a) SRT 40 days
100

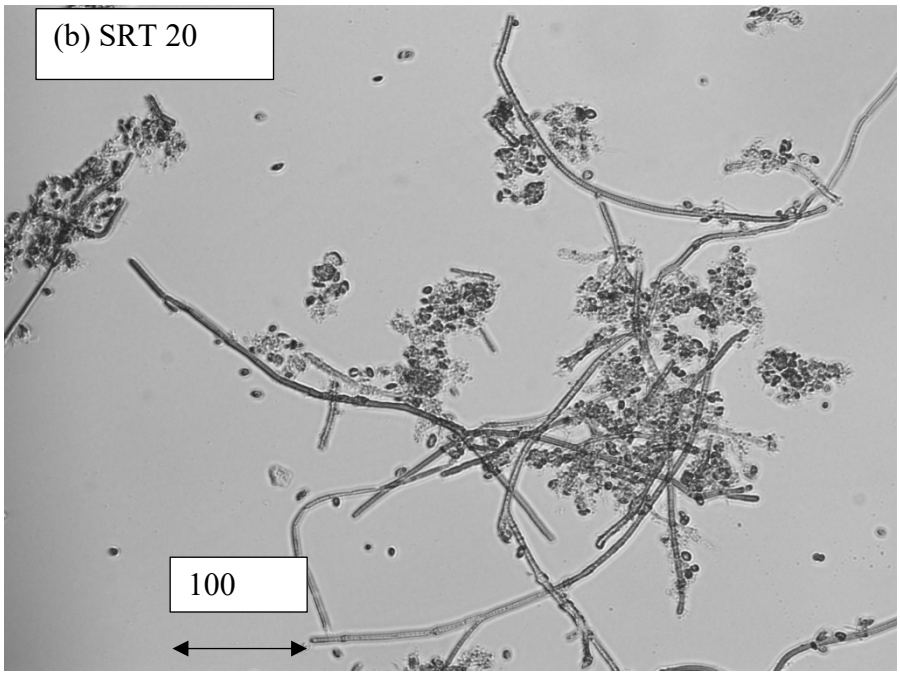
(b) SRT 20
100

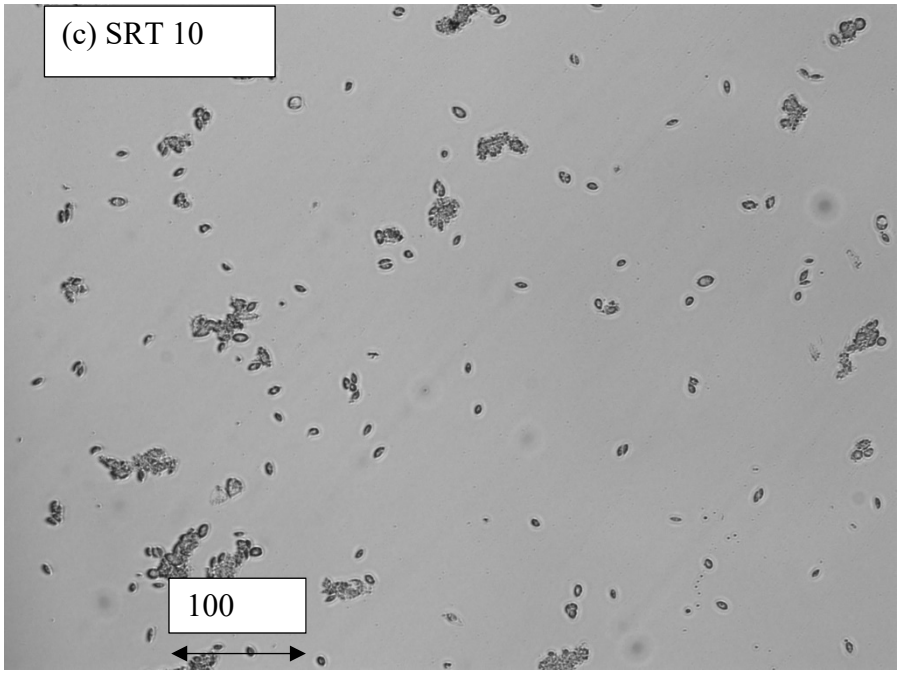

Figure 5-5 Microscopic images representing the morphology of *C. vulgaris* in (a) EK-MPBR SRT of 40 days, (b) EK-MPBR SRT of 20 days, (c) EK-MPBR SRT of 10 days taken on the last day of the experimental period.

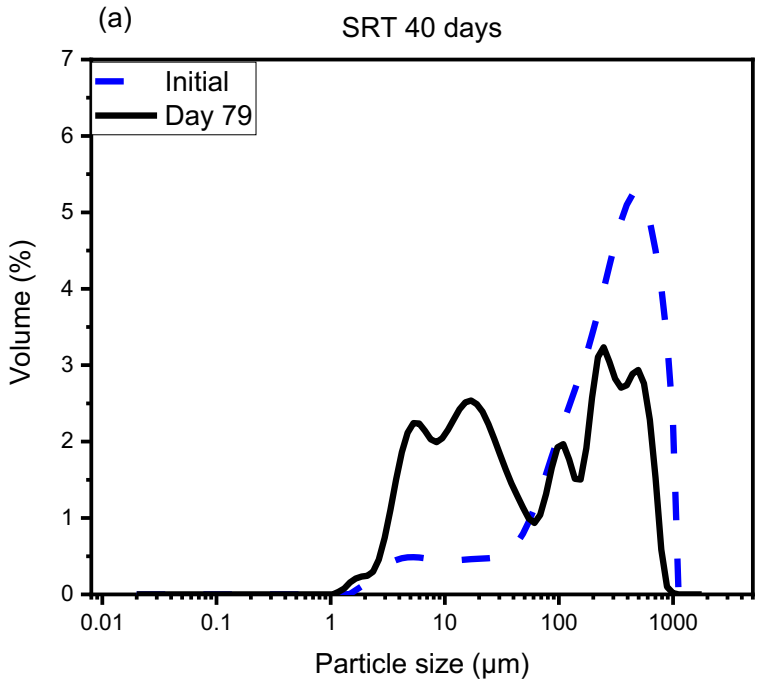

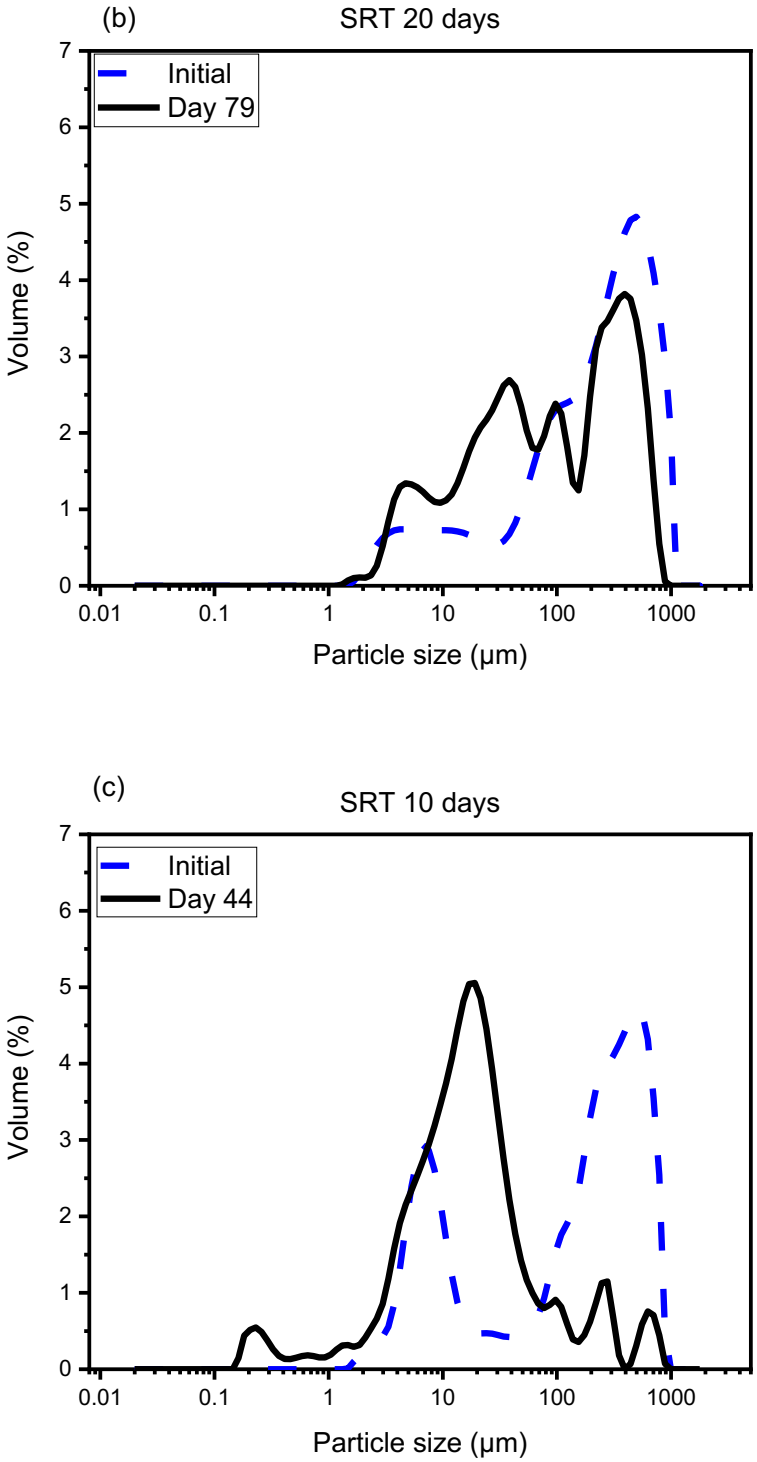

Figure 5-6 Initial and final particle size distribution of the floc suspension in EK-MPBRs (a) SRT of 40 days (b) SRT of 20 days (c) SRT of 10 days.

The joint microscopic and PSD results suggest that for SRTs of 40 and 20 days, with the same microalgal consortium, the increase of SRT from 20 to 40 led to a reduction in the number of larger flocs. This reduction was more noticeable in SRT of 40 days compared to that of SRT of 20. This could be due to the higher MLSS concentration in the suspension in EK-MPBR with SRT of 40 days with almost the same amount of nutrient as in SRT of 20 days resulting in competition for algal and bacterial communities and, therefore, inhibitory effect of this competition on bacterial growth. Furthermore, increased MLSS could improve the chance of cell breakage induced by electrophoretic movements [17]. At SRT of 10, however, the portion of individual algal cells was dominant. This could be attributed to the less self-shading inside the reactor caused by the smaller MLSS concentration, which promoted the growth of the algae in SRT of 10. Another possible mechanism could be the stronger electrophoretic movements for smaller particles which increase the chance of cell breakage in lower concentrations.

5.4 Conclusion

Three modified membrane photobioreactors with the incorporation of low voltage DC electric field and *Chlorella vulgaris* were studied with the variation in SRT. In this novel study, the biomass production and the nitrogen and phosphorus removal efficiency of EK-MPBRs were determined. SRT of 10 days provided better biomass productivity along with improved nutrient removal compared to SRT of 20 and 40 days. SRT variation, however, showed negligible impact on COD removal. The electric field increased the portion of small flocs over the experimental period for all three EK-MPBRs caused by the breakage of the cells introduced by electrophoresis.

5.5 References

1. Khan, F.A.; Ansari, A.A. Eutrophication: an ecological vision. *The botanical review* **2005**, *71*, 449-482.
2. Priyadharshini, S.D.; Babu, P.S.; Manikandan, S.; Subbaiya, R.; Govarthanan, M.; Karmegam, N. Phycoremediation of wastewater for pollutant removal: A green approach to environmental protection and long-term remediation. *Environmental pollution* **2021**, *290*, 117989.
3. Karthik, V.; Saravanan, K.; Bharathi, P.; Dharanya, V.; Meiaraj, C. An overview of treatments for the removal of textile dyes. *Journal of chemical and pharmaceutical sciences* **2014**, *7*, 301-307.
4. Verma, R.; Suthar, S.; Chand, N.; Mutiyar, P.K. Phycoremediation of milk processing wastewater and lipid-rich biomass production using Chlorella vulgaris under continuous batch system. *Science of the total environment* **2022**, *833*, 155110.
5. Bilad, M.; Arafat, H.A.; Vankelecom, I.F. Membrane technology in microalgae cultivation and harvesting: a review. *Biotechnology advances* **2014**, *32*, 1283-1300.
6. Nezammahalleh, H.; Ghanati, F.; Adams II, T.A.; Nosrati, M.; Shojaosadati, S.A. Effect of moderate static electric field on the growth and metabolism of Chlorella vulgaris. *Bioresource technology* **2016**, *218*, 700-711.
7. Serra-Maia, R.; Bernard, O.; Gonçalves, A.; Bensalem, S.; Lopes, F. Influence of temperature on Chlorella vulgaris growth and mortality rates in a photobioreactor. *Algal research* **2016**, *18*, 352-359.
8. Petrus, L.; Noordermeer, M.A. Biomass to biofuels, a chemical perspective. *Green chemistry* **2006**, *8*, 861-867.
9. Stelte, W.; Sanadi, A.R.; Shang, L.; Holm, J.K.; Ahrenfeldt, J.; Henriksen, U.B. Recent developments in biomass pelletization–A review. *Bioresources* **2012**, *7*, 4451-4490.
10. Gao, F.; Peng, Y.-Y.; Li, C.; Cui, W.; Yang, Z.-H.; Zeng, G.-M. Coupled nutrient removal from secondary effluent and algal biomass production in membrane photobioreactor (MPBR): effect of HRT and long-term operation. *Chemical engineering journal* **2018**, *335*, 169-175.

11. Solmaz, A.; Işık, M. Optimization gapsof membrane photobioreactor; the effect of hydraulic retention time on biomass production and nutrient removal by mixed microalgae culture. *Biomass and bioenergy* **2020**, *142*, 105809.
12. Geada, P.; Rodrigues, R.; Loureiro, L.; Pereira, R.; Fernandes, B.; Teixeira, J.A.; Vasconcelos, V.; Vicente, A.A. Electrotechnologies applied to microalgal biotechnology–Applications, techniques and future trends. *Renewable and sustainable energy reviews* **2018**, *94*, 656-668.
13. Gusbeth, C.A.; Eing, C.; Göttel, M.; Frey, W. Boost of algae growth by ultra short pulsed electric field treatment. In Proceedings of the 2013 Abstracts IEEE international conference on plasma science (ICOPS), 2013; pp. 1-1.
14. Vandamme, D.; Pontes, S.C.V.; Goiris, K.; Foubert, I.; Pinoy, L.J.J.; Muylaert, K. Evaluation of electro-coagulation–flocculation for harvesting marine and freshwater microalgae. *Biotechnology and bioengineering* **2011**, *108*, 2320-2329.
15. Zenouzi, A.; Ghobadian, B.; Hejazi, M.; Rahnemoon, P. Harvesting of microalgae Dunaliella salina using electroflocculation. *Journal of agricultural science and technology* **2013**, *15*, 879-887.
16. Coustets, M.; Joubert-Durigneux, V.; Hérault, J.; Schoefs, B.; Blanckaert, V.; Garnier, J.-P.; Teissié, J. Optimization of protein electroextraction from microalgae by a flow process. *Bioelectrochemistry* **2015**, *103*, 74-81.
17. Amini, M.; Mohamedelhassan, E.; Liao, B. The Biological Performance of a Novel Electrokinetic-Assisted Membrane Photobioreactor (EK-MPBR) for Wastewater Treatment. *Membranes* **2022**, *12*, 587.
18. Zhang, M.; Leung, K.-T.; Lin, H.; Liao, B. Membrane fouling in a microalgal-bacterial membrane photobioreactor: Effects of P-availability controlled by N: P ratio. *Chemosphere* **2021**, *282*, 131015.
19. Lee, J.-C.; Park, R.; Yoo, K.S.; Kim, H.-W. Coupling cold plasma and membrane photobioreactor for enhanced fouling control during livestock excreta treatment. *Chemosphere* **2021**, *265*, 129031.
20. Güneş, G.; Taşkan, E. Quorum quenching strategy for biofouling control in membrane photobioreactor. *Chemosphere* **2022**, *288*, 132667.

21. Borea, L.; Ensano, B.M.B.; Hasan, S.W.; Balakrishnan, M.; Belgiorno, V.; de Luna, M.D.G.; Ballesteros Jr, F.C.; Naddeo, V. Are pharmaceuticals removal and membrane fouling in electromembrane bioreactor affected by current density? *Science of the total environment* **2019**, *692*, 732-740.
22. Millanar-Marfa, J.M.J.; Borea, L.; Hasan, S.W.; de Luna, M.D.G.; Belgiorno, V.; Naddeo, V. Advanced membrane bioreactors for emerging contaminant removal and quorum sensing control. In *Current developments in biotechnology and bioengineering*; Elsevier: 2020; pp. 117-147.
23. Corpuz, M.V.A.; Borea, L.; Senatore, V.; Castrogiovanni, F.; Buonerba, A.; Oliva, G.; Ballesteros Jr, F.; Zarra, T.; Belgiorno, V.; Choo, K.-H. Wastewater treatment and fouling control in an electro algae-activated sludge membrane bioreactor. *Science of the total environment* **2021**, *786*, 147475.
24. Zhang, M.; Lee, E.; Vonghia, E.; Hong, Y.; Liao, B. Introduction to aerobic membrane bioreactors: Current status and recent developments. In *Current developments in biotechnology and bioengineering*; Elsevier: 2020; pp. 1-23.
25. Luo, Y.; Le-Clech, P.; Henderson, R.K. Simultaneous microalgae cultivation and wastewater treatment in submerged membrane photobioreactors: a review. *Algal research* **2017**, *24*, 425-437.
26. Miner, G. Standard methods for the examination of water and wastewater. *American water works association. Journal* **2006**, *98*, 130.
27. Wei, F. Monitoring and analysis methods of water and wastewater. *China environmental science press, Beijing* **2002**.
28. Federation, W.E.; Association, A. Standard methods for the examination of water and wastewater. *American Public Health Association (APHA): Washington, DC, USA* **2005**, *21*.
29. Luo, Y.; Le-Clech, P.; Henderson, R.K. Assessment of membrane photobioreactor (MPBR) performance parameters and operating conditions. *Water research* **2018**, *138*, 169-180.

30. Honda, R.; Teraoka, Y.; Noguchi, M.; Yang, S. Optimization of hydraulic retention time and biomass concentration in microalgae biomass production from treated sewage with a membrane photobioreactor. *Journal of water and environment technology* **2017**, *15*, 1-11.
31. Zhang, M.; Yao, L.; Maleki, E.; Liao, B.-Q.; Lin, H. Membrane technologies for microalgal cultivation and dewatering: Recent progress and challenges. *Algal research* **2019**, *44*, 101686.
32. Praveen, P.; Xiao, W.; Lamba, B.; Loh, K.-C. Low-retention operation to enhance biomass productivity in an algal membrane photobioreactor. *Algal research* **2019**, *40*, 101487.
33. Megharaj, M.; Pearson, H.; Venkateswarlu, K. Removal of nitrogen and phosphorus by immobilized cells of Chlorella vulgaris and Scenedesmus bijugatus isolated from soil. *Enzyme and microbial technology* **1992**, *14*, 656-658.
34. Noguchi, M.; Hashimoto, C.; Honda, R.; Teraoka, Y.; Yang, S.; Ninomiya, K.; Takahashi, K. Utilization of anaerobic digestion supernatant as a nutrient source in microalgal biomass production with a membrane photobioreactor. *Journal of water and environment technology* **2017**, *15*, 199-206.
35. Solmaz, A.; Işik, M. Effect of sludge retention time on biomass production and nutrient removal at an algal membrane photobioreactor. *Bioenergy research* **2019**, *12*, 197-204.
36. Zhang, M.; Leung, K.-T.; Lin, H.; Liao, B. Effects of solids retention time on the biological performance of a novel microalgal-bacterial membrane photobioreactor for industrial wastewater treatment. *Journal of environmental chemical engineering* **2021**, *9*, 105500.
37. Meng, F.; Chae, S.-R.; Drews, A.; Kraume, M.; Shin, H.-S.; Yang, F. Recent advances in membrane bioreactors (MBRs): membrane fouling and membrane material. *Water research* **2009**, *43*, 1489-1512.

Chapter 6 Effects of solid retention time on the membrane performance of a novel electrokinetic-assisted membrane photobioreactor (EK-MPBR)

Abstract

The effect of solid retention time (SRT) on the fouling behaviour of electrokinetic-assisted membrane photobioreactors (EK-MPBR) was examined in this study. Three SRTs (10, 20, and 40 days) were studied in treating synthetic municipal wastewater using microalgae *Chlorella vulgaris*. SRTs of 40 and 20 were run in parallel for 80 days, followed by another run of SRT of 10 days for 45 days. A similar fouling trend was observed in SRTs of 10 and 20 days, while SRT of 10 days had no fouling within the first 40 days of operation and had lower pore blocking despite a higher portion of smaller flocs. SRT of 40 days had 75 % more fouling than SRT of 20 days. While SRTs correlated with the fouling precursors, such as soluble microbial product (SMP) and extracellular polymeric substances (EPS), to a different extent, it was found that it had little correlation with fouling as a result of the abundance of these precursors in the suspension. The low voltage direct current applied electric field (4 mA) appeared to affect the particle size of the biomass suspension and, thus, contributed mainly to the fouling prevention of EK-MPBRs with different SRTs. Backwash flux resulting from the applied electric field was calculated and contributed to a greater extent in the SRT of 10 days compared to the prolonged SRT of 20 and 40 days. In summary, SRT of 10 and 20 showed similar and much better membrane performance than that of SRT of 40 days in EK-MPBRs. Biomass concentration, the zeta potential of flocs, and electrophoretic force played a significant role in membrane fouling of EK-MPBRs.

Keywords: Membrane photobioreactor, Solid retention time, Electrokinetic, Membrane fouling

6.1 Introduction

By combining a membrane separation unit with microalgae cultivation, membrane photobioreactor (MPBR) has emerged as one of the promising wastewater treatments and phycoremediation techniques. MPBRs utilize microalgae or microalgal biomass to intake nutrients from wastewater. This leads to the moderation of nutrients such as nitrogen and phosphorus, the main pollutants of the wastewater discharges. Compared to other biological wastewater techniques, MPBRs provide better nutrient removal and simultaneous microalgae production [1,2]. Despite the advantages of MPBR over conventional wastewater treatment systems [3,4], membrane fouling remained a drawback in utilizing MPBRs. Some techniques have been studied and developed to control fouling in MPBRs, such as quorum quenching, controlling solid retention time (SRT) and nutrient compositions [5-7]. Utilizing an electric field to control fouling is a relatively recent approach, especially in MPBRs.

Electrical approaches such as electrocoagulation and electrooxidation under the electric field have shown great potential for fouling mitigation due to their low operational cost compared to other fouling control methods [8,9]. A recent study has demonstrated the advancement of electric-assisted fouling control in MPBRs [10]. They observed improved nutrient removal and reduced fouling rate in MPBRs with an applied electric field. In addition to this literature, another group used *Chlorella vulgaris* as biomass and observed better nutrient removal and fouling control than the control MPBR [11]. However, this field has the potential to further improve the performance of EK-MPBRs in terms of fouling control and nutrient removal. Furthermore, a combination of factors such as SRT and electric field and their effect on fouling control has not been investigated yet.

This study incorporated a novel electrified MPBR (EK-MPBR) design and studied the effect of different SRTs on the fouling behaviours of EK-MPBRs. Microalgae *Chlorella vulgaris* was used to treat synthetic municipal wastewater. The performance of EK-MPBRs with three different SRTs of 10, 20, and 40 was compared and is reported in this literature. Furthermore, the effect of electrophoresis and electroosmosis on the fouling inhibition was investigated in the current study to further examine the potential of the electrified MPBRs as a promising wastewater treatment technique.

6.2 Materials and methods

6.2.1 EK-MPBR set-up and operation

Three lab-scale electric-assisted membrane photobioreactors (EK-MPBRs) were constructed for treating synthetic municipal wastewater using graphite as an anode and stainless steel mesh as a cathode. A detailed schematic diagram of the experimental set-up of EK-MPBR was provided in our previous publication [11]. The effective volume of the reactors is 10 L, where the membrane modules were submerged. A direct current (DC) electric field was applied during the operation through a modified design of the conventional MPBR. The cathode, and stainless steel sheets were placed underneath the membrane to provide support and current simultaneously. The graphite sheets, or anode, were placed facing the membrane on each side of the membrane module at a distance of approximately 0.03 m. Polyvinylidene fluoride (PVDF) flat sheet membranes with a pore size of 0.1 μm were utilized and placed on both sides of the membrane module between the cathode and anode. The microalgae strain was freshwater *Chlorella Vulgaris* (CPCC 90) purchased from the Canadian Phycological Culture Centre (University of Waterloo, ON, Canada). The pre-cultured microalgae were cultivated in a modified mineral salt medium (MSM), according to the literature[12]. Two aeration stone was placed under the membrane module to deliver CO_2 to the microalgae and help to mix the suspension and fouling prevention. The overall aeration intensity in each EK-MPBR was 2.2 ± 0.05 L/min. The hydraulic retention time (HRT) was kept constant through the permeation flux of approximately 8.5 L/m^{2}h for the three EK-MPBRs during the entire experimental period. The solid retention time (SRT) was the variable of this study and was kept at 40, 20, and 10 during the operation of the EK-MPBRs for 80, 80, and 45 days, respectively. When the transmembrane pressure (TMP) reached at about 35 kPa, physical cleaning was performed to maintain the flux. At the end of each run, physical cleaning followed by chemical cleaning was conducted to measure each membrane module's filtration resistance of each membrane module.

6.2.2 Membrane filtration evaluation

Membrane filtration resistance was calculated based on Darcy's law as the following equations [13]:

$$R = \frac{\Delta P}{J\mu} \tag{6.1}$$

$$R_t = R_m + R_p + R_c \quad (6.2)$$

Where, ΔP is the transmembrane pressure (kPa), J is the permeate flux (L/m^2.h), μ is the dynamic viscosity of the permeate (Pa.s), and R is the membrane resistance (m^{-1}); $R_t, R_m, R_p,$ and R_c are total resistance to filtration, virgin membrane, pore blocking, and cake layer resistance, respectively.

At the end of each run, R_t, the total resistance, was calculated based on the final permeability and transmembrane pressure in the EK-MPBR. R_c and R_p can be obtained by measuring the permeability of the membrane after physical and chemical cleaning, respectively. R_m was measured before the start of the experiment using tap water through the virgin membrane [13].

6.2.3 Particle size distribution (PSD)

Malvern Mastersize 2000 instrument (Worcestershire, UK) was used to determine the particle size distribution of the mixed liquor. The samples were automatically measured in triplicate with a detection range of 0.02-2000 μm.

6.2.4 Quantitative and qualitative analysis of extracellular polymeric substances (EPS) and soluble microbial product (SMP)

Lowry's method was carried out to measure protein content in SMP and EPS using BSA as the standard [14]. The carbohydrate content in SMP and EPS with glucose as standard and the Gaudy method was also used [15]. The proteins and carbohydrates were normalized as the sum of protein and carbohydrate as total EPS and SMP.

The extraction method of EPS was the modified method used in literatures and is described as follows [16-18]. The microalgal suspension was centrifuged at 4400 xg for 15 min. The supernatant was filtered through a 0.45 μ filter and collected as SMP. The pellet was then added to 25 ml of 1.5 M NaCl at 30°C for one hour, followed by centrifugation at 10000 x g for 15 min. The filtered supernatant (0.45 μ filter, Nitrocellulose filter paper (Merk, Ireland)) was collected as EPS and was further analyzed for protein and carbohydrate measurements.

6.2.5 Sludge volume index (SVI) and zeta potential

SVI was tested according to APHA 21st Edition [19]. The zeta potential of the flocs was measured by using a NanoBrook ZetaPlus (Brookhaven, USA). Samples were diluted in 1 mM KCl solution. Each sample was triplicated by the instrument to confirm the zeta potential value. Zeta potential was calculated according to Smoluchowski's equation [20].

6.2.6 Statistical analysis

The comparison of SMP and EPS at different SRTs was performed using an analysis of variance (ANOVA). If $P<0.05$, the difference is considered statistically different.

6.3 Results

In this section, the parameters affecting membrane performance and fouling, including transmembrane pressure (TMP), flux, particle size distribution (PSD), and fouling precursors such as EPS and SMP were measured in replicate are presented.

6.3.1 Membrane fouling performance

Figure 6.1 represents the time-course monitoring of TMP and flux for the three EK-MPBRs. The development of TMP over time is an indicator of the fouling of the membrane and the EK-MPBRs represented different fouling development. Between days 1 to 10, attributed to the initial fouling stage, EK-MPBRs with SRT of 20 and 10 showed relatively similar patterns, during which SRT of 10 days showed a slightly sharper TMP increase). SRT of 40 days, however, exhibited earlier and sharper fouling in the same period. After day 11 and the initial TMP increment, SRT of 40 showed much faster fouling compared to the other two EK-MPBRs. A slight increase in TMP (low fouling rate) with experimental time was observed for SRT of 20 days, while no fouling was observed for SRT of 10 days within the first 40 days of operation. The first phase of physical cleaning happened on day 11 in SRT of 40 as opposed to day 74 in SRT of 20. More frequent and diverse rate of fouling has been observed in SRT of 40 which suggests more sever fouling in SRT of 40 compared to SRT of 10 and 20 days. The shortened SRT of 20 and 10 days, showed less frequent fouling in a way that the physical cleaning of 74 days was sufficient for SRT of 20 days and no fouling occurred during the operation of SRT of 10 days for the first 40 days. Fouling

started to develop after day 40 for SRT of 10 days. The different fouling behaviours of the EK-MPBRs under different SRTs could be explained by the changes in MLSS concentration, sludge properties, and electrophoretic phenomena, which will be investigated in the preceding sections.

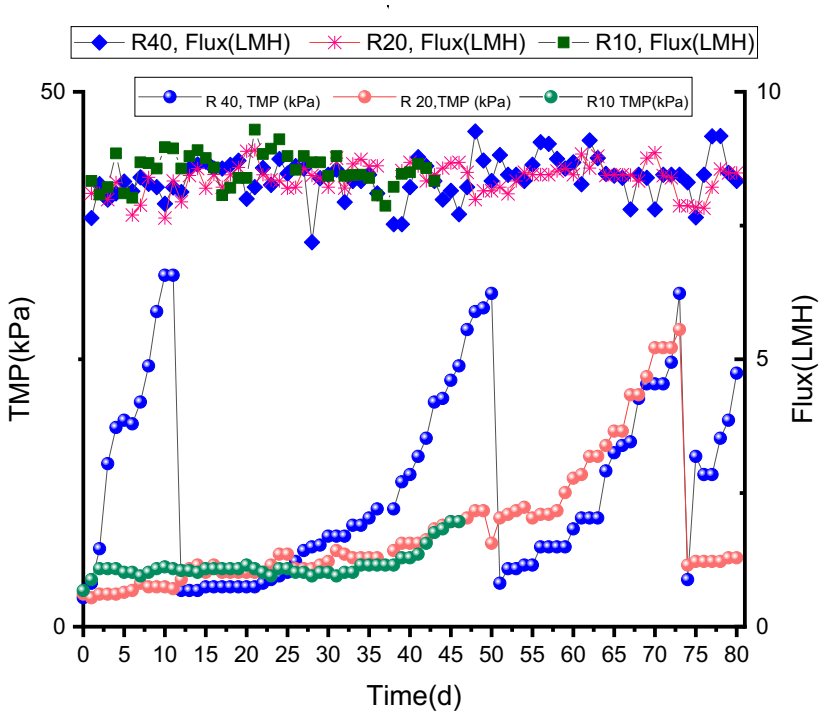

Figure 6-1 Membrane flux and TMP over the experimental period.

6.3.2 Optical image of the cake layer

As presented in Figure 6.2, the optical image of the cake layer formed on the membrane surface for each EK-MPBR was visually different in terms of colour and thickness. The pictures were taken at the end of experimental periods from the cake layer formed on membrane surface. The cake layer formed in EK-MPBR with SRT of 40 days showed thicker and greenish cake layer formation compared to the other two reactors.

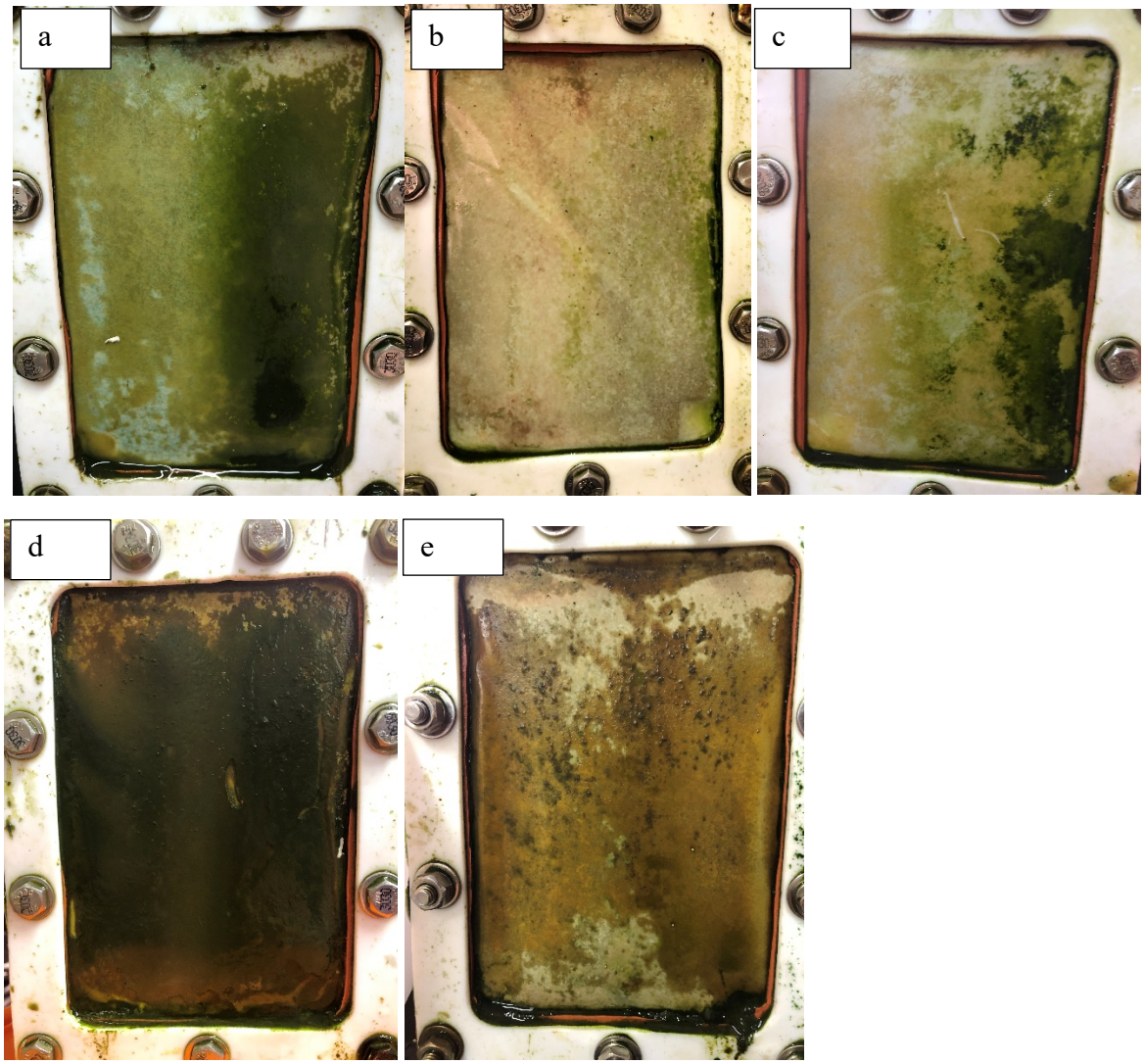

Figure 6-2 Optical image of the cake layers on the membrane surface on the last day of the operation in EK-MPBRs with SRTs of a) 40 days b) 20 days c) 10 days d) cake layer of the fouled membrane for SRT of 40 days before the first physical cleaning on day 12 e) cake layer of the fouled membrane for SRT of 20 days taken on day 74.

6.3.3 Resistance of membrane filtration

The permeability of the membranes were measured at the end of each run and after physical and chemical cleaning. The results are summarized in Table 6.1 for all three EK-MPBRs. This measurement aims to identify the contribution of different fouling mechanisms, such as pore blocking and cake/gel layer formation. The membrane resistance in SRT of 40, 20, and 10 days was greatly different in values. However, as the final TMP in the MPBRs were different, the direct

evaluation and comparison of the values is not recommended and should be with regard to the contribution and dominant mechanism in each EK-MPBR. In terms of the contribution of the resistances, all three SRTs revealed cake/gel layer formation as the major contributor to the total resistance among which SRT of 40 days showed the highest gel/cake layer filtration resistance. SRT of 10 days showed the lowest pore clogging filtration resistance as compared to SRT of 20 and 40 days.

Table 6-1 Compositions of membrane filtration resistances

	$R_m(\times 10^{12}\ m^{-1})$	$R_p(\times 10^{12}\ m^{-1})$	$R_c(\times 10^{12}\ m^{-1})$	$R_t(\times 10^{12}\ m^{-1})$
R40	0.39 (2.56%)	2.54(16.81%)	12.18 (80.63%)	15.11 (100%)
R20	0.38 (2.87%)	0.96 (7.24%)	11.91 (89.89%)	13.25 (100%)
R10	0.36 (7.7%)	0.3 (6.15%)	4.03 (86.15%)	4.67(100%)

6.3.4 Particle size distribution (PSD) of biomass in the suspension

Particle size distribution (PSD) as a factor determining membrane fouling rate was measured and presented in Figure 6.3. As shown in this Figure, the development of PSD over the experimental period differed as SRT was shortened. The EK-MPBRs with SRT 40 and 20 were started with a relatively identical biomass consortium and showed a unimodal PSD with the major portion of particles being in size range of 110 to 1000 μm. Both EK-MPBRs of SRT 40 and 20 days showed a change from unimodal to polymodal distribution at the end of the experiment. A comparison between the two EK-MPBRs shows that PSD at SRT of 40 days showed that the prolonged SRT from 20 to 40 days led to a greater portion of small particles with the size range of 2 to 70 μm. At SRT of 10 days, however, the initial biomass consortium appeared to be different with regard to the size with, an observed bimodal distribution on day 1. SRT of 10 days showed a gradual change with the dominancy of the particle with a size ranging from 20 to 80 μm. SRT of 10 days had a significantly larger portion of smaller flocs in PSD as compared to that of SRT of 20 and 40 days. As for all three EK-MPBRs, the operation and the electric field increased the portion of smaller particles over the course of the experiment.

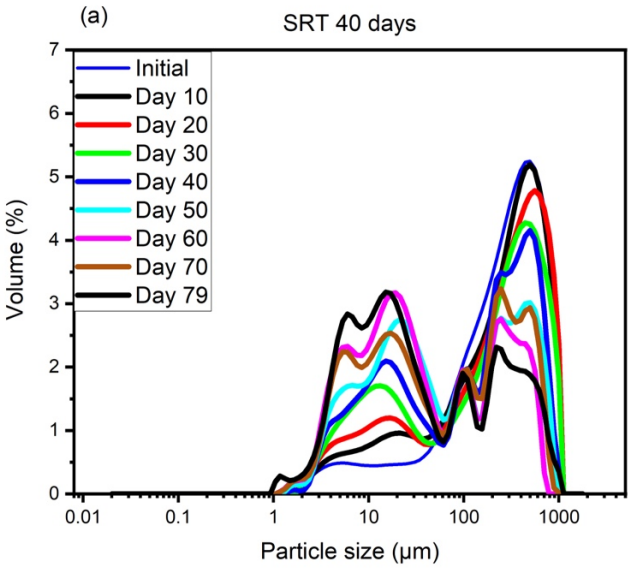
(a)
SRT 40 days
Initial
Day 10
Day 20
Day 30
Day 40
Day 50
Day 60
Day 70
Day 79
Volume (%)
Particle size (μm)
0.01
0.1
1
10
100
1000
0
1
2
3
4
5
6
7

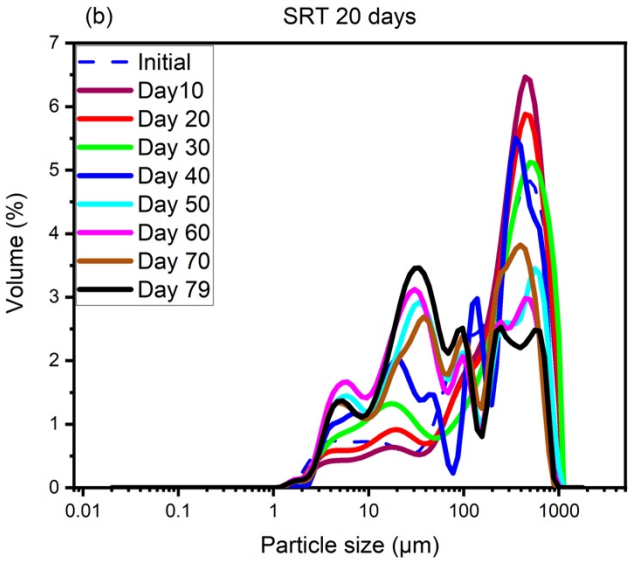
(b)
SRT 20 days
Initial
Day10
Day 20
Day 30
Day 40
Day 50
Day 60
Day 70
Day 79
Volume (%)
Particle size (μm)
0.01
0.1
1
10
100
1000
0
1
2
3
4
5
6
7

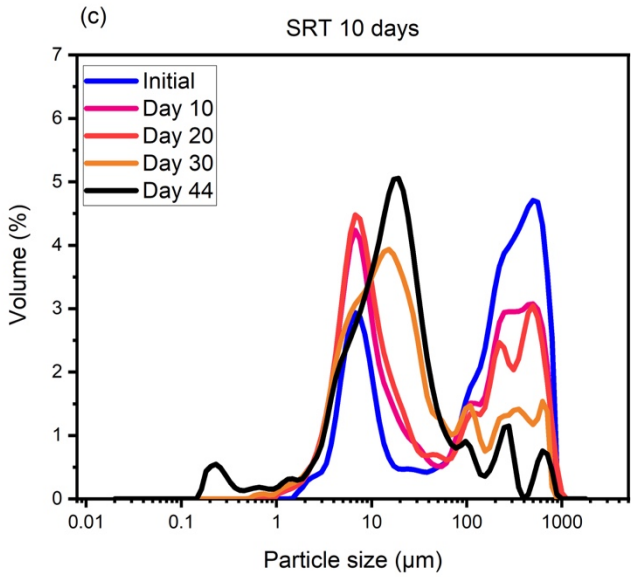

Figure 6-3 Particle size distribution of EK-MPBRs a) SRT of 40 days, b) SRT of 20 days and c) SRT of 10 days.

6.3.5 Floc size distribution of the cake layer

Figure 6.4 illustrates the PSD of the cake layer in EK-MPBRs for SRT of 40, 20, and 10 days. All three EK-MPBRs showed polymodal distribution among which SRT of 40 days showed a larger portion of smaller particles between 1 to 10 µm. The volume of middle range particle sizes (50-200 µm) of SRT 10 days was relatively higher. On the other hand, the cake layers from SRT of 20 and 40 days had a larger portion of larger flocs (approximately 500-1000 µm). This observation further supports the PSD of biomass as represented in Figure 6.3 (a and b).

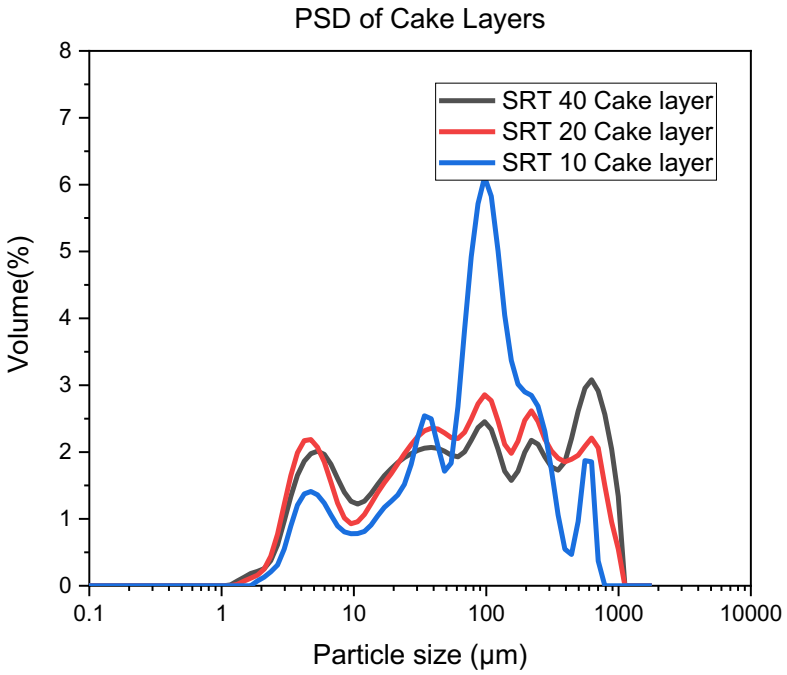

Figure 6-4 Floc size distribution of the cake layer for EK-MPBRs with SRTs of 10, 20, and 40 days.

6.3.6 Extracellular polymeric substances (EPS) and soluble microbial products (SMP) content

A comparable EPS and SMP content were observed at SRTs of 40, 20, and 10 days. In all three reactors, total SMP content decreased under the applied electric field starting on day 5 and continued to decline until day 12 after which the fluctuation was observed in both reactors. The overall total SMP, protein and carbohydrate for the SRTs of 40, 20, and 10 days were not statistically different based on ANOVA ($P = 0.06$). The average total SMP for SRTs of 40, 20, and 10 days was 7.07 ± 0.06, 7.15 ± 0.06, and 10.7 ± 2.92 mg/L, respectively. Since the reactors with SRTs of 40 and 20 days were run in parallel, the same day comparison of total SMP was performed and showed comparable concentration throughout the experimental period of 80 days ($P = 0.97$). The ratio of protein to carbohydrate (PN/PS) remained relatively constant during the experiment (0.86± 0.35, 1.15 ±0.65, and 3.47 ± 0.94 for SRTs of 40, 20, and 10 days ($P > 0.05$). On the contrary, total EPS results revealed that despite comparable EPS concentration at SRTs of 40 and 20 days, the difference between EPS at SRT of 10 and that of the prolonged SRTs of 20 and 40

was statistically significant ($P < 0.05$). The variation of EPS with SRTs is represented in Figure 6.5. The overall EPS concentration for SRTs of 40, 20 and 10 days was 10.22 ± 1.07, 11.76 ± 2.6, and 21.27 ± 4.43 mg/g MLSS, respectively. Furthermore, protein was the dominant component of EPS in all three SRTs for almost the entire operational periods. The same day comparison of total EPS for SRTs of 40 and 20 showed comparable results throughout the run ($P=1$). The average PN/PS of the last 10 days of the operations were 1.48 ± 0.6, 0.85 ± 0.24, and 3.84 ± 1.48 for SRTs of 40, 20, and 10 days, respectively. As shown in Figure 6.6 (c), the protein concentration and the ratio of PN/PS significantly changed during the operation of EK-MPBR with SRT of 10 days ($P <0.05$).

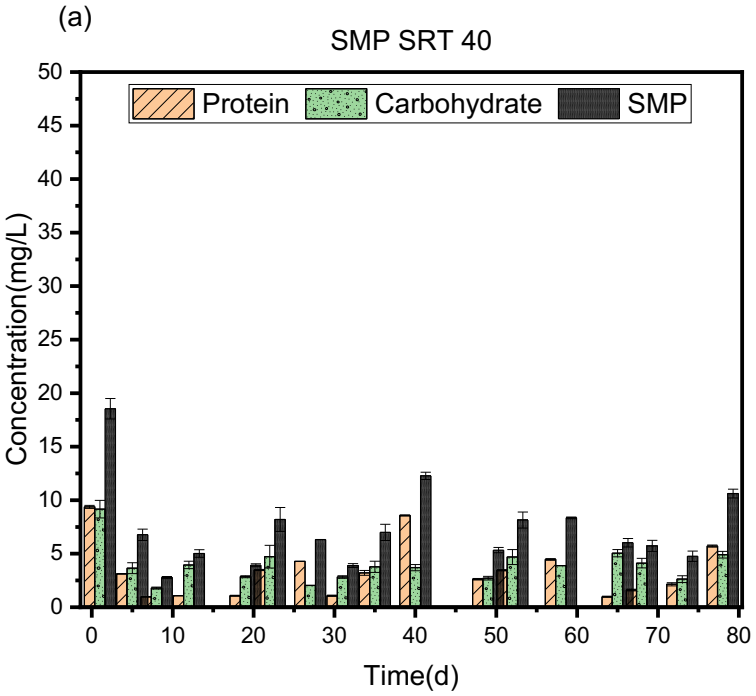
(a)
SMP SRT 40
Protein
Carbohydrate
SMP
Concentration(mg/L)
Time(d)
0
5
10
15
20
25
30
35
40
45
50
0
10
20
30
40
50
60
70
80

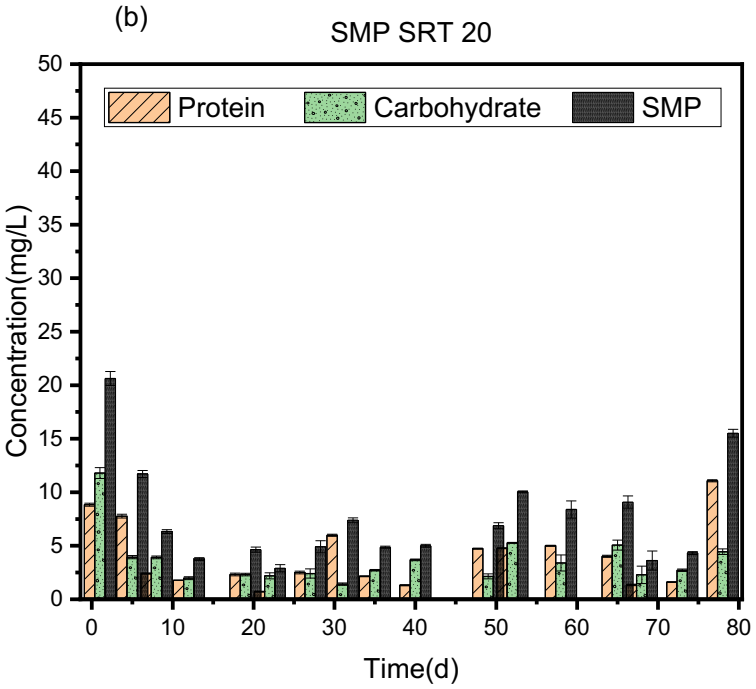
(b)
SMP SRT 20
Protein
Carbohydrate
SMP
Concentration(mg/L)
Time(d)
0
5
10
15
20
25
30
35
40
45
50
0
10
20
30
40
50
60
70
80

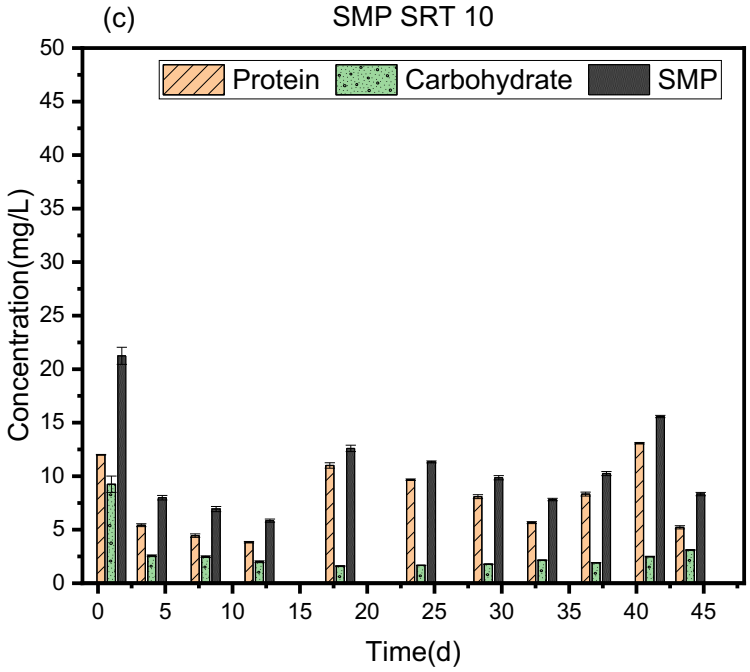

Figure 6-5 SMP composition of EK-MPBRs with SRTs of a)40 days b)20 days c) 10 days. Values and error bars represent average and standard deviation from two technical replicate measurements (n = 2), respectively.

(a)

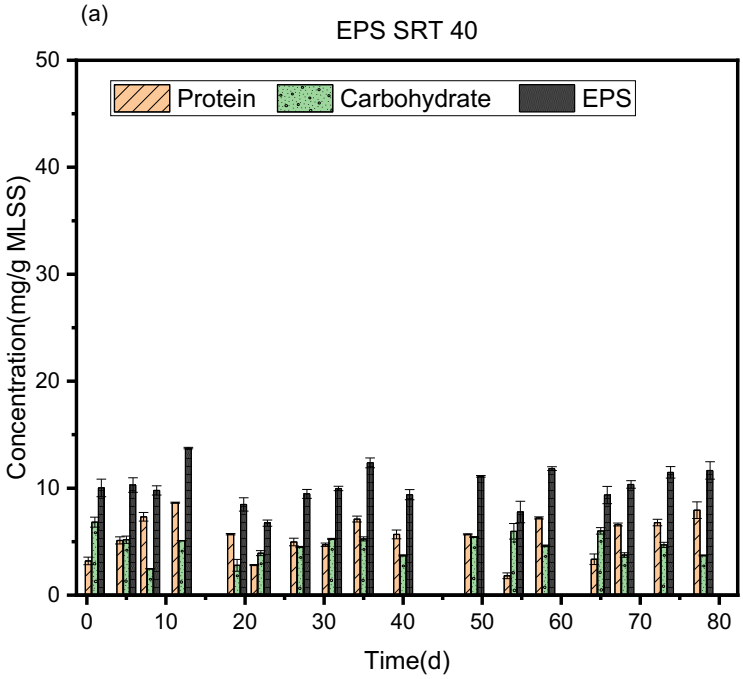
EPS SRT 40
Protein
Carbohydrate
EPS
Concentration(mg/g MLSS)
Time(d)
0
10
20
30
40
50
60
70
80

(b)

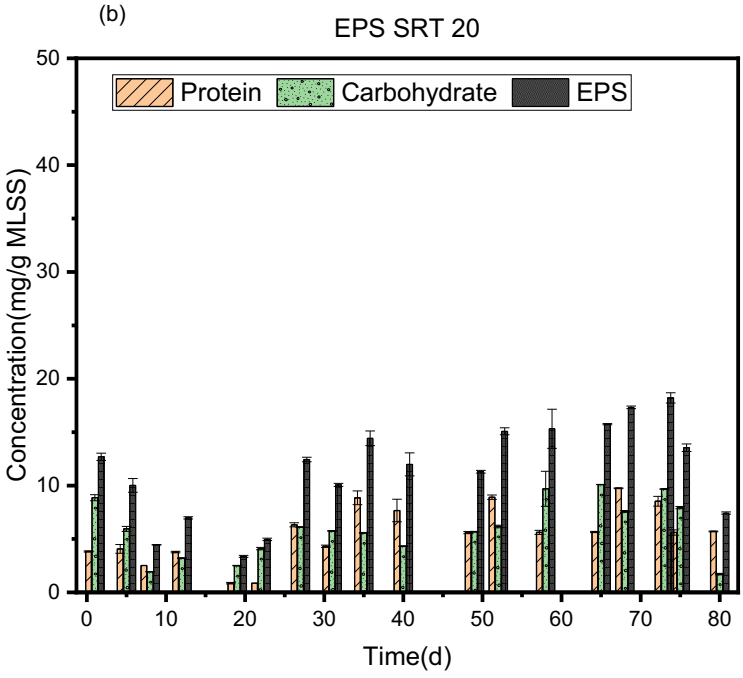
EPS SRT 20
Protein
Carbohydrate
EPS
Concentration(mg/g MLSS)
Time(d)
0
10
20
30
40
50
60
70
80

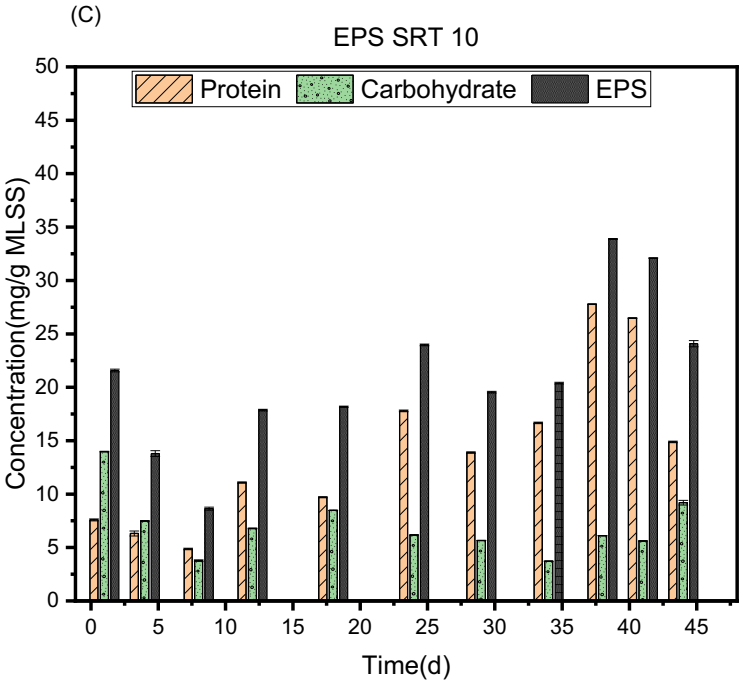

Figure 6-6 EPS composition of EK-MPBRs with SRTs of a)40 days b)20 days c) 10 days. Values and error bars represent average and standard deviation from two technical replicate measurements (n = 2), respectively.

6.3.7 Voltage changes vs. transmembrane pressure (TMP)

The voltage changes could also be an indicator of cake layer formation and fouling of the membrane. Thus, the time-course monitoring of the voltage was recorded and presented in Figure 6.7.

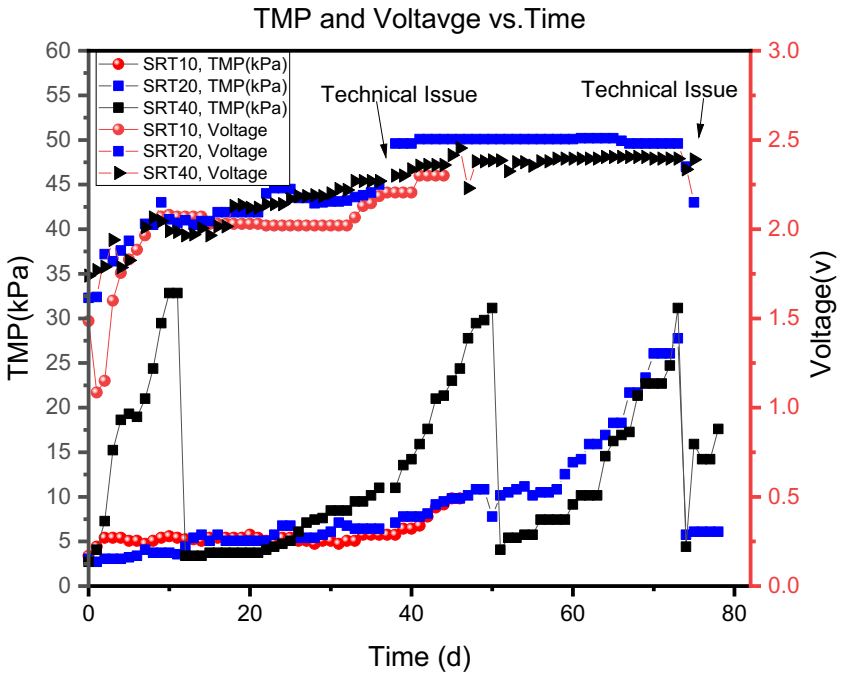

Figure 6-7 Voltage and TMP variation in EK-MPBRs.

The equilibrium phase occurred at approximately day 2 at SRT of 40 days and day 7 at SRT of 20 and 10 days. The average voltage for SRTs of 40, 20, and 10 days was 2.23, 2.28 and 2.00 v, respectively. The next phase, during which the cake layer started to grow on the membrane surface and caused TMP increase occurred on day 32, 22, and 18 at SRTs of 10, 20 and 40 days, respectively. After physical cleanings, the voltage dropped and continued to increase with the formation of a new cake layer. At SRT of 40 days, the trend of voltage variations after physical cleanings (days 11, 50, and 73) differed each time. Both SRTs of 40 and 20 days encountered technical issues that led to power interruption on days 36 and 75.

6.3.8 Backwash flux and electric field affect

By introducing an electric field to the biomass, the particles will acquire a more negative charge and repel from the surface of the membrane, which is also negatively charged. This phenomenon, which is called electrophoretic movement, is in the opposite direction of permeate being pumped through the membrane. Since the electric field was continuously applied, the effect of electrophoresis and backwash flux is studied to quantify the potential effect of electrophoresis in

the fouling control. The electrophoresis induced flux could be calculated based on the following formulas.

$$E = \frac{\Delta U}{d} = \frac{I}{\sigma A} \tag{6.3}$$

$$J_{backwash} = \frac{Q_p}{A} = 3.6 \times 10^6 . v_p \tag{6.4}$$

$$v_p = \frac{\varepsilon \zeta}{\mu} E \tag{6.5}$$

Where E is the electric field strength $(^{v}/_{m})$, ΔU is the voltage (V), d implies the distance between the cathode and anode (m), I is the current (A), and σ is the conductivity of the biomass suspension$(^{S}/_{m})$ [17,21]. In the second and third equations, v_p is the electrophoretic velocity $(^{m}/_{s})$, ζ is the zeta potential of the particles (v), ε is the permittivity of the electrolyte $(^{F}/_{m})$, μ is the viscosity of the permeate $(Pa.s)$, $J_{backwash}$ is the electrophoretic equivalent of backwash flux $(^{L}/_{(m^2.h)})$, and Q_p is the flow rate of permeate water $(^{m^3}/_{s})$.

In this study, the applied current was kept constant at the value of 0.004 A, and the average zeta potential for SRT of 40, 20 and 10 days was -25.0 ± 4.7, -23.5 ± 5.2, and -28.71 ± 8.5 mv, respectively. The calculated electrophoretic velocity at 25 ◦ c and backwash flux is calculated and summarized in Table 6.2.

Table 6-2 Electric field parameters and backwash flux in EK-MPBRs

	ΔU (v)	Zeta potential (mv)	$v_p(\times 10^{-7})$ (m/s)	$J_{backwash}$ $(^{L}/_{(m^2 h)})$	$\frac{J_{backwash}}{Q_p}$ (%)
SRT 40 days	2.23	-25.0 ± 4.7	1.67 ± 0.28	0.60 ± 0.01	6.9 ± 0.01
SRT 20 days	2.28	-23.5 ± 5.2	1.61 ± 0.31	0.58 ± 0.02	6.7 ± 0.02
SRT 10 days	2.00	-28.71 ± 8.5	1.78 ± 0.54	0.64 ± 0.34	7.4 ± 0.04

As represented in Table 6.2, SRT of 10 days had higher zeta potential and, thus, better potential backwash flux. While the repulsive force for SRTs of 20 and 40 were fairly similar, the repulsive

force caused by the electric field on each side of the membrane module led to 0.7 % and 0.5 % higher backwash flux in SRT of 10 days compared to that of SRT of 20 and 40 days, respectively. Since this effect is continuous, it can have a major influence on membrane fouling and is worth considering [17].

6.3.9 Sludge volume index (SVI)

SVI is a widely used settleability potential of the biomass and an indicator of the fouling potential. In order to measure this index, biomass suspension of EK-MPBRs was analyzed for SVI measurement at room temperature (25.7 ± 0.7 ° c). The results are presented in Figure 8. For all three EK-MPBRs, the applied electric field improved the settleability of the biomass. EK-MPBRs with SRTs of 40 and 20 days showed almost similar and better settleability compared to SRT of 10. SRT of 40 days showed an overall better settleability for nearly the entire operation except for days 35 to 45 and the end of operation, even with a higher biomass concentration. The shortened SRT to 20 and 10 days which interfered the settleability improvement caused by the electric field.

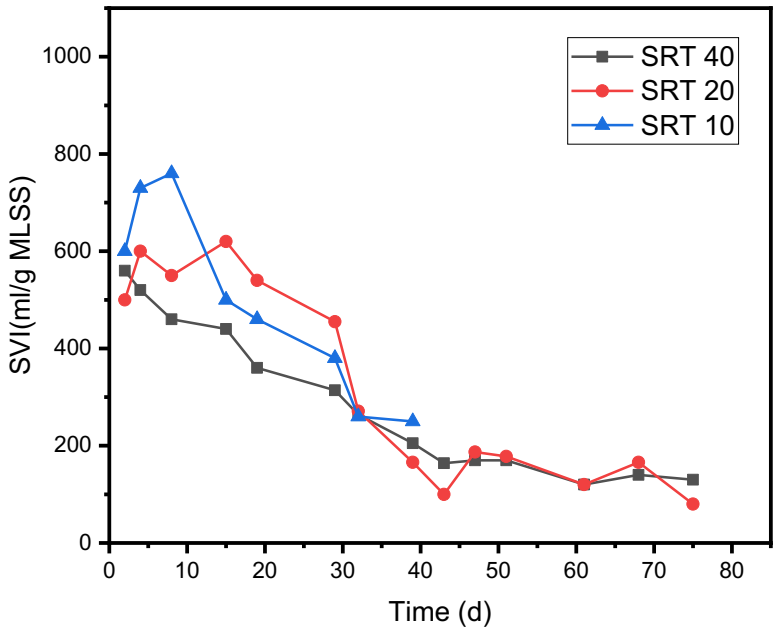

Figure 6-8 Sludge volume index over the experimental period.

6.4 Discussion

6.4.1 Sludge properties

As presented in Figure 6.3, the overall SRT of 10 days exhibited a higher portion of smaller flocs as compared to SRTs of 20 and 40 days. Larger flocs with a size range of >100 μm, which can be attributed to the presence of bacteria and contamination in biomass, remained high, whereas their percentage declined at SRTs and 40 and 20 days. It is well accepted that the prolonged SRT promotes the existence of bacterial contamination in the microalgae suspension and further supports the observation of a higher portion of large flocs at SRTs of 40 and 20 days compared to that of SRT of 10 days [22]. In addition, the significant decrease in the range of floc size at SRT of 10 days could be due to more influence of the applied electric field on the biomass inside the reactors at a younger age. It has been argued that the electric field could inhibit the bacteria's growth and prevent cell agglomeration [11]. The relatively higher value of zeta potential at SRT of 10 days could be related to the more influence of the electric field at SRT of 10 days and, therefore, lower bacterial contamination. Furthermore, the electrostatic repulsion between the cells would increase with the increased surface charge, which is presented as zeta potential (ζ). The higher absolute value of ζ could prevent the algal cell agglomeration and the formation of larger flocs. The positive correlation between the average zeta potential value and the magnitude of reduction in the portion of flocs at SRTs of 20 and 40 days are further aligned with the effect of zeta potential in preventing cell agglomeration. The fraction of PN/PS in EPS is a major contributor to the surface charge of the flocs [23], indicating that higher zeta potential at SRT of 10 days might be due to the higher PN/PS ratio (3.84 ± 1.48) compared to that of SRT of 20 (0.8 ± 0.24) and 40 days (1.48 ± 0.6). This agrees with the finding of Shadi Hassan et al.[24].

The particle size range of 1 to 100 μm could represent individual cells. In all three EK-MPBRs, this portion increased due to the applied electric field. It has been argued that the electrokinetic phenomena would reduce the size of the algal cells due to the electrophoresis and electroosmosis phenomena that will be discussed further[10].The comparison of the initial line graphs in Figure 6.3 reveals that an SRT of 10 days recorded a higher portion of small flocs at the beginning compared to that of SRTs of 20 and 40 days. This relatively different initial condition can also contribute to the higher percentage of smaller cells (1 to 100 μm) at an SRT of 10 days.

The comparative graph (Figure 6.8) represents the settleability of the flocs in relation to SRTs. Both sets of SRT of 40 and 20 days showed better settleability compared to the shortened SRT of 10 days even at a higher MLSS concentration. This could be due to the lower ZP value of longer SRTs of 40 and 20 days compared to 10 days of SRT.

6.4.2 Membrane fouling performance

In addition to the factors affecting membrane fouling in MPBRs such as PSD, SMP and EPS, EK-MPBRs can be studied in terms of the change of these precursors under the electric field effect [25,26]. In addition, this study focuses on the impact of SRTs on the fouling formation in EK-MPBRs. As shown in Figure 6.1, TMP development varied for different SRTs, among which SRT of 40 days showed the fastest fouling rate. For the entire operating time of 80 days for SRTs of 40 and 20 days, the cleaning cycle was required significantly less frequently, from three to only once, with a shortening SRT from 40 to 20 days, respectively. The initial fouling stage in SRT of 40 days could be attributed to the first stage of fouling which is pore blocking and happens within the first few days of the operation. The presence of a higher volume of smaller flocs in SRT of 40 days compared to SRT of 20 days could lead to faster fouling development in SRT of 40 days. This finding has confirmed the study of others (e.g. [27] that particle size distribution is a significant contributor and can be used to indicate the rate of membrane fouling). A comparison between the PSD in Figure 6.3 (a), (b), and (c) further highlights the relationship between the portion of smaller flocs (< 100 μm) and the rate of fouling development. As shown in this Figure, a higher tendency for fouling growth was observed in SRT of 10 days, as compared to SRT of 20 days in the first few days of operation, containing more smaller flocs in the suspension. However, a contradictory trend between PSD and fouling development has occurred between SRT of 40 days and 10 days, in which the higher percentage of small individual cells (< 100 μm) in SRT of 10 days did not cause more severe fouling in SRT of 10 days and during the stage of pore clogging. In order to explain this difference in the trend, other underlying factors affecting fouling in EK-MPBRs should be considered, such as MLSS concentration. Despite particle size, MLSS concentration is another governing factor contributing to membrane fouling [2]. The higher biomass concentration at SRT of 40 days compared to the shortened SRTs of 20 and 10 days can explain faster fouling

development during the operational period. This agrees with the finding of Zhang et al. [27] that the higher biomass concentration leads to more fouling in MPBRs.

Followed by pore blocking phenomena, cake/gel layer formation happens that is affected by factors such as SMP and EPS. As shown in Figure 6.5, the SMP component of the biomass varied with SRTs as SRT of 10 days, having slightly higher overall SMP content in all three SRTs. It is clear that introducing an electric field reduced the SMP component, especially in the first few days of operation. In addition to the effect of applied current, SMP appeared to be hardly affected by SRT changes, and the overall SMP remained comparable. This agrees with the finding of others that SMP is a minor contributor to the fouling under the applied electric field [10,11] .As such, a slightly higher average SMP at SRT of 10 days (3 mg/L higher compared to SRT of 20 and 40 days) might not significantly affect the TMP increase. However, a positive correlation has been observed between the TMP increase and total SMP concentration. For instance, the higher SMP concentration on days 42, 80 and 60 aligned with the higher TMP on the exact days in SRT of 40 days. Moreover, the gradual increase in SMP component at SRTs of 20 and 10 days shows a direct correlation between TMP and SMP increase. This agrees with the finding of other literature [22,28].

EPS is another fouling precursor affecting cells' binding and cell-membrane attachment (i.e. formation of gel/cake layer). The comparable average total EPS at SRTs of 20 and 40 days and yet different fouling development rates could suggest that EPS was not the major contributor to the fouling, and other fouling mechanisms should be considered. As shown in Figure 6.6, the highest value of total EPS was observed at an SRT of 10 days, while the TMP development at this SRT revealed little correlation between EPS content and fouling development. This agrees with the finding of Shadi et el., where the observed adverse correlation between EPS and the membrane fouling in an electrified MBR [24]. In addition, the comparison between EPS content of SRTs of 20 and 40 days can suggest that despite the time difference in SRT, the average EPS content was comparable. At SRT of 10 days, however, the shortened SRT appeared to affect total EPS significantly by 80 % compared to SRT of 20 days and 100 % compared to SRT of 40 days. The prolonged SRT revealed the effect of SRT in increasing EPS protein (EPSp) content respective to the increased SRT, especially during the last days of operation and reaching stable conditions. However, the electric field appeared to be effective in removing EPS carbohydrate (EPSc),

especially during the first few days of operation, where EPSc was reduced by 64 % at SRT of 40 days, 73 % at SRT of 20 days, and 78 % at SRT of 10 days. The lowest ratio of PN/PS in EPS was observed at SRT of 20 days, while the highest was accounted for SRT of 10 days, and the nonlinear correlation between this value and SRT can suggest that the study of the EPS effect on fouling behaviour when an electric field is applied is complex and requires further investigations.

6.4.3 EF contribution to the fouling behaviour

The two main mechanisms electric field can contribute to the fouling control are electroosmosis and electrophoresis [24]. Electroosmosis can remove the bound water around the cells and make them smaller, reducing the specific resistance of the membrane formed by the cake layer [29]. This study agrees with this statement and shows the shrinkage of the cells in all SRTs of 40, 20, and 10 days (Figure 6.3). Despite SRT, all three EK-MPBRs showed more portions of smaller particles at the end of the operational period, which can be attributed to electrophoresis.

As shown in Figure 6.3 and Figure 6.4, despite a higher portion of small particles (<100 μm) at SRT of 10 days, the less of them were found in the cake layer compared to SRT of 40 and 20 days, meaning that they were more easily repelled from the membrane by the electric field, which is called electrophoresis, due to the smaller floc size and more negatively zeta potential. Electrophoresis is a movement in that charged particles move towards the opposite electrode. As both algal cells and the membrane are negatively charged, it can be estimated that the particles would move toward graphite sheets located outside the membrane module. The magnitude of this electrophoresis depends on various parameters such as particle size and zeta potential [24]. The magnitude of backwash flux was higher for SRT of 10 days compared to fairly similar backflush flux at the other two sets of SRT of 20 and 40 days (Table 6.2). As such, the less pore blocking (Table 6.1) can suggest the more significant effect of electrophoresis and the associated backwash flux at SRT of 10 days. Although the backwash flux contribution compared to the total flux was negligible, studies have found the impact of backwash flux in forming loosely attached and highly permeable cake layers as a result of electrophoretic movement on the surface of the membrane[17]. As shown in Figure 6.7, after each physical cleaning at SRT of 40 days, the voltage becomes stable faster compared to the beginning of the experimental period, which can further support the loosely

attached, probably thinner cake layer under the continuous effect of the electric field. This is in accordance with the observation of other literature [11,17].

SRT of 40 and 20 days had almost the same composition in terms of the size of the flocs forming the cake layer in Figure 6.4 except for the portion of particles with the size of approximately 600 μm. This higher portion of the large flocs can be attributed to the age of the cake layer and the frequency of the cake layer formed on the surface of the membrane, which was the highest among other SRTs.

Electrophoretic mobility is also affected by biomass viscosity. Sludge volume index (SVI) can be used as an indicator of the viscosity of the flocs as the higher viscosity would attribute to higher settleability [30]. The SVI values for all three EK-MPBRs are presented in Figure 6.8. Both SRTs of 40 and 20 days showed relatively similar settleability potential during the stable phase (day 30 onward), implying almost the same viscosity. SRT of 10 days, however, exhibited less and unstable settleability potential.

This can suggest the presence of flocs with less viscosity in SRT of 10 days remain suspended during the settlement time. This coagulation potential can be beneficial in fouling prevention and is affected by both zeta potential and the size of the cells [24]. It is well believed that larger particles can lead to faster settlement. Given the distinctively highest portion of smaller particles at SRT of 10 days and having the highest value of zeta potential can explain the lower viscosity and, as a result, higher electrophoretic mobility at SRT of 10 days compared to the other SRTs. It can be estimated that an SRT of 10 days can show less fouling and better membrane fouling in the long run, as compared to that of SRT of 40 days.

6.5 Conclusion

In EK-MPBR, SRT contributed differently to the fouling behaviour, depending on MLSS concentration and the size of the flocs. The fastest fouling was observed in SRT of 40 days, with the highest pore blocking and cake layer formation, as compared to the other two EK-MPBRs. SRT of 10 days exhibited similar fouling behaviour to SRT of 20 days but with no obvious membrane fouling during the first 40 days of operation except for the TMP jump in the first few

days operation due to less pore blocking and more repulsive electrophoresis force at SRT of 10 days. Electric filed contributed nonlinearly with SRT changes and, consequently, influenced fouling patterns differently based on the size and EPS component of the algal cells. In summary, shorter SRTs (10 and 20 days) had a lower fouling rate as compared to the prolonged SRT of 40 days. Biomass concentration, the zeta potential of flocs, and electrophoretic force played a significant role in controlling membrane fouling in EK-MPBRs.

6.6 References

1. Sheng, A.; Bilad, M.; Osman, N.; Arahman, N. Sequencing batch membrane photobioreactor for real secondary effluent polishing using native microalgae: Process performance and full-scale projection. *Journal of cleaner production* **2017**, *168*, 708-715.
2. Lee, W.; Kang, S.; Shin, H. Sludge characteristics and their contribution to microfiltration in submerged membrane bioreactors. *Journal of membrane science* **2003**, *216*, 217-227.
3. Marbelia, L.; Bilad, M.R.; Passaris, I.; Discart, V.; Vandamme, D.; Beuckels, A.; Muylaert, K.; Vankelecom, I.F. Membrane photobioreactors for integrated microalgae cultivation and nutrient remediation of membrane bioreactors effluent. *Bioresource technology* **2014**, *163*, 228-235.
4. Gao, F.; Li, C.; Yang, Z.-H.; Zeng, G.-M.; Feng, L.-J.; Liu, J.-z.; Liu, M.; Cai, H.-w. Continuous microalgae cultivation in aquaculture wastewater by a membrane photobioreactor for biomass production and nutrients removal. *Ecological engineering* **2016**, *92*, 55-61.
5. Lafi, H. Effect of organic carbon to nutrients (nitrogen and phosphorus) ratios on the performance of a novel microalgal-bacterial membrane photobioreactor. 2021.
6. Güneş, G.; Taşkan, E. Quorum quenching strategy for biofouling control in membrane photobioreactor. *Chemosphere* **2022**, *288*, 132667.
7. Liao, Y.; Bokhary, A.; Maleki, E.; Liao, B. A review of membrane fouling and its control in algal-related membrane processes. *Bioresource technology* **2018**, *264*, 343-358.

8. Sarkar, B.; De, S. Electric field enhanced gel controlled cross-flow ultrafiltration under turbulent flow conditions. *Separation and purification technology* **2010**, *74*, 73-82.
9. Yu, B.; Sun, J.; Zhao, K.; Ma, F.; Sun, L.; Shao, J.; Tian, J.; Hu, C. Mitigating membrane fouling by coupling coagulation and the electrokinetic effect in a novel electrocoagulation membrane cathode reactor. *Water research* **2022**, *217*, 118378.
10. Corpuz, M.V.A.; Borea, L.; Senatore, V.; Castrogiovanni, F.; Buonerba, A.; Oliva, G.; Ballesteros Jr, F.; Zarra, T.; Belgiorno, V.; Choo, K.-H. Wastewater treatment and fouling control in an electro algae-activated sludge membrane bioreactor. *Science of the total environment* **2021**, *786*, 147475.
11. Amini, M.; Mohamedelhassan, E.; Liao, B. The Biological Performance of a Novel Electrokinetic-Assisted Membrane Photobioreactor (EK-MPBR) for Wastewater Treatment. *Membranes* **2022**, *12*, 587.
12. Zhang, M.; Leung, K.-T.; Lin, H.; Liao, B. Effects of solids retention time on the biological performance of a novel microalgal-bacterial membrane photobioreactor for industrial wastewater treatment. *Journal of environmental chemical engineering* **2021**, *9*, 105500.
13. Lin, H.; Xie, K.; Mahendran, B.; Bagley, D.; Leung, K.; Liss, S.; Liao, B. Sludge properties and their effects on membrane fouling in submerged anaerobic membrane bioreactors (SAnMBRs). *Water research* **2009**, *43*, 3827-3837.
14. Classics Lowry, O.; Rosebrough, N.; Farr, A.; Randall, R. Protein measurement with the Folin phenol reagent. *Journal of biologocal Chemistry* **1951**, *193*, 265-275.
15. Gaudy, A. Colorimetric determination of protein and carbohydrate. *Industrial water wastes.* **1962**, *7*, 17-22.
16. Lv, J.; Zhao, F.; Feng, J.; Liu, Q.; Nan, F.; Xie, S. Extraction of extracellular polymeric substances (EPS) from a newly isolated self-flocculating microalga Neocystis mucosa SX with different methods. *Algal research* **2019**, *40*, 101479.
17. Zhang, J.; Satti, A.; Chen, X.; Xiao, K.; Sun, J.; Yan, X.; Liang, P.; Zhang, X.; Huang, X. Low-voltage electric field applied into MBR for fouling suppression: Performance and mechanisms. *Chemical engineering journal* **2015**, *273*, 223-230.

18. Luo, X.; Zhang, H.; Zhang, J. The influence of a static magnetic field on a Chlorella vulgaris-Bacillus licheniformis consortium and its sewage treatment effect. *Journal of environmental management* **2021**, *295*, 112969.
19. Federation, W.E.; Association, A. Standard methods for the examination of water and wastewater. *American Public Health Association (APHA): Washington, DC, USA* **2005**, *21*.
20. Shaw, D.J. *Introduction to colloid and surface chemistry*; Butterworths: 1980.
21. Zhang, S.; Yang, K.; Liu, W.; Xu, Y.; Hei, S.; Zhang, J.; Chen, C.; Zhu, X.; Liang, P.; Zhang, X. Understanding the mechanism of membrane fouling suppression in electro-anaerobic membrane bioreactor. *Chemical engineering journal* **2021**, *418*, 129384.
22. Zhang, M.; Leung, K.-T.; Lin, H.; Liao, B. Evaluation of membrane fouling in a microalgal-bacterial membrane photobioreactor: Effects of SRT. *Science of the total environment* **2022**, 156414.
23. Mikkelsen, L.H.; Keiding, K. Physico-chemical characteristics of full scale sewage sludges with implications to dewatering. *Water research* **2002**, *36*, 2451-2462.
24. Hasan, S.W.; Elektorowicz, M.; Oleszkiewicz, J.A. Correlations between trans-membrane pressure (TMP) and sludge properties in submerged membrane electro-bioreactor (SMEBR) and conventional membrane bioreactor (MBR). *Bioresource technology* **2012**, *120*, 199-205.
25. Wang, Z.; Wu, Z.; Tang, S. Extracellular polymeric substances (EPS) properties and their effects on membrane fouling in a submerged membrane bioreactor. *Water research* **2009**, *43*, 2504-2512.
26. Azizi, S.; Hashemi, A.; Shariati, F.P.; Tayebati, H.; Keramati, A.; Bonakdarpour, B.; Shirazi, M.M.A. Effect of different light-dark cycles on the membrane fouling, EPS and SMP production in a novel reciprocal membrane photobioreactor (RMPBR) by C. vulgaris species. *Journal of water process wngineering* **2021**, *43*, 102256.
27. Zhang, M.-j. Microalgal-Bacterial Membrane Photobioreactor (MB-MPBR) for Wastewater Treatment and Membrane Fouling Characterization. Lakehead University, 2020.

28. Low, S.L.; Ong, S.L.; Ng, H.Y. Characterization of membrane fouling in submerged ceramic membrane photobioreactors fed with effluent from membrane bioreactors. *Chemical engineering journal* **2016**, *290*, 91-102.
29. Ibeid, S.; Elektorowicz, M.; Oleszkiewicz, J. Modification of activated sludge properties caused by application of continuous and intermittent current. *Water research* **2013**, *47*, 903-910.
30. Jin, B.; Wilén, B.-M.; Lant, P. A comprehensive insight into floc characteristics and their impact on compressibility and settleability of activated sludge. *Chemical engineering journal* **2003**, *95*, 221-234.

Chapter 7 **Conclusions and future work**

7.1 Conclusions

Electro-phycoremediation is a newly developed technique that has proven to be effective in improving nutrients removal from wastewater. Furthermore, the integration of an electric field with the membrane separation process was able to successfully mitigate membrane fouling issues and increase the membrane's lifetime. The incorporation of a low voltage electric field with a membrane photobioreactor (MPBR) using *Chlorella vulgaris* as biomass is a novel approach that has been developed and investigated in this literature. This thesis focuses on the effect of an electric field on the biological performance of the microalgae *Chlorella vulgaris* and compares the membrane performance in an electrokinetic-assisted membrane photobioreactor (EK-MPBR) with a control MPBR. In addition, the effect of solid retention time (SRT) on the biological and membrane performance of EK-MPBR in treating synthetic municipal wastewater was studied.

Low voltage electric field influenced nitrogen and phosphorus removal efficiency. Over 50 % more phosphorus removal was seen in the EK-MPBR compared to the control MPBR, which could be due to electrochemical reactions around the electrodes. Lower nitrogen removal in EK-MPBR, however, shows interference with the nitrogen removal mechanism of microalgae induced by the electric field. Smaller flocs and lower pH were observed in EK-MPBR which might lead to a change in the growth mechanism of the microalgae. Comparable biomass production was achieved in EK-MPBR compared to the control MPBR.

The applied electric field impacted the fouling behaviour and membrane performance of EK-MPBR. Improved sludge settleability and less fouling were observed in EK-MPBR compared to MPBR. The fouling and cleaning frequency was lowered by 50 % in EK-MPBR compared to the control MPBR. The cake layer resistance was lower in the EK-MPBR while more pore blocking occurred in EK-MPBR compared to the control MPBR. The smaller flocs contributing to this more pore blocking could be attributed to the cell shrinkage caused by the electrophoretic movements under the electric field effect. The contribution of other fouling precursors such as SMP and EPS revealed that the SMP component was reduced in EK-MPBR which could explain less fouling. On

the other hand, the electric field and the electrochemical reactions led to lower contamination and, therefore, fewer bacteria and EPS concentration in the algal biomass. In summary, the study showed that electric fields could contribute to the fouling precursors to a varying extent and their attribution to the membrane performance.

In EK-MPBR, variation of SRT had little impact on the phosphorus removal efficiency while the nitrogen removal was improved by shortening SRT from 40 days to 20 and 10 days. Shortening SRT from 20 to 10 days was also beneficial to biomass productivity despite the relatively similar productivity of SRT of 20 and 40 days. The higher biomass productivity could be due to higher nutrients to biomass ratio in SRT of 10 days compared to that of SRT of 40 and 20 days. COD removal was hardly affected by SRT variation in EK-MPBR and the discharge standard was met regardless of SRT changes. PSD and microscopic images of biomass in EK-MPBRs show that changes in the size of the algal cells and agglomeration are in correlation with SRT.

Furthermore, SRT impacted membrane fouling by changing the particle size, zeta potential of the flocs, and biomass concentration. SRT of 40 days had more fouling with a higher cake layer and pore blocking resistance when compared to the relatively similar fouling behaviour observed in SRTs of 20 and 10 days. Reducing the SRT from 20 to 10 days was found to have little correlation with the fouling pattern, as both SRTs exhibited similar patterns of TMP increase and fouling behaviour in the first 45 days. The electric field appeared to impact EK-MPBRs depending on their biomass properties and size. The effect of the electric field on repelling the particles from the membrane surface was quantified as backwash flux which showed better efficiency with smaller particles in a lower concentration of algal biomass. In summary, the combination of interrelated factors in electrified membrane photobioreactors suggests that SRTs of 10 and 20 days were beneficial in controlling the membrane fouling in EK-MPBRs.

In summary, electro-phycoremediation is a promising technology to improve phosphorus removal from synthetic municipal wastewater. It is also effective in enhancing biomass production along with controlled fouling of the submerged membrane. The modified design of the electrokinetic-assisted membrane photobioreactors could effectively improve the membrane performance of EK-MPBR compared to a control MPBR. Phosphorus removal was significantly higher compared to the conventional MPBRs while nitrogen removal interfered with the applied electric field. The SRT variation in EK-MPBRs contributed differently to the membrane and biological performance.

EK-MPBRs are in their early stage of development and more studies are required to address the challenges in this area and its implication for industrial application. In this thesis, the modified design was better able to alleviate fouling, but there is still room for further improvement in nitrogen removal. However, this research can help promote membrane-assisted wastewater treatment technologies with controlled membrane fouling.

7.2 Future work

EK-MPBR is a recently developed technology for simultaneously removing the nutrients (N and P) and microalgae production integrated that utilizes an electric field. Despite the advantages of this technology over conventional MPBRs, such as controlled fouling and better phosphorus removal, some challenges need to be studied and overcome further as the application of the electric field and its contribution to the performance of MPBRs is complex and requires further investigation. To date, this is the first study that examines the effect of low voltage DC electric field in treating synthetic wastewater in MPBR using *Chlorella vulgaris*. While the modified design of the MPBR was able to eliminate the membrane fouling in the current study, further modifications could be investigated to improve the mixing condition in the reactor. The effect of electrode material in improving nutrient removal could also be a focus of further studies in this area.

Currently, both continuous and intermittent electric field has been studied in electrokinetic-assisted MBRs. However, the combination of the intermittent electric field with an MPBR has not been investigated yet. Research in this area could lead to further optimization of this technique with regard to energy cost and efficiency. Aeration intensity and illumination optimization are other factors that can contribute to the energy optimization of EK-MPBRs.

The effect of HRT and nitrogen to phosphorus (N/P) ratio in the feed is worth studying as they are proven to be effective in MPBR performance. However, the integration of electrokinetic phenomena with phycoremediation has made this field complex and a thorough investigation of the interrelated factors and the relationship between them need to be considered for future studies.

One of the challenges in MPBRs is their effectiveness in treating real wastewater with higher concentrations of nutrients compared to synthetic municipal wastewater. Further studies on the assessment of EK-MPBRs with various type of wastewater should be investigated. Such research could bridge the gap between the laboratory and industrial implications of this recent field.

Electric fields can contribute differently to the mechanisms of nitrogen and phosphorus removal. To date, there are limited studies to investigate the removal efficiency of the electrified microalgae *Chlorella vulgaris* in an MPBR on a molecular level. The study of underlying phenomena could provide the knowledge needed for future improvement of EK-MPBRs.

In order to enhance the potential of scalable EK-MPBR, future work should focus on improving the backwash flux force and consider the pump suction force. Current work is limited by the relatively low electrostatic repulsion force that has not been effective in preventing poor blocking as much as expected. Such enhancement can profoundly enhance the fouling control in EK-MPBRs. More stable and durable electrode materials can promote this technology, especially for long-term operations.